Chem Soc Rev

Molecular containers assembled through the hydrophobic effect

Journal:	*Chemical Society Reviews*
Manuscript ID:	CS-REV-05-2014-000191.R1
Article Type:	Review Article
Date Submitted by the Author:	29-May-2014
Complete List of Authors:	Jordan, Jacobs; Tulane University, Chemistry Gibb, Bruce; Tulane University, Chemistry

Molecular containers assembled through the hydrophobic effect

Jacobs H. Jordan and Bruce C. Gibb

Department of Chemistry, Tulane University, New Orleans, LA 70118, USA

Abstract

This review focuses on molecular containers formed by assembly processes driven by the Hydrophobic Effect, and summarizes the progress made in the field over the last ten years. This small but growing facet of supramolecular chemistry discusses three classes of molecules used by researchers to investigate how self-assembly can be applied to form discrete, mono-dispersed, and structurally well-defined supramolecular entities. The approaches demonstrate the importance of preorganization of arrays of rigid moieties to define a specific form predisposed to bind, fold, or assemble. As the examples demonstrate, studying these systems and their properties is teaching us how to control supramolecular chemistry in water, shedding light on aspects of aqueous solutions chemistry, and illustrating novel applications that harness the unique properties of the Hydrophobic Effect.

1.0 Introduction

Why water?

Chemists are spoilt for choice when it comes to solvent;[1] in contemporary chemistry there are literally dozens of different solvents to chose from, each with their own unique properties to fit a task. So why would a chemist focus on just one? And why would an organic chemist focus on one that doesn't dissolve most organic molecules? Why would an organic chemist choose water as a solvent? One reason that may be suggested is the environment. Green chemists might argue that we should aim for water as the default solvent; that organic chemists should be systematically converting – by whatever means possible – the cornucopia of organic reactions in the literature into water-based processes. Of course, whether or not this is possible, or even desirable, is debatable. And so for this and many other reasons organic chemists focus on organic solvents.

But there is no debating that supramolecular chemists should be very interested in water.[2] With important exceptions, the expertise in controlling and utilizing non-covalent forces that the field has built up over the last few decades has been grounded in organic solvents. And yet aqueous chemistry is fundamental to the biosphere, hydrosphere, lithosphere and the atmosphere.[3] Choose just one of these (the biosphere?), and one tiny fraction of it (Homo Sapiens?), and consider all of the key non-covalent interactions going on in aqueous solution.[4] Opportunities abound.

But there are problems. Although pure water is relatively well understood, there are still some controversies arising from its dynamic structure. The idea of memory water and poly-water may have been refuted,[5] but the recent debate about the ability of water to store charge[6] should remind us that its complicatedness – its complexity (in the sense of emergence) – provides many opportunities to be led astray.

Moving away from the controversial, just the slightest complication to the pure water picture and our view becomes somewhat murky.[7] Hence, a simple(!) air-water interface, or a change in pressure or temperature leads to debate and controversy. Dissolve something in water, be it a salt or a relatively hydrophobic, organic molecule and the water becomes murkier still. That is not to say that progress isn't being made. For example, the Jones and Ray Effect (a minimum in the surface tension of electrolyte solutions at 1 mM concentrations) – a phenomenon that caused considerable debate last century – now seems to be resolved.[8] More generally, it now seems clear that certain kinds of ions do accumulate at the air water interface, and that the ensuing models can now bridge the divide between physical chemists who point out that surface tension increases in solutions as a function of increasing salt concentrations can

only be accounted for by a depletion of ions from the air-water interface, and atmospheric chemists who can only explain aerosol properties by having ions accumulate on droplet surfaces.[9] Progress is also being made in regards to the solvation of hydrophobic surfaces, although the focus has primarily been on convex[10] and flat surfaces[11] and is only more recently turning to concave surfaces.[12] This noted, there is still plenty to discover about the Hydrophobic Effect (most simply put, why oil and water don't mix) and the Hofmeister Effect (how salts effect the properties of water and aqueous solution). Water science is a rich field barely scratch by supramolecular chemistry. But one thing is for sure, dissolve benzene and sodium chloride in water and there are six non-covalent interactions to consider (water-water, salt-salt, benzene-benzene, water-benzene, water-salt and benzene-salt). Rich pickings for supramolecular chemists.

Topic boundaries of the review

This review focuses on one small but growing area of supramolecular chemistry in aqueous solution. As the title suggests, the topic is molecular containers that are formed by assembly processes driven by the Hydrophobic Effect. But when is a container a container? What is an assembly? And which assemblies are, or are not, driven by the Hydrophobic Effect? We take the following perspectives.

The definition of a molecular container can be approached quantitatively or qualitatively, although both are subjective and arbitrary. Quantitatively, in our minds a molecular container envelops at least 83% of a smaller guest. This is based on our experiences at the macroscopic scale. Thus, in the extreme a container encloses 100% and there is no opportunity for the inner contents to escape without the opening of the container itself. Opening the container may be irreversible (an egg), but most containers can be opened and closed repeatedly because they have a screw-top or lid, and in our minds a molecular container is more akin to the plastic boxes devised by Earl Tupper (Tupperware®) than it is to an open cage-like structure. Our envisioned containers therefore possess the equivalent of at least five of six sides and envelop roughly 83% (100% $\times$ 5/6) of its contents, and the addition of a lid leading to 100% encapsulation and complete isolation from the external medium. Qualitatively, we view a molecular container as fully preventing guest exchange unless the container is opened. In the case of a true molecular container bond breakage may be required to do this, but in the context of assembled containers then disassembly (removing the lid) suffices to allow guest entry or egression.

The extent by which a container envelops is not the only quality colored by our macro-scale view, so too is our definition of the type of construction material used to form the molecular

walls. Thus, our definition includes structurally well-defined, mono-dispersed chemical entities with kinetically stable walls, but not those that are fluxional and/or poorly defined. We therefore do not include the topic of fluxional foldamers (but see below), even though we acknowledge that defining these as fluxional and/or poorly defined is colored by how they are analyzed.

In chemistry, self-assembly is the process in which a relatively disordered system of pre-existing molecules or ions forms a more organized structure as a result of specific, local interactions among the subunits. And so the systems under review here are principally molecules that form dimers, trimers, tetramers etc. and in doing so modify (put the lid on) or create the container. We have however intentionally chosen the more vague term “assembly” for the title rather than “self-assembly” so that structurally well-defined self-folding molecules can be included. In our minds there are too many similarities and overlaps between self-assembling and self-folding molecules to completely exclude the latter. Again, we acknowledge the vagaries in deciding what is and what is not a kinetically or thermodynamically stable entity.

Which assemblies are, or are not, driven by the Hydrophobic Effect? That depends on the definition of the Hydrophobic Effect. Our view is that it is the phenomenon of the separation of hydrophobes from water and/or the desolvation of hydrophobic surfaces that is primarily driven by the highly cohesive nature of water. More specifically, it is an observed effect arising from the strong hydrogen bonding within water and, to a lesser extent, the van der Waals forces between solutes. The simple face-to-face cyclohexane dimer in water illustrates this idea perfectly. But it doesn’t take much structural diversity to make things ambiguous. Is a similar face-to-face dimer of cyclohexanol driven by the Hydrophobic Effect? Or is that hydrogen bond important? Our drawing of the line in this regard is based on the following: 1) the system in question must be in water. Systems with co-solvents were not included (mostly); 2) no systems involving covalent, or strong non-covalent interactions such as metal coordination, are discussed in detail. Reversible[13] and irreversible covalent bond[14] formation and metal-ligand driven assembly[15] are very important topic in self-assembly but are excluded here; 3) There must be both structural features in the solute and empirical evidence that desolvation of hydrophobic surfaces is key to assembly.

Finally, in this paper we have tried to summarize the progress made in the field over the last ten years. During this time-period we have attempted to be as comprehensive as possible. However, as is always the case, the topic of “molecular containers assembled through the hydrophobic effect” did not appear out of the ether. Consequently, where appropriate we have stretched back in the literature to before 2004.

2.0 Classes of Self-Assembling Molecules

2.1 Deep-Cavity Cavitands

2.1.1 Investigating the Properties of Deep-Cavity Cavitands

a) Synthesis, Structure and Coatings

The water-soluble deep-cavity cavitands discussed here have their roots in analogous organic-soluble deep-cavity cavitands devised by the Gibb group.[16] Available in two linear steps from the respective resorcinarene, hosts such as **1** possess deeper pockets than those popularized by Cram and others, and acted as a proof-of-concept for the facile formation of relatively rigid (non-collapsing) binding pockets.

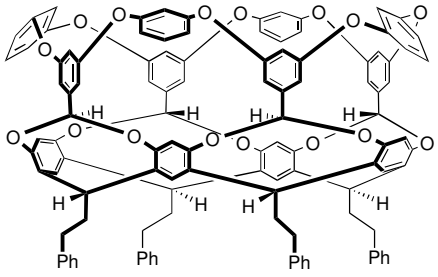

1

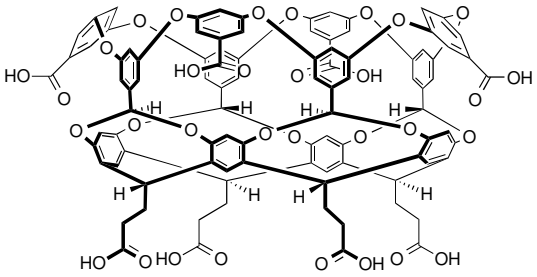

2

Building on this early work, the Gibb group reported the first example of a water-soluble deep-cavity cavitand (**2**) that binds and assembles into well-defined supramolecular entities via the hydrophobic effect; a host that is commonly called octa-acid (OA).[17] The synthesis of OA **2**[18] involves six steps from the requisite resorcinarene, only one of which requires chromatographic separation. Consequently, gram quantities of **2** are readily available. Briefly (Scheme 1), the resorcinarene scaffold was built up by first stereoselective bridging resorcinarene **3** with the corresponding benzal bromide (1-3-dibromo-5-(dibromomethyl)benzene) to afford the deep-cavity cavitand octabromide **4**.[16e, 19] Subsequently, an eight-fold Ullmann ether reaction is introduced to provide rigidity to the cavity and introduce functionality at the rim in the form of hydroxyl groups (**5**). Oxidation then gives crude OA **2**. Esterification followed by chromatographic purification, then hydrolysis of the octa-ester **6** affords OA **2** in six linear steps.

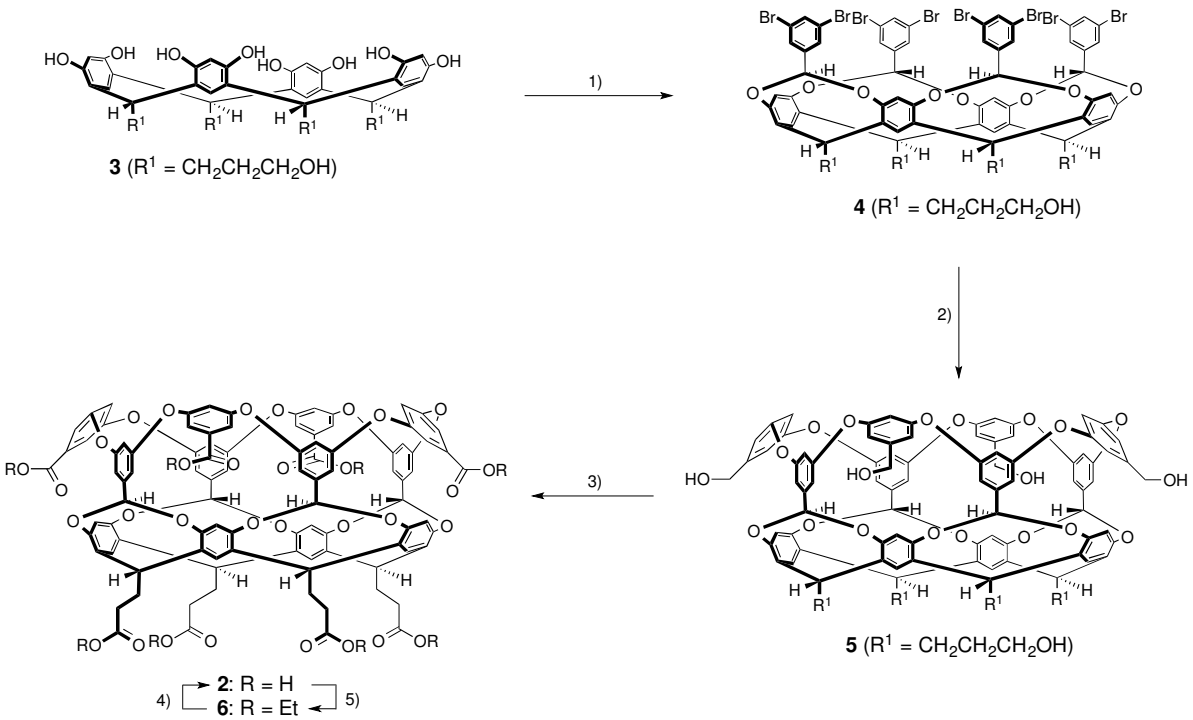

3 (R^1 = $CH_2CH_2CH_2OH$)

4 (R^1 = $CH_2CH_2CH_2OH$)

5 (R^1 = $CH_2CH_2CH_2OH$)

Scheme 1: Synthesis of Octa Acid (OA) 2. Reagents are: 1)) 3,5-dibrombenzal bromide, DBU, DMA; 2) 3,5-dihydroxybenzyl alcohol, K_2CO_3, CuO, Pyr; 3) $KMnO_4$, DMA, *t*-BuOH; 4) HCl, EtOH/$CHCl_3$; 5) LiOH, DMA, H_2O.

Taking OA **2** as a representative of this class of molecule, these hosts possess a ca. 0.8 nm diameter wide and ca. 0.8 nm deep hydrophobic pocket comprised primarily of eight aromatic rings (Figure 1). Atop the cavity, forming a rim around the portal, are four more aromatic rings orthogonal to the C_4 axis of the host that 'stitch' the bowl together. The rim defined by these four rings is relatively hydrophobic and is key to the predisposition[20] of the molecules to assemble into supramolecular capsules. In addition, they provide diverging functionalization points for water solubilizing groups (R_1, in this case four carboxylic acids), as well as four converging (*endo*) positions for groups that modulate the shape and properties of the hydrophobic pocket (R_2). Four more functional groups for water-solubilization can be found at the termini of the pendant groups that hang down from the main bowl structure (R_3).

By virtue of its eight carboxylic acid/carboxylate groups OA **2** is soluble in tens of micromolar concentration at pH 7, and greater than one hundred millimolar concentrations at pH 9 or above. As is outlined in this section, this deep-cavity cavitand has been the most utilized and studied of this family of hosts. Key to this point is not only its good water solubility, but also its good behavior under a variety of conditions. Thus, whereas at above pH ≈ 10 and concentrations less than 10 mM random aggregation of the host is rare, the presence of guests from as small as propane[21] to as large as cholesterol[17] trigger quantitative dimerization into

mono-dispersed capsular complexes. We attribute the good behavior of OA **2** not only to the fact that it has eight water-solubilizing groups, but also to the fact that they are distributed in an pseudo square anti-prismatic or anti-cubic array that spreads the negative charges evenly (but not uniformly) around its outer surface (eight, maximally distant points on the surface of a sphere define an anti-cube). The distortion to the anti-cube – that the upper portal face is larger than its opposing face, and the carboxylates on the rim are below the lip of the pocket – means that the charge distribution is not even; the upper portal face is a relatively hydrophobic surface and likely contributes to the predisposition of these hosts to assemble.

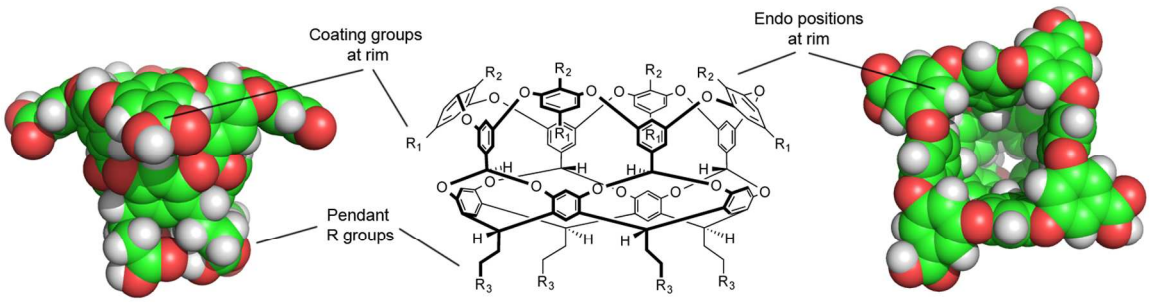

Figure 1: Structure of Octa-Acid **2**. The space-filling model on the left is from the same perspective as the chemical structure in the center. The space-filling model on the right looking down into the pocket of the host is from 'above' as viewed from the chemical structure.

Before discussing the different derivatives of these water-soluble deep-cavity cavitands it is worth noting the fine balance between charge number/charge distribution and the water solubility of these hosts; a concept that applies to the design of water-soluble hosts and self-assembling subunits in general. Cavitands **7**, possessing only four carboxylic acid groups, aggregates in aqueous solution and DMSO is required as a co-solvent to give interpretable NMR spectra.[22] It is a similar story for host **8** (R = 3,5-benzene dicarboxylic acid), whose eight water-solubilizing groups are all on one end of the molecule. This host is too amphiphilic and also undergoes aggregation in aqueous solution.

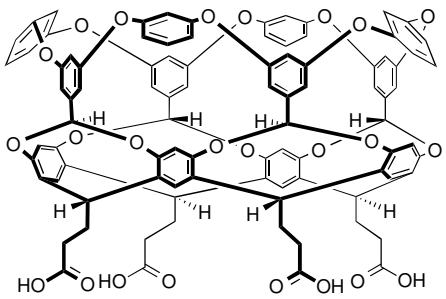

7

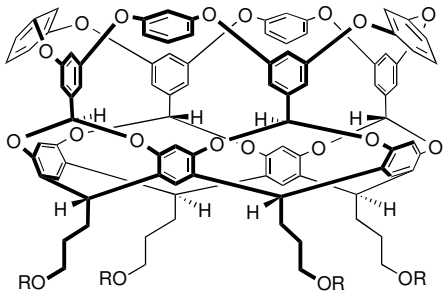

8

As well as these anionic hosts, neutral and cationic derivatives have also been synthesized. Examples of these are highlighted in the following sections. Here we briefly highlight some examples from these two classes for illustrative purposes.

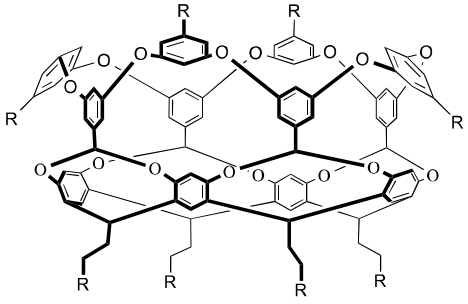

5 (R = CH_2OH)

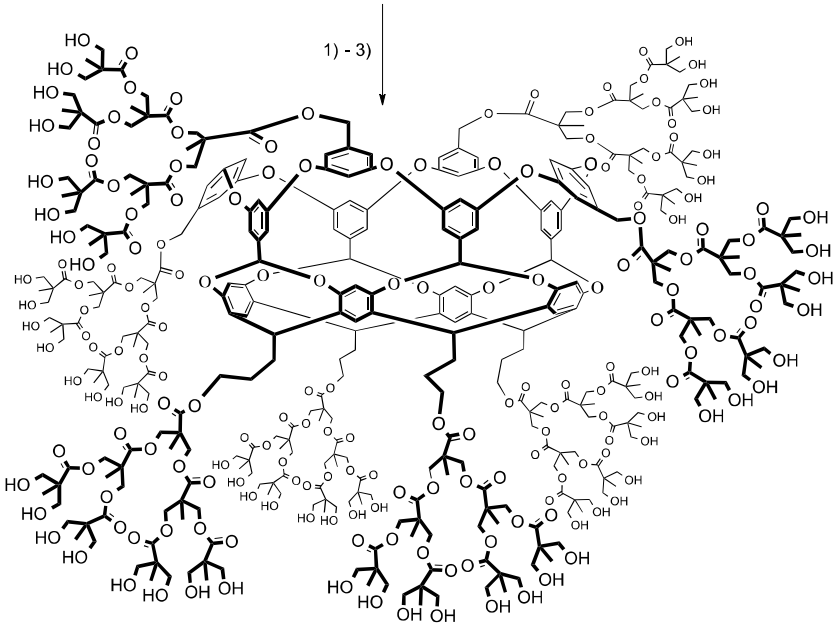

9

Scheme 2: Synthesis of dendronized cavitand **9**. Conditions are: 1) Acetonide-protected *bis*(hydroxy-methyl)propanoic anhydride, DMAP; 2) Dowex acid resin; 3) Repeat coupling and deprotection steps 1) and 2) twice.

The first example of a neutral water-soluble host was third generation (G3) dendrimer **9** (Scheme 2) from the Grayson group.[23] The G3 host **9** was prepared by three successive rounds of coupling, and deprotection starting from the precursor compound octol **5**. Thus, the eight hydroxy moieties were dendronized with an acetonide-protected anhydride and deprotected using a solid-phase acid resin to give the G1 cavitand with 16 hydroxyl groups. Two successive rounds of protection-coupling-deprotection gave the G3 cavitand with 64 water-solubilizing hydroxyls on the termini of the dendritic chains. Three generations of dendrimer were necessary for full water solubility. Thus the corresponding G2 cavitand required at least 20% methanol solutions for dissolution. Although possessing the same type of properties of OA **2** (see below), guest affinities to the G3 cavitand **9** were generally lower than with OA **2**. This was attributed to self-inclusion of the dendritic arms within the hydrophobic concavity.

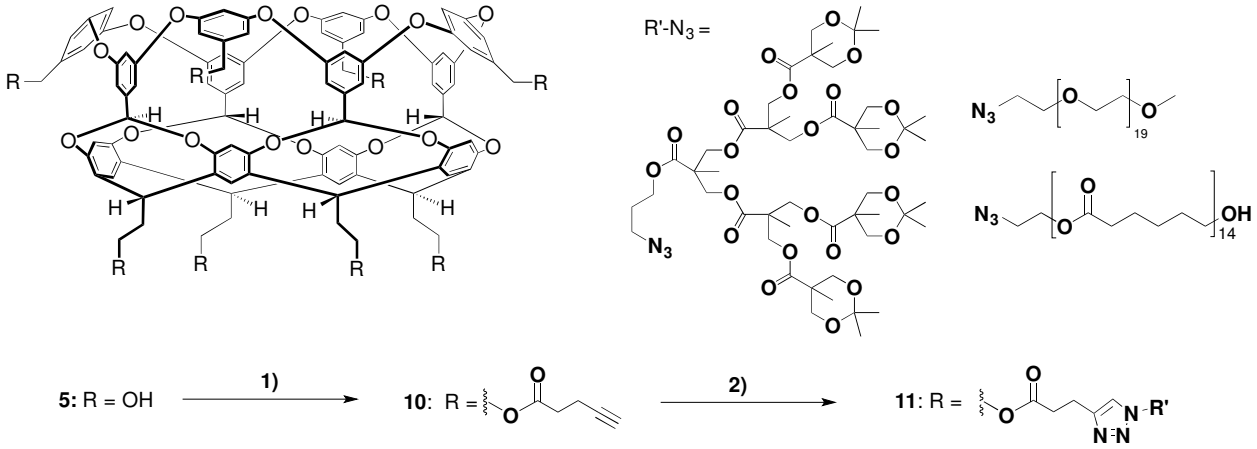

Scheme 3: "Click" chemistry for diverse water-soluble cavitands. Conditions are: 1) 4-pentynoic acid, *N*,*N*'-dicyclohexylcarbodiimide, DMAP, pyr/CH_2Cl_2; 2) Various azides, Cu(I)Br/Cu/*N*,*N*,*N*',*N*',*N*''-pentamethyldiethylenetriamine/CH_2Cl_2.

In an alternative approach, Grayson introduced a range of surface modifications using Cu(I) catalyzed aza-alkyne cycloaddition ("click") chemistry. Thus, the octol **5** was treated with a carbodiimide in the presence of 4-pentynoic acid to give the activated core cavitand **10** with eight alkynes protruding from the exterior (Scheme 3). Subsequently, treatment of **10** with an excess of the requisite azide under "click" conditions led to an array of coated hosts (**11**) including two with dendrons, and several with polymer coats such as polycaprolactone (PCL), and polyethylene glycol (PEG). All of the functionalized cavitands were highly mono-disperse and were characterized by MALDI-TOF MS analysis. The PCL-grafted cavitand showed increased solubility in organic solvents, whilst the PEGylated cavitand showed increased

solubility in polar solvents such as methanol (> 88 mg/ml), ethanol (> 24 mg/ml) and water (> 33 mg/ml).

The first example of water-soluble cavitands coated with cationic groups, host **12** and its octa-triethyl ammonium derivative, have been recently reported by the Ramamurthy group.[24] The initial studies on these hosts suggest that at low pH, **12** undergoes a degree of aggregation, but that it is better behaved as a complex with different guests. Preliminary host-guest and photochemical studies suggest properties similar to OA **2**. On the other hand, preliminary work with the corresponding octa-triethyl ammonium derivative suggest a poorly behaved host at neutral pH. Interestingly, host **12** also allowed the first glimpse in the gas phase of the 1:1 and capsular complexes made by these types of hosts.[25]

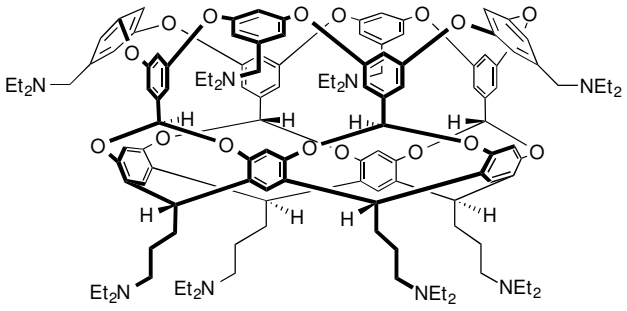

12

b) Factors Affecting Complexation and Assembly

Both the nature of the host and guest are important in the complexes formed by deep-cavity cavitands. To date the following host-guest complexes have been identified with deep-cavity cavitands: 1:1, 1:2, 2:1, 2:2, 4:2 and 6:3. We will focus first on guest effects and the formation of 1:1 and 2:1 complexes to highlight why one or the other forms.

Guest Effects

The Gibb group first identified the key point about forming 1:1 complexes with OA **2** in a study of the binding of a range of cyclic and acyclic aliphatic carboxylates.[26] ^{1}H NMR showed that these amphiphilic guests bound with their hydrophobic chains in the pocket of host **2**, and their polar carboxylates exposed to the free aqueous medium. Consequently, by binding in the orientation specific manner the 'upper' surface of the host defined by the portal to the pocket and its attendant rim is rendered more hydrophilic and assembly to the capsular state is switched off. A later study with related molecules confirmed these findings.[27]

In the study of cyclic and acyclic aliphatic carboxylates,[26] Isothermal Titration Calorimetry (ITC) were utilized to examine three cyclic and three acyclic carboxylates typified by hexanoate **13** and adamantane carboxylate **14** (Figure 2). All of the examined carboxylates were found to associate with a K_a of between 10^3 and 10^6 M^{-1}, with the weakest being haxanoate (K_a = 3.64 × 10^3) and the strongest proving to be adamantane carboxylate (K_a = 1.14 × 10^6). Butanoate, with a short propyl chain, did not bind. Apparently, the propyl chain was unable to effectively compete with the hydrophlicity of the carboxylate. A linear trend was observed for the relationship between ΔG° for complexation and the number of carbon atoms in the guest (N_c). ΔG° values become more favorable with increasing number of N_c, with the gradients $d\Delta G^\circ/dN_c$ for the acyclic acids and cyclic acids respectively being similar to those observed for the transfer of hydrocarbons from water to organic solvents.

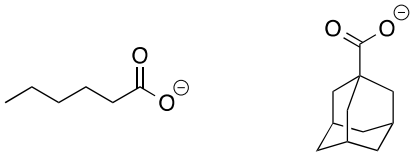

13 **14**

Figure 2: Representative carboxylate guests for 1:1 complexes with OA **2**.

Examining how the enthalpy and entropy changes as a function of N_c revealed two trends. First, for the acyclic guests as N_c increased both the entropy and enthalpy terms for complexation became more favorable. In contrast, enthalpy-entropy compensation was observed with the cyclic guests; with increasing N_c the entropy component of binding became less favorable, while the enthalpy component became more favorable. This was interpreted to arise from increasing host-guest contacts with larger guests being countered by restricted motion within the cavity.

For both series, the thermodynamics of complexation as a function of temperature displayed near perfect enthalpy-entropy compensation so that ΔG° was nearly independent of T. In all cases the exothermicity of complexation increase with T confirming that the heat capacity change (ΔC°_p) upon complexation was negative. The obtained values were generally equal to and/or greater than those seen with cyclodextrins, perhaps reflective of the more hydrophobic pocket of the deep-cavity cavitand. Expanding on this work, the same authors recently examined the binding of a series of cyclic aliphatic and aromatic carboxylates as part of the fourth statistical assessment of modeling of proteins and ligands (sampl.eyesopen.com).[28]

Another illustrative example of the formation of 1:1 complexes is the binding of 'hydrophobic' anions to the cavity of OA **2**.[29] This work examined the effects of different salts on

the binding of adamantane carboxylate **14**. There was only a slight change in the free energy of guest binding (~0.5 kcal mol^{-1}) between the absence and presence of salting-out salts such as sodium fluoride. In contrast to this were the series of salting-in sodium salts (chlorate, iodide, thiocyanate and perchlorate) which demonstrated a trend towards a decreasing free energy of complexation. Underlying this free energy change was a dramatic decline in the contribution to the free energy by enthalpy and a concomitant increase in the contribution made by entropy; so much so that in the presence of sodium perchlorate, guest binding was entirely entropy driven and the binding of **14** was actually endothermic.

^{1}H NMR showed that fundamental to the reported changes in thermodynamics with salting-in salts was anion binding to the pocket of the host competing with the complexation of **14**. Subsequent NMR titrations of salt to OA **2** without **14** revealed association constants ranging from <1 M^{-1} in the case of sodium nitrate, to 95 M^{-1} in the case of sodium perchlorate. This first reported instance of inorganic anion binding to a hydrophobic pocket again demonstrates that like **13** or **14**, very small charged guests lead to 1:1 complexes.

It is understood that anionic amphiphiles and simple anions form 1:1 complexes with OA **2** because the upper portal region of the complex remains quite hydrophilic. If on the other hand the binding of a guest renders the portal region of OA **2** hydrophobic then, there is a thermodynamic preference for a second host molecule to cap the complex and form an encapsulation complex. In fact, the first complexes reported with OA **2** were 2:1 host-guest complexes with steroids.[17] In this report a number of steroid guests were encapsulated including estradiol **15**, progesterone **16** and cholesterol **17** (Figure 3). In each case, because of the chirality of the guest the 2:1 host-guest complexes could be identified from symmetry arguments of the ^{1}H NMR data alone. In addition though, 2D NOESY NMR confirmed the spatial proximity of the host-host interactions and the host-guest interactions from the two sets of non-equivalent hydrogens in each hemisphere of the capsule. Guests such as **15** and **16** formed very stable and structurally defined complexes, with a K_a for the former (empty capsule to full capsule) estimated to be > 1 x 10^8 M^{-1}. Strong as these complexes are however, they were 'denatured' when methanol was added to the solution. It is noteworthy that the steroids such as cholesterol **17**, although greatly solubilized by the host, did not form kinetically stable complexes (on the NMR time scale). In such cases, the length of guest is too large for the capsule and as a result the two hemispheres of the capsule cannot clamp down on one another and must remain partially solvated.

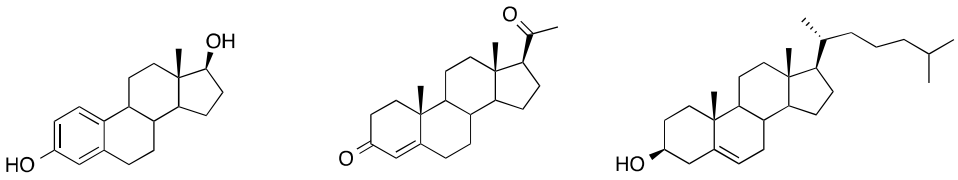

15 **16** **17**

Figure 3: Example of steroids that from 2:1 host-guest complexes with OA **2**.

The stability of 2:1 host-guest capsular complexes involving OA **2** to co-solvent induced denaturation has been examined using ^{1}H NMR.[30] In this study, a series of capsular complexes of trioxolane guests, e.g. **18**-**20** (Figure 4) were investigated. The trioxolanes varied from practically insoluble to sparingly soluble in aqueous media, yet nevertheless were fully dissolved in a 2:1 solution of OA **2** in aqueous buffer. ^{1}H NMR demonstrated that all of these trioxolanes were readily taken up as a kinetically and thermodynamically stable 2:1 complex. The denaturation experiments of the different complexes utilized a series of per-deuterated water miscible solvents, namely: acetone-d_6, dimethylsulfoxide-d_6 (DMSO-d_6) methanol-d_4, ethanol-d_6, isopropanol-d_8, acetonitrile-d_3, and tetrahydrofuran-d_8 (THF-d_8); as well as trifluoroethanol (TFE). Overall, **18** formed the weakest of the complexes, and a 1:1 ratio of the host and guest did not form any 1:1 or 2:1 complex in 50% aqueous acetone. On the other hand, under identical conditions guest **19** formed 78% 1:1 and no 2:1 complex. Because of solubility issues with **20**, only a 2:1 host-guest ratio could be examined in 50% aqueous acetone, in which case the mixture formed essentially only the 2:1 complex.

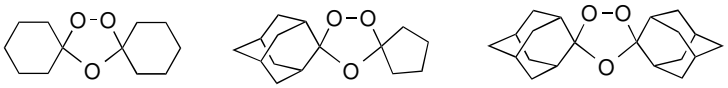

18 **19** **20**

Figure 4: Examples of Encapsulated trioxolanes

The different cyclic alkyl groups of **19** proved illuminating in so much as it was possible to observe the denaturation of the 2:1 capsular complex to form the 1:1 complex in which the adamantyl group is bound, and ultimately the breakdown of this complex with even higher equivalents of added co-solvent. Overall, for the different solvents examined, the ability to denature the complex formed by **19** was: acetonitrile-d_3 > THF-d_8 > TFE > *i*-PrOD-d_8 > acetone-d_6 > ethanol-d_6 > methanol-d_4 ≈ DMSO-d_6. Thus it was observed that whereas acetonitrile denatures most of the capsular complex at 30% by volume, a 70% aqueous solution of DMSO was needed to bring about the same extent of decomplexation.

In related work it has been shown that a fully fitting and rigid guest is not a prerequisite for capsule formation, but that even small straight-chain alkanes can lead to assembly.[31] In this work, the authors investigated the binding of the alkanes *n*-pentane through *n*-octadecane (C_{18}). Although, the latter guest was reportedly (*vide infra)* too large to form a kinetically stable complex, the C_5-C_{17} guests did form stable complexes with assembly/disassembly rates slower than the NMR timescale. As was noted for the aforementioned steroid and trioxolane complexes, for the free host the diffusion constant (*D*) as determined by pulse-gradient stimulated spin-echo (PGSE) NMR experiment was 1.82×10^{-6} cm^2 s^{-1}, considerably larger than that for the capsular complexes ($D = 1.36 \times 10^{-6}$ cm^2 s^{-1}).

More specifically, the guests *n*-pentane through *n*-heptane were found to form stable 2:2 complexes with OA **2**. These were the first examples of multiple molecules binding within the capsule formed by the host. Apparently there is too much empty space in the capsule when only one molecule is encapsulated. For the longer alkanes examined, the complexes formed were 2:1 in stoichiometry; the one exception being intermediately sized *n*-octane which formed both 2:1 and 2:2 capsules in a temperature dependent ratio (the quaternary complex dominating at higher temperature).

The propensity for deep-cavity cavitands to tend towards capsule formation was further investigated by comparing a series of guests of roughly equal volume but differing polarity/water solubility (Figure 5).[32] In these instances, it was shown that as the number of oxygen atoms increased in the series the stability of the corresponding capsular complexes decreased.

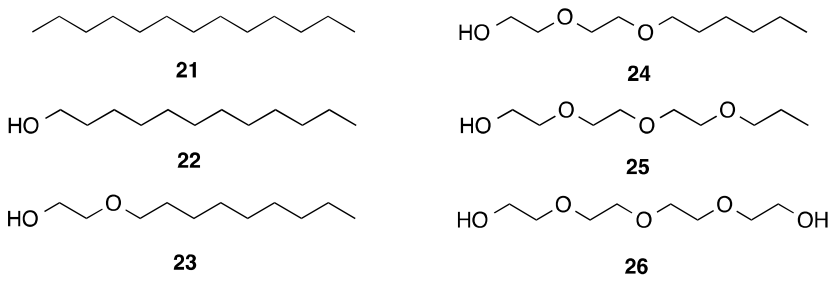

Figure 5: Approximately isosteric guests of varying polarity;

Competition experiments between the varying guests indicated that both tridecane (C_{13}) **21** and dodecanol **22** bound strongly and favored 2:1 capsule formation, with the former possessing a binding affinity an order of magnitude greater than the latter. This was attributed to both the hydrophilicity of the polar hydroxyl group of **22** and its ability to hydrogen bond and be freely solvated by waters, and the loss of C-H···π interactions between the host and guest upon replacement of the terminal methyl of **21**. Both tridecane **21** and dodecanol **22** adopt an

extended, pole-to-pole motif within the capsule (for guest packing within the capsule formed by OA **2** see Section 2.1.1.e), and for the methylene groups at C-1 and C-11 of **22** the $\Delta\delta$ values indicated that the hydroxyl moiety was bound more deeply in one half of the capsule that the methyl group was in the other.

While the other guests **23** and **24** had clearly defined NMR signals indicative of 2:1 complexation, 2-[2-(2 propoxyethoxy)ethoxy] ethanol (tri(ethylene glycol) propyl ether) **25** exhibited broadened signals which were confirmed by PGSE NMR to be due to a capsule of low stability. Furthermore, *bis* [2-(2-hydroxy-ethoxy)ethyl] ether tetra(ethylene glycol) **26** did not show any signals indicative of capsule formation and indeed was confirmed by PGSE NMR to form only a 1:1 complex. An interesting side-note regarding **26** is that opinion is split about whether it is hydrophilic or hydrophobic. At least by the metric of binding to OA **2** the answer is clear; it is relatively hydrophobic.

To recap, the question of whether a 1:1 or a capsular complex is formed with cavitands such as OA **2** rests in large part on the nature of the guest. If the guest is highly water soluble, or at least can adopt a binding orientation that projects a polar group to the portal of the host, then only a 1:1 complex will be formed. If on the other hand the guest binds and the net polarity of the portal/rim region of the host-guest complex is hydrophobic, then a capsular complex is preferentially formed; and the more hydrophobic the guest the stronger the capsular complex that is formed.

Host Effects

In addition to the nature of the guest, the structure of the host also plays a role in the assemblies seen. This was first demonstrated with the deep-cavity cavitand TEMOA (tetra-*endo*-methyl octa-acid, **27**). In an analogous procedure to that utilized in the synthesis of OA **2**, TEMOA **27** was synthesized by the eight-fold Ullmann reaction of octabromide **4** (Scheme 1) with 3,5-dihydroxy-4-methylbenzyl alcohol. This afforded four methyl substituents in place of the corresponding protons at the hydrophobic rim, which after oxidation, esterification and purification, and hydrolysis led to host **27**.[33]

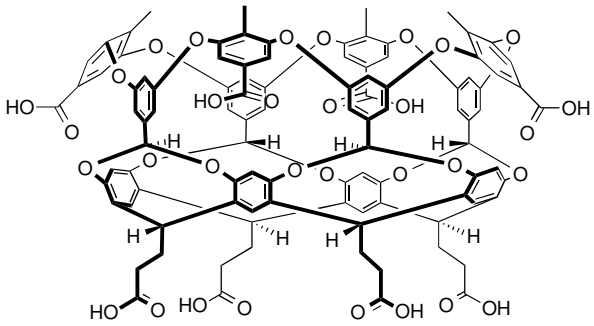

27

The four *endo* methyl groups of **27** provide for a slightly deeper cavity with a narrower portal region. Furthermore, the methyls crenellate the rim of the cavity and consequently disrupt 2:1 capsule formation. As a result, its properties are quite different from OA **2**. For example, as a function of guest size the assembly of OA **2** is straightforward: with small guests such as methane and ethane it forms 1:1 complexes (*vide infra*), but with bigger guests a 2:2 and then a 2:1 capsule is formed (*vide supra*). In contrast, diffusion NMR experiments revealed that TEMOA **27** forms 1:1 assemblies for methane, ethane, *n*-heptane and *n*-octane, a mixture of 1:1 and 2:2 complexes with propane, *n*-butane, and *n*-hexane, and only capsular assemblies for *n*-pentane (2:2) and the longer chain alkanes C_9 to C_{14} (2:1)[31, 33] Why? It would appear that because the methyl groups at the rim of **27** reduce its predisposition to dimerize, 1:1 complexes are preferentially formed even with some hydrophobic guests. This occurs with methane and ethane because they are too small and the 2:2 complexes would have too much void space, and with *n*-heptane (C_7) and *n*-octane (C_8) because in both cases two guests cannot fit in the capsule and the 2:1 complexes again would have too much empty space. In contrast, *n*-pentane can form a relatively stable 2:2 complex, and the longer chain alkanes C_9 to C_{14} form relatively stable 2:1 capsular complexes. The guests propane, *n*-butane, and *n*-hexane are intermediate between the 'islands of stability' defined by *n*-pentane, and the alkanes C_9 to C_{14}.

The unusual assembly properties of TEMOA **27** are reflected in what happens with mixtures of it and OA **2**.[34] In the described work NMR was used to probe the extent of hetero-capsule formation when these two hosts are combined, i.e., whether a guest or guests were complexed inside $\mathbf{2}_2$, $\mathbf{27}_2$, or **2.27**. A range of *n*-alkanes (C_5 to C_{16}) was used in this study.

A combination of ^{1}H and NOESY NMR confirmed the possibility of hetero-capsule formation, and that the ratio of the homo- and hetero-capsular complexes varied depending on the nature of the included guest. Thus 24% of the hetero-complex involving **2** and **27** was formed in the presence of *n*-heptane (C_7), whereas 74% was formed in the presence of *n*-tridecane (C_{13}). Overall, the extent of hetero-capsule formation was high for guests *n*-pentane, *n*-hexane and C_9-C_{14}, and small for C_7, C_8, C_{15}, and C_{16} (Figure 6). It was noted that there was a

reasonable correlation between the extent of this hetero-capsule formation and the measured hydrodynamic volumes of the homo-capsular complexes formed by TEMOA **27** alone in the presence of the same guests (Figure 6). These results were interpreted as follows. First, the guests *n*-heptane (C_7) and *n*-octane (C_8) formed limited amounts of hetero-capsular complex because they are poor templates of both homo- and hetero-capsules. As a result, it is energetically preferential for TEMOA **27** to form 1:1 complexes and allow OA **2** to from stable homo-capsular complexes. In other words, these guests promote self-sorting of OA **2**. For the guests C_9 through C_{14}, the higher amounts of hetero-capsular complex formed was attributed to the more efficient packing of the (singular) guest within the capsular complexes compensating for the limited ability of **27** to assemble. The reason why the largest guests examined (C_{15} and C_{16}) formed below statistical amounts of hetero-complex was not discussed.

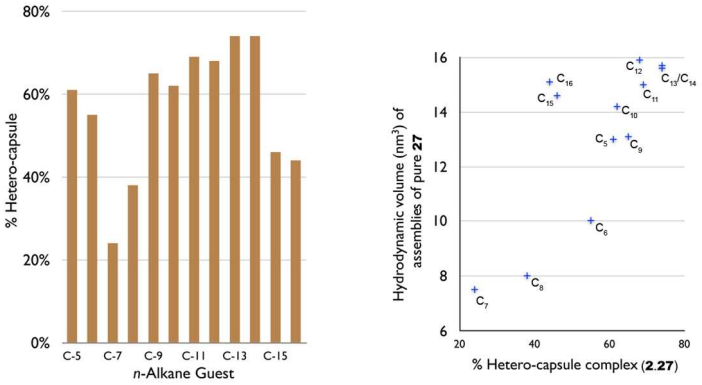

Figure 6: Left panel: Extent of hetero-capsule formation for hosts **2** and **27** in the presence of *n*-alkane guests. Right panel: Correlation between the extent of hetero-capsule (**2**.**27**) formation and the hydrodynamic volumes of the corresponding complexes formed by **27** alone; guest size for each point are indicated.

The point that the methyl groups of deep-cavity cavitand TEMOA **27** reduce its predisposition to form a dimer capsule suggests that other assembly pathways may be more favorable to this host. Relatively recently this has indeed been shown to be the case.[35] Thus, whereas OA **2** has only been observed to assemble into dimers, TEMOA **27** can form dimeric, tetrameric and even hexameric capsules depending on the size of the guest that is encapsulated (Figure 7a).

The different assembly states of TEMOA **27** were identified by investigating a series of homologous *n*-alkanes, from *n*-tetradecane (C_{14}) to *n*-hexacosane (C_{26}). While the C_{14} guest bound in the typical 2:1 fashion previously observed with OA **2**, (^{1}H and PGSE NMR), longer alkane chains (C_{17} – C_{20}) formed pseudo T_d (D_{2d}) 4:2 host-guest complexes. Models suggest that the inner volume of this tetrameric host shell to be 1400-1500 Å^3, i.e., this assembly is more voluminous than the familiar resorcinarene hexamer.[36] In contrast, the intermediate length

guests, the C_{15} and C_{16} alkanes, showed broad and/or poorly resolved NMR spectra suggesting that mixtures of assembly products were formed. Furthermore, although this was also the case with the C_{21} to C_{23} guests, with *n*-tetracosane (C_{24}) only one highly symmetric assembly product was observed in a 2:1 host-guest ratio. PGSE diffusion NMR examination of the host-guest signals indicated a diffusion coefficient of 9.6×10^{-7} $cm^2 s^{-1}$, which after correction for the higher working concentrations revealed a hydrodynamic volume of 48.9 nm^3. In short, C_{24} formed a nonary 6:3 host-guest complex with overall O_h symmetry and an estimated internal volume of between 3200 and 3700 $Å^3$. The same complex was also observed for the longer guests *n*-pentacosane (C_{25}) and *n*-hexacosane (C_{26}), but unfortunately the kinetics of complex formation with even longer alkanes were too slow to investigate the formation of still larger assemblies. The precise packing arrangement of the two or three guests in the pseudo T_d and O_h capsules could not be surmised from the given data, but from the highfield positioning of the shielded guest methyl signal and the large anisotropy of the guest signals it was assumed that, to take the pseudo T_d capsule as an example, the guests adopt one of three different arrangements in which each end of a guest occupies one cavity of a host: an X-motif, a double U-motif, or a 'catenated 'double U-motif (Figure 7b).

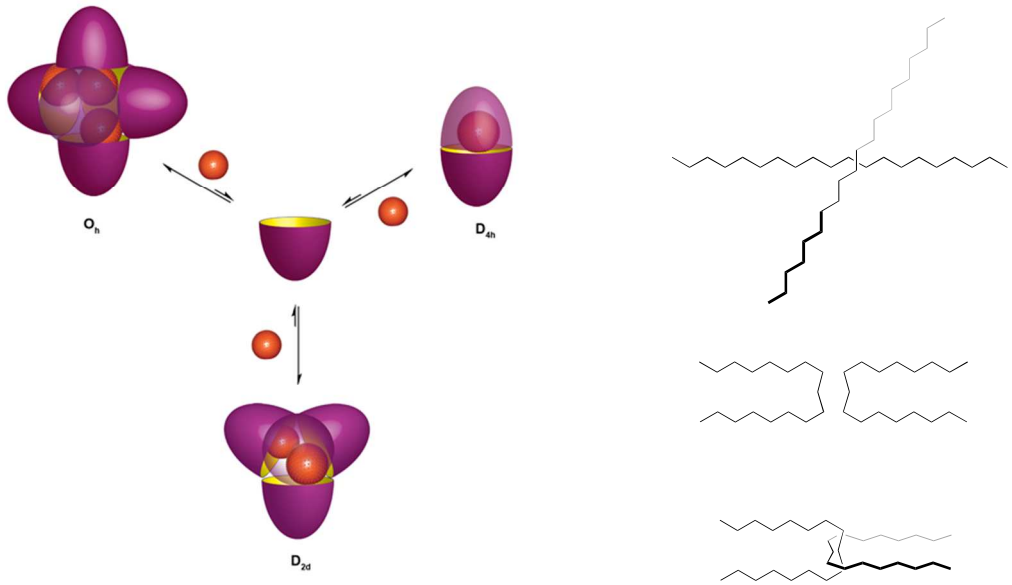

Figure 7: a) Different assemblies observed with TEMOA **27**. b) Different packing motifs within the tetramer of TEMOA **27**.

c) Environment Inside the OA Capsule

We have noted that OA **2** and TEMOA **27** are predisposed to form respectively dimeric, and dimeric, tetrameric and hexameric assemblies depending on the guests. In addition, the

aforementioned studies reveal that it is the Hydrophobic Effect that drives the formation of these supramolecular entities. If this is indeed the case, then desolvation of the pocket and rim of the host, and of course desolvation of the guest molecules, must both be key. This leads to the question, are there any water molecules within the cavity of these capsular complexes? It is noteworthy that molecular dynamics simulations have indicated that water molecules are included within the hydrophobic concavity of free OA **2**.[37] These calculations suggest that on average there are 4.34 ± 0.04 water molecules inside the hydrophobic pocket of the free host. Nature simply abhors a vacuum. Furthermore, these simulations reveal that during a wetting event the number of water molecules fluctuate, with four being the most probable (or lowest free energy) and the maximum number being seven. Overall, ΔG_{hyd} of the cavity was estimated to be -5 kcal mol^{-1}, with $\Delta H_{hyd} \approx$ -20 kcal mol^{-1} and $T\Delta S_{hyd} \approx$ 15 kcal mol^{-1}. This study also determined that these hydrophobic pocket waters are stabilized by their interaction with the bulk. Thus, when a hydrophobe approaches the portal of the pocket the cavity is rapidly and completely dewetted. Is there complete dewetting when a capsule is formed? The use of fluorescent probes as guests has addressed this question. For example, the ratio of the I_1 and I_3 vibronic bands in the fluorescence spectrum of pyrene **28** (Figure 8) confirm that no waters are present in the complex of **28** with OA **2**.[38] Furthermore, a more comprehensive study suggests that – at least for sizeable guests that fill most of the cavity – this is the case regardless of the nature of the guest encapsulated.[39] To take one example from a series of guests investigated, coumarin-1 **29**, whose fluorescent quantum yield and lifetime increase with a decrease in solvent polarity, also demonstrated a low polarity environment inside the capsule. Overall these results suggest that, as would be expected considering the nature of the host, the environment inside the OA **2** dimer is benzene-like. To the authors' knowledge, a study of the environment within the TEMOA tetramer or hexamer has not been undertaken.

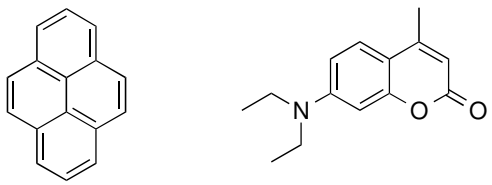

28 **29**

Figure 8: Molecular probes to examine the inner environment of the OA **2** dimer.

d) Kinetics of Capsule Opening and Closing

The very earliest studies with these container molecules demonstrated that for most hydrophobic guests the exchange between the free and the encapsulated state is slow on the

NMR timescale; the lifetimes of many complexes are > 0.1 s. This point noted, there remains the idea that very small (atomic or diatomic) guests such as molecular oxygen might be able to enter an occupied capsule via partial opening (breathing) of the equatorial seam of the container. The first detailed analysis focusing on this possibility came from measurements of the rate constants for the quenching of excited singlet and triplet guests by singlet oxygen.[40] These guests included (Figure 9) T_1 excited dimethyl benzil **30** (phosphorescence) and S_1 excited phenanthrene **31** (fluorescence), and covered excited-state lifetimes from 0.05 to 922 μs. Two classes of guests were observed, those that were quenched by oxygen when enclosed within the capsule, and those that were not. The latter were a mixture of singlet and triplet guests and therefore the spin state of the guest was dismissed as an explanation for why these guests were not quenched. Rather the obtained results reflected the guest-dependent accessibility of oxygen to the bound guest; if the guest had an excited lifetime of less than 5 μs it was inaccessible to oxygen.

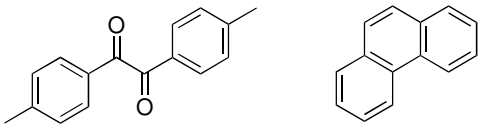

30 **31**

Figure 9: Molecular probes to examine the opening and closing of the OA **2** dimer.

To investigate the formation/dissociation dynamics of the encapsulation complexes formed by OA **2**, the Bohne group measured the real-time kinetics of formation of the 1:1 and 2:1 host-guest complexes formed between OA **2** and pyrene **28** (Figure 10).[41]. Pyrene **28** formed the expected 2:1 host-guest complex in aqueous solution, and upon encapsulation there was a marked red shift (5-6 nm) in its excitation and absorption spectra. This could not be attributed to dimerization of the guest as no excimer emission or spectral broadening was observed. Further evidence for the encapsulation of a single molecule of **28** within the OA **2** dimer was that its fluorescence lifetime was nearly three times longer than free **28** in aqueous borate buffer (361 ± 1 ns vs. 130 ± 1 ns), whilst the quenching rate by iodide anion was roughly four orders of magnitude slower ($5.9 \pm 0.7 \times 10^5$ $M^{-1}s^{-1}$ vs. $1.0 \pm 0.2 \times 10^9$ $M^{-1}s^{-1}$). As the iodide quenching rate constant was similar to that observed for oxygen quenching of the triplet excited **28** within the OA **2** dimer,[38] this suggested a similar mode of action, namely, a partial opening of the capsular complex allowing small guest entry and egress.

Measurements of the fluorescent intensity change of the complex as a function of added OA **2** were carried out and the observed trend fitted the expected 2:1 binding isotherm with an overall β_{21} of 3.2×10^{12} M^{-2}. Subsequent stopped-flow experiments successfully probed Eq. 1 (Figure 10), and identified a fast reaction for the formation of the 1:1 complex with a K_{11} value of $K_1 = (4.5 \pm 0.6) \times 10^5$ M^{-1}. Hence a K_{21} value of $K_{21} = (7 \pm 1) \times 10^6$ M^{-1} could be calculated (Eq. 4). The K_{11} and K_{21} values represented the first view of the difference between forming a 1:1 complex (desolvating half the guest and the pocket) and capping this complex (desolvating half the guest a pocket, and the two rims of the subunits). This clamping down of the two hemispheres in the second step leads to an association constant K_{21} one order of magnitude larger than the formation of the 1:1 complex, and is why K_{11} of the transient 1:1 complex could only be determined from kinetic experiments.

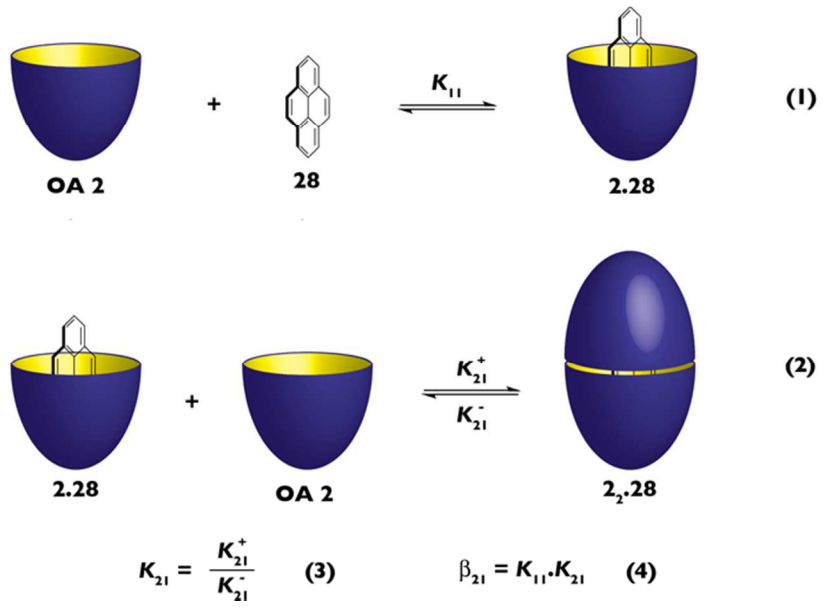

Figure 10: Assembly States and kinetic parameters for the complex formed between OA **2** and pyrene **28**.

The lifetime of the capsular complex encapsulating **28** was also determined in this study. Thus the k_{21}^+ and k_{21}^- values ($(2.6 \pm 0.2) \times 10^6$ M^{-1} s^{-1} and 0.37 ± 0.06 s^{-1} respectively) were obtained from global fitting of the slow change in fluorescence intensity attributed to the second step of the assembly (Eq. 2), and how this was modulated as a function of OA **2**. This gave a lifetime for the $\mathbf{2}_2$.**28** complex of 2.7 s. While the aforementioned entrance/egress of small molecules occurred on the microsecond timescale, these results suggest that for the complex with **28** the 'breathing' of the complex was on the order of 10^5 times faster than the release of **28**.

e) Movement of Internalized Guests and Guest Packing Motifs

The shape of guests such as steroids forces them to bind along the long Y-axis of the capsule (Figure 11).[17] Whilst their rigidity precludes their rotation around the X or Z axes of the capsule, even such rigid guests are capable of rotation around their Y-axis. The net effect of this movement is that by NMR the two hemispheres of the capsule are non-equivalent but each maintains its C_4 symmetry. In contrast, although flexible and highly mobile guests such as ethylene glycol monononyl ether **23** have been shown to bind in a similar pole-to-pole manner (Figure 11), the two hemispheres of the capsule appear equivalent because on the NMR timescale the guest can freely tumble around the X or Z-axis of the container.[32]

In an effort to gain a better understanding of the mobility of molecules within the capsule formed by OA **2**, the Turro and Ramamurthy groups used a combination of NMR and EPR experiments to analyze the movement of encapsulated guests within different complexes.[42] Their approach was to classify guests according to whether not they were capable of rotation around their X or Z axis, and if so, the temperature required to do so and whether or not the rotation was faster or slower than the NMR timescale. The ^{1}H and NOESY NMR data gathered in this study indicates that as in the case of ethylene glycol monononyl ether **23**, the NMR spectra of complexes of guests such as 1-methyl-4-(octyloxy)benzene **32** (Figure 11) show the two capsule hemispheres to be equivalent. Furthermore, the data also showed that the guest rotation around the X or Z axis needed to induce this equivalence did not involve disassembly/reassembly of the capsule. In addition, the accompanying EPR studies revealed that, as the guest was increased in length so the rate of rotation around the Y-axis decreased.

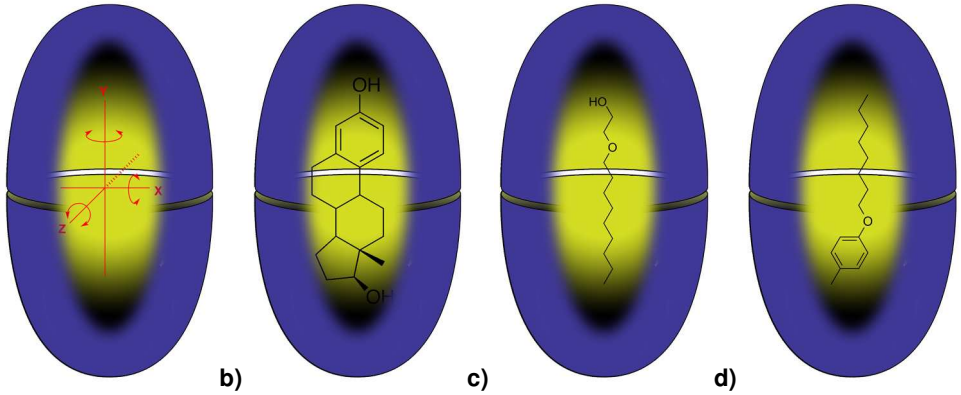

Figure 11: a) Axes within the capsule; b)-d) Encapsulated guests illustrating predominant packing motif: b) Estradiol **15**; c) Ethylene glycol monononyl ether **23**; d) 1-methyl-4-(octyloxy)benzene **32.**

Although not specifically discussed in Section 2.1.1.c, the binding of *n*-alkanes from C_5 to C_{17} inside the dimer formed by OA **2** gave valuable early information about how guests pack within the capsule.[31] Thus, ^{1}H NMR investigations focusing on the spectral difference between the free and the bound state of the guest revealed pole-to-pole guest binding. Because of the tapering nature of these deep-cavity cavitands, a general rule is that the more deeply an atom resides in a host the more it is upfield shifted relative to the free state. Most simply put, at the base of the pocket the aromatic walls of the host are closest together and therefore exert the largest shift in the NMR signals of atoms located there. In contrast, at the equator the greater separation of the aromatic rings results in smaller upfield shifts. Hence an evaluation of the $\Delta\delta$ value of the free versus bound signals from the guest gives valuable information about the time-averaged guest-packing motif within the host dimer. For all the *n*-alkane guests examined it was the terminal methyl groups that displayed the largest $\Delta\delta$ value, with upfield shifts as high as -3.15 ppm in the case of C_{12}. In contrast the guest protons midway along the alkane chain were the least shifted, indicating they reside near the equatorial region of the capsule.

Space-filling models illustrate that C_{12} is just slightly longer than the Y-axis of the capsule and can therefore occupy the cavity in an essentially fully extended conformation (Figure 12a). Guests longer than this must however compress somewhat to be accommodated. Do these compressed guests adopt any distinct form? NOESY and COSY NMR experiments were also utilized to elucidate the conformational preferences of these guests, and the former revealed stronger NOE C_i–C_{i+1} and C_i–C_{i+2} correlations between the terminal methyl groups and the penultimate methylenes than for the methylenes at the center of the cavity. In addition, C_i–C_{i+3} and C_i–C_{i+4} were also observed with the longer guests. As with previous work from the Rebek group,[43] the inference from this data was that guests such as C_{14} adopt helical conformations within the cavity of the OA **2** dimer (Figure 12b). Models demonstrate that the helical motif allows both for maximal C–H···π interactions with the cavitand walls and for maximal packing within the cavity; two factors that counter the strain of contiguous *gauche* dihedrals down the length of the chain.

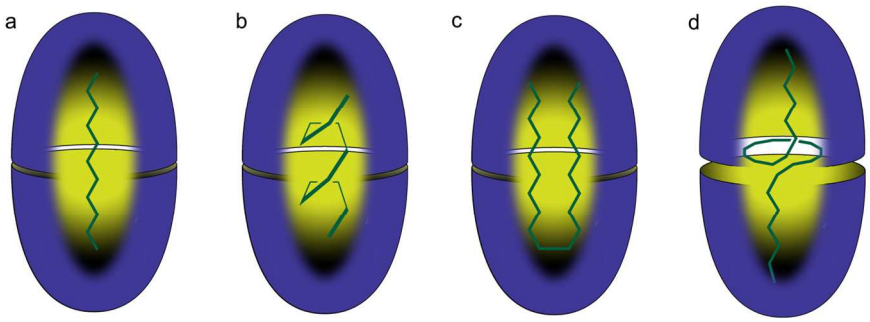

Figure 12: Schematic representations of observed binding motifs within deep-cavity cavitand hosts.

Two recent papers have demonstrated that other motifs are also possible. In the first, the Prabhakar and Ramamurthy groups examined the binding of phenyl-substituted hydrocarbons (Figure 13) to the capsule formed by OA **2** using a combination of NMR and molecular dynamics (MD) simulations.[44]

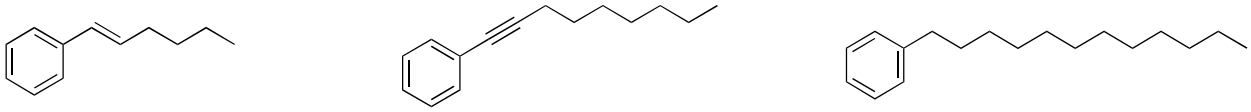

33 **34** **35**

Figure 13: Guests for probing conformational preferences within the dimer of OA **2**.

As expected, small guests such as **33** were found to pack the cavity in an essentially fully extended manner, with the phenyl group in one hemisphere and the methyl binding to the polar region of the other. The case of **34** is very similar, but being 4 Å longer the guest must adopt a slightly compressed motif and its movement within the cavity is restricted. At room temperature the guest signals are broadened somewhat, but these are seen to sharpen as the temperature is increased. For the longer guests examined, e.g., **35**, both NMR and the MD simulations demonstrate that these molecules are forced to fold into J- or U-shaped motifs. Such motifs are frequently observed in fatty acids bound to fatty acid binding proteins,[45] and have also been observed with similar guests binding to cucurbiturils.[46] Overall, it was noted that the inclusion of saturation in the hydrocarbon sidechain has a pronounced effect on the conformational options available to the guest. In passing, it is perhaps worth noting that these J- and U-motifs suggest a mechanism by which the ends of very flexible guests (e.g., Figure 12c and 12d) can exchange hemispheres without complex disassembly.

The second paper in question reveals a further packing motif. This study concerned a combined study of long *n*-alkanes within the capsule formed by OA **2** and the hexalenediamine-linked dimer (HOA) **36**.

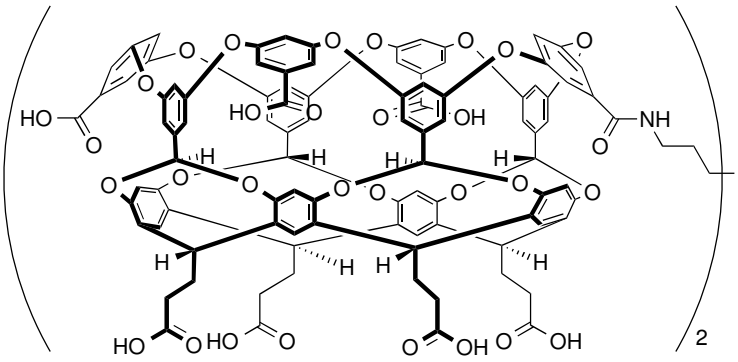

36

This covalently-linked dimer of OA was readily synthesized by taking advantage of a modification to the esterification of OA **2** (Scheme 1) that gave a high yield of the corresponding hepta-ester with one free carboxylate group at the rim of the cavitand. Two equivalents of the hepta-ester were then covalently linked using 1,6-hexanediamine and HBTU as a coupling agent to give the corresponding tetradeca-ester, subsequent hydrolysis of which gave HOA **36**. [47]

The covalent linking of OA **2** in this manner results in a host with quite different assembly modes and subtle differences in guest packing. Regarding the former, the possible complexes/assembly products pertinent to this discussion are: the open 1:2 host-guest complex; the 1:1 capsular complex; the 2:2 bis-capsule complex; and the 2:2 capsular complex (Scheme 4). The 2:2 bis-capsule complex possesses two essentially independent inner volumes, whereas the 2:2 capsular complex possesses a single inner space more capacious than the 2:2 bis-capsule complex because the internal volume is comprised of the binding pockets of four cavitands plus a central, pseudo tetrahedral space, defined by the four cavitands.

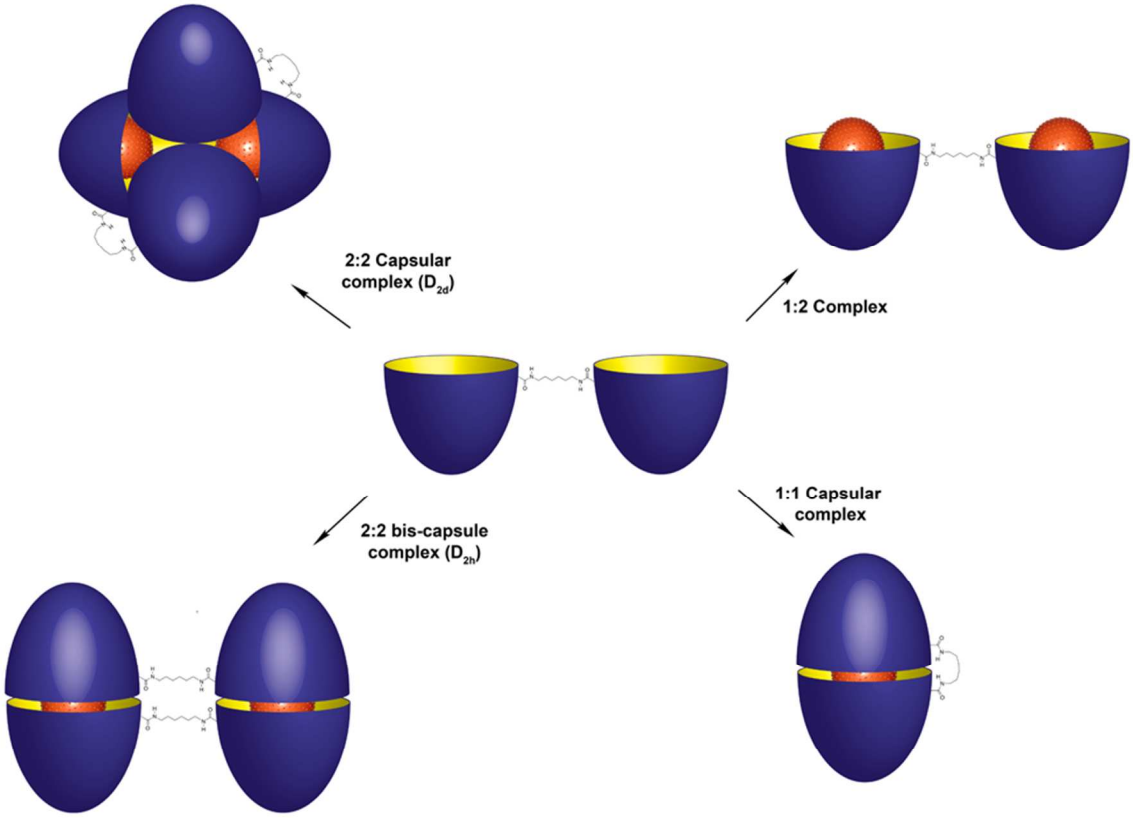

Scheme 4: Assemblies of HOA **36**.

As extensive NMR analysis reveals OA **2** and HOA **36** have quite different properties. Earlier work had reported that for *n*-alkanes the guest-size limit of OA **2** was C_{17},[31] but this proved to be largely the result of poor solubility and poor uptake and not a limiting factor of the host itself. Thus, in this more recent report a combination of heating and sonication allowed encapsulation of guests inside of the OA **2** dimer as large as *n*-hexacosane (C_{26}). As noted previously, guests up to twelve carbon atoms (dodecane) adopt extended motifs with contiguous *anti* dihedral angles, whereas longer guests adopt a more compressed motif. These E/C (extended/compressed) motifs cannot be readily distinguished by NMR, although helical motifs (Figure 12b) can.

For alkane guests exceeding eighteen carbon atoms (*n*-octadecane) it is not possible to pack OA **2** in either of these motifs. Instead, NMR demonstrates that guests such as *n*-eicosane (C_{20}) pack the cavity by adopting a U-shaped motif (Figure 12c). This motif holds true for guests up to *n*-tricosane, however the largest guests seen to unequivocally bind to the capsule formed by OA **2** (C_{24} to C_{26}) cannot adopt this U-shape. Instead, for these guests the motif appears to be akin to a spinning-top (Figure 12d) whereby the two terminal ends of the alkane chain are

nestled in the poles of each cavitand and the central portion of the hydrophobic chain sandwiched between the two aromatic rims of the host.

HOA **36** was found to form a 1:1 capsular complex in the presence of short *n*-alkanes (C_6, C_8 and C_{10}) as well as *n*-hexadecane (C_{16}), and in each case the packing motif of the guest was as is observed with OA **2**. However packing of alkane chains with eighteen to twenty-three carbons displayed very different binding profiles, while packing of guests with more than twenty-three carbons did not occur as the linker prevented sufficient separation of the two hemispheres of HOA **36** to allow the guest to adopt the spinning-top motif.

For the longer alkanes (C_{18} to C_{23}), NMR experiments revealed two complexes for each guest: one with a lower energy E/C conformation and one with a higher energy U-shaped motif. Unusually, as the guest size was increased so the amount of the lower energy E/C motif increased. PGSE NMR unraveled this conundrum. Whereas the diffusion constants for the complexes with the U-shaped motif were the same as for the 1:1 complex between HOA **33** and *n*-dodecane C_{12} (D = 1.31 × 10^{-6} cm^2 s^{-1}), the complexes with the E/C motif had significantly smaller diffusion rates (D = 0.95 × 10^{-6} cm^2 s^{-1}) corresponding to a dimer host structure. Although it was not possible to unequivocally differentiate between the 2:2 bis-capsule complex and the 2:2 capsular complex (Scheme 4), the ^{1}H NMR data supported the latter. Furthermore, as the 2:2 capsular complex is necessarily more capacious than the 2:2 bis-capsule complex, this assumption fits with the guest motif changing to a more relaxed E/C motif as the guest size increases. In summary, whereas OA **2** accommodates very large guests by adopting a high energy spinning-top motif (the motif of last resort), HOA **36** accommodates such guests by switching from a 1:1 capsular complex to a more voluminous 2:2 capsular complex.

We complete this section by noting that it is not just highly flexible guests than can be persuaded to adopt unusual conformations or motifs within the confines of these supramolecular capsules. For example, a comprehensive NMR examination of piperidine derivatives **37**-**41** (Figure 14) revealed that the conformational preferences of **37**, and **39**-**41** within the capsule formed by OA **2** were similar to that seen in solutions; these guests adopt a conformation in which the OR group is exclusively equatorial.[48] On the other hand, when **38** is encapsulated within the OA **2** dimer it adopts a 53:47 mixture of the equatorial and axial conformers that interconvert slowly on the NMR timescale. Apparently, the *n*-Pr group is just the right size to reduce the energy difference between the more stable equatorial conformer and the axial form, where as an ethyl group is too small and a *n*-butyl group too big. Such precise control of one molecule in a homologous series suggests interesting possibilities vis-à-vis reaction control (see Section 2.1.2.b).

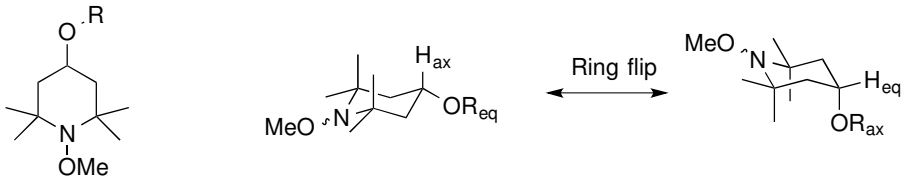

37: R = Et
38: R = *n*-Pr
39: R = *n*-Bu
40: R = *n*-pentyl
41: R = *n*-hexyl

Figure 14: Piperidine guests encapsulated within the OA **2** dimer, and their conformational options.

f) Communication through the Capsule

As has been reviewed, when a guest is bound inside the dimer formed by OA **2** it is not completely isolated from the bulk. Thus even during occupancy, guests can be exposed to small co-guests such as molecular oxygen via capsule 'breathing'. Furthermore, as we highlight in this section, direct communication between bound guests and the bulk is also possible through the walls of the host.

The communication between molecules entrapped within the OA **2** dimer and molecules in free solution has been extensively investigated. As detailed below, to date the following systems have been explored: 1) confined excited singlet or triplet donors and a free acceptor (respectively singlet-singlet and triplet-triplet energy transfers); 2) a confined radical and one free in the bulk (spin-spin exchange); 3) an encapsulated, excited molecule and a radical in free solution; 4) internalized fluorescence resonance energy donors and external acceptors (FRET), and; 5) confined electron donors and free acceptors (electron transfer).

The Turro group has led investigations into the ability of guests inside the capsule to 'communicate' through the walls of the host with guests in bulk solution.[49] The first example of communication involved a superexchange process whereby the orbitals of a guest nitroxide interact with those of a nitroxide solute in free solution through the bond orbitals of the host. The guests utilized for this study were **42** and **43** (Figure 15). Encapsulation of paramagnetic guest ^{14}N labeled **42** inside the capsule lead to broadening of the ^{1}H NMR spectrum of the complex. Although this is good evidence of complex formation, conformation of guest internalization was sought using ^{14}N labeled diamagnetic guest **43**. This similarly sized molecule resulted in a 2:1 host-guest complex that was readily characterized by ^{1}H NMR. Subsequent analysis of the Electron Paramagnetic Resonance (EPR) rotational correlation times and hyperfine coupling constants for the complex between OA **2** dimer and the ^{14}N labeled **42** confirmed encapsulation.

As anticipated by the researchers, EPR studies of the capsular complex of diamagnetic ^{14}N guest **43** demonstrated that positively charged ^{14}N labeled solute **44** bound to the outside of the capsule, but the negatively charged **45** did not. Furthermore, using the capsular complex containing the ^{15}N paramagnetic guest **42**, EPR demonstrated a strong electron spin-electron spin interaction between the encapsulated guest and the cationic ^{14}N solute **44**. As expected however, the same experiment using the anionic ^{14}N solute **45** indicated no interaction with the anionic capsular complex.

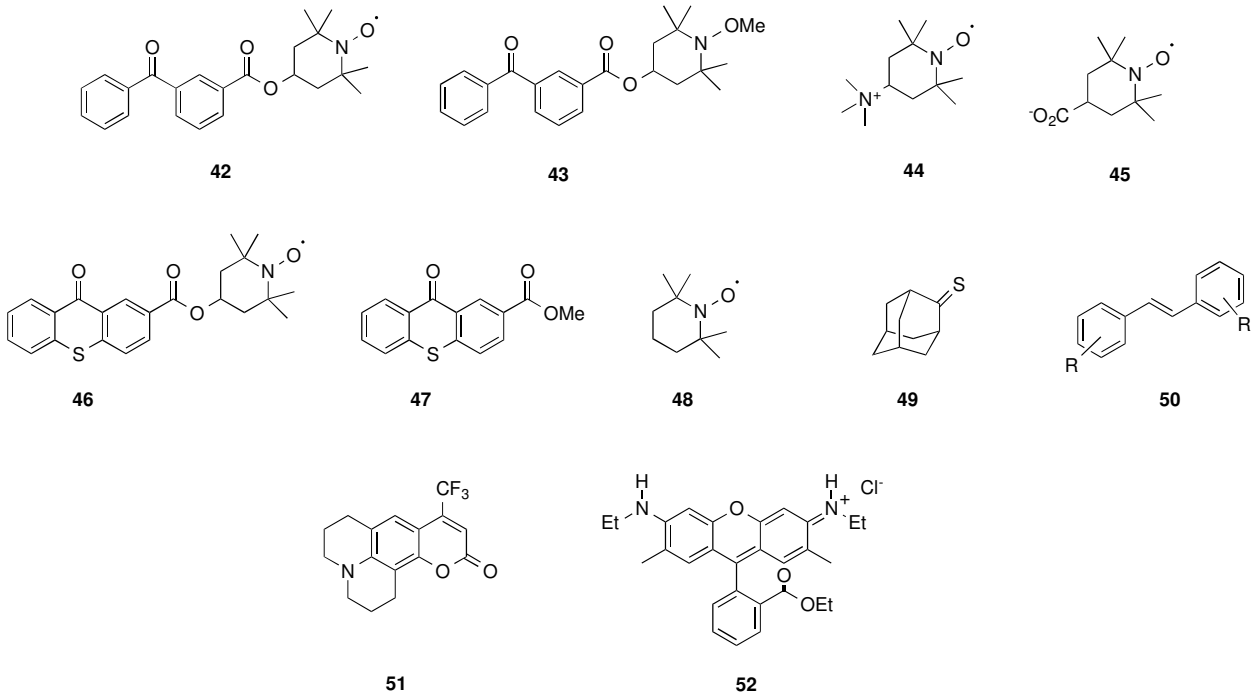

Figure 15: Guests and solutes used by the Turro and Ramamurthy groups to explore through-the-wall communication in the OA **2** dimer.

Building on this steady-state EPR work, the Turro and Ramamurthy groups used time-resolved EPR to gain a better understanding of superexchange between an encapsulated guest and a solute.[50] Key to this work was the encapsulation complex formed between ^{15}N thioxanthone guest **46** (Figure 15) and the dimeric capsule formed by OA **2**. Steady state EPR spectroscopy demonstrated that encapsulated ^{15}N **46** possessed the expected increased rotational correlation time and decreased hyperfine coupling constant (relative to free solution) indicative of restricted motion within a non-polar environment. Separately, transient triplet-triplet absorption measurements upon ^{14}N **46** and **47** in acetonitrile revealed that upon irradiation at 355 nm their thioxanthone moieties were readily excited to the triplet state, but that in this case

of ^{14}N **46** this was rapidly quenched by the adjacent nitroxide. Furthermore, time-resolved EPR of ^{14}N **46** in acetonitrile (355 nm, 5 ns) demonstrated that during this quenching process the spin-polarized triplet states of the thioxanthone moiety transferred their spin polarization to the nitroxide. A similar time-resolved EPR experiment with ^{15}N guest **46** encapsulated within the OA **2** dimer revealed the same phenomenon, but that confinement resulted in a longer spin polarization lifetime for the nitroxide. Following this, an analogous experiment but with the addition of ^{14}N solute **44** in bulk solution demonstrated that spin polarization of the incarcerated guest could be transferred to the cationic solute. Thus the time-resolved EPR kinetic traces of spin polarization for both the ^{15}N guest **46** and the ^{14}N solute **44** revealed a reduced lifetime of the former, and a delayed rise-time of the spin polarization of the latter. That association with the outside of the capsule is key was demonstrated in two ways: by the addition of cucurbit[8]uril that strongly sequesters **44**, or by using anionic guest **45** that is repelled from the surface of the host. In both cases no superexchange between encapsulated guest and solute occurred. As excited thioxanthone **47** and benzil **30** (Figure 9) guests led to opposite signs of spin polarization of nitroxides, it was concluded that the principle mechanism for the formation of polarized nitroxides involved the electron spin polarization transfer mechanism.[51]

A different viewpoint on the barrier engendered by the wall of the capsule formed by OA was obtained by examining the communication (exited spin state-radical spin transfer) between solutes **44**, **45** and **48**, and a range of eight internalized guests including benzil **30** (Figure 9), thione **49**, and stilbene **50** (R = 4-Me, Figure 15). The cationic, anionic and neutral states of the nitroxide radicals **44**, **45** and **48** allowed control of the lifetime of the solute-capsule encounter complex, and in the case of the cationic solute **44** NMR signal relaxation times suggested that it specifically associates at the equator of the capsule. These results also suggested that **48** has no specific interaction with the capsule, whilst not unexpectedly **45** is repelled from it. Although the guests examined formed both 2:2 and 2:1 host-guest complexes and formed a range of excited states, quenching of the excited, entrapped guest by the nitroxide solute **44** revealed only two distinct systems: 1) triplet states that are quenched dynamically by cationic nitroxide **44**; 2) triplet and excited singlet states that are quenched via a static process. Moreover, the decay curves and lifetimes of the encapsulated, excited state guests revealed that regardless of the lifetime of the former, they are quenched with almost identical rate constants. In contrast the latter group all have short (< 5 μs) lifetimes. *En masse*, a detailed analysis of these results supported the hypothesis that if a guest relaxed more slowly than 5 μs then its relaxation is controlled by through the wall quenching as a result of diffusion controlled encounter complexes,

whereas guests with lifetimes shorter than 5 μs undergo static relaxation in the cavity of the capsule.

As an alternative to this short range (Dexter type) superexchange, the Ramamurthy group have used femtosecond (fs) up-conversion to study longer range Förster resonance energy transfers (FRET) between an encapsulated donor and an cationic acceptor associating with the outer surface of the OA **2** capsule.[52] In these experiments the (bound) donors were coumarin dyes such as **51**, whilst the acceptor in free solution was Rhodamine 6G **52** (Figure 15). A combination of steady-state fluorescence and ^{1}H NMR confirmed that the different donors examined were bound within the dry interior of the capsule, whilst fluorescence, ^{1}H, and diffusion NMR spectroscopies revealed that the cationic acceptor had an affinity for the outside of the negatively charged capsule.

The accompanying time-resolved fluorescence studies involving the encapsulated coumarin dye and the externally bound **52** revealed a rapid decay of the excited state of the donor. This was attributed to an ultrafast FRET process arising from the close proximity of donor and acceptor; a hypothesis that was confirmed by the rapid rise on the acceptor emission observed in a fs up-conversion experiment. Calculations from these studies suggested that the donor-acceptor distance in these systems was a mere 13 Å.

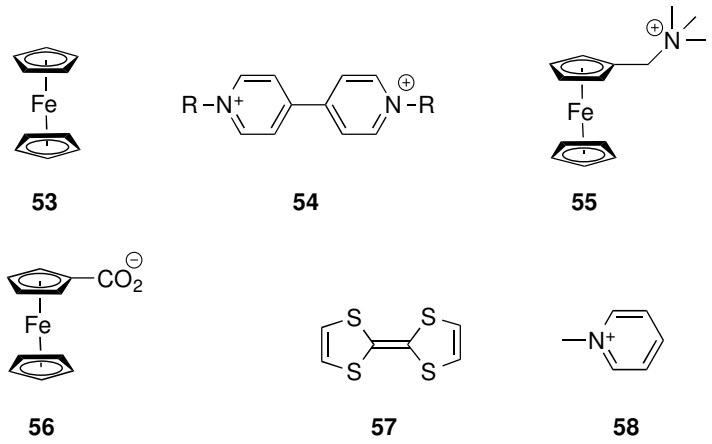

53 **54** **55**

56 **57** **58**

Figure 16: Guests and solutes used to study electron transfer through the walls of the OA **2** capsule.

It is not only spin and energy that can be transferred through the walls of the capsule formed by OA **2**; electron transfer is also possible. In a step towards this, the Kaifer group examined the properties of encapsulated ferrocene **53** (Figure 16).[53] A combination of ^{1}H and PGSE NMR experiments demonstrated that **53** formed a 2:1 host-guest complex with OA **2**. Neither cyclic voltammetry (CV) nor square-wave voltammetry (SWV) detected any faradaic

response from the encapsulated **53**, and a series of experiments varying the host-guest ratio indicate that inside the OA **2** dimer the guest does not give rise to a measurable current–potential response.

Whereas ferrocene **53** is strongly bound within the host capsule, ^{1}H and PGSE NMR clearly showed that methyl, ethyl, and *n*-butyl viologen **54** (R = Me, Et and *n*-Bu respectively) bind to the exterior of empty OA **2** dimer. Indeed, two molecules of viologen bind to this empty capsule, suggesting that the four carboxylates at each pole are the viologen-specific binding site. That noted, this was the first example of an empty capsule formed by OA **2**; all work prior, and the vast majority of subsequent work, demonstrates that an internalized guest is required for capsule formation. These facts suggest that there is also likely association of the viologens with the equatorial carboxylates of the capsule that helps to hold the empty capsule together.

CV studies of viologens **54** associated with OA **2** demonstrate the two expected reduction steps (to radical cation and then to the neutral), but with substantially reduced current levels. Furthermore, these studies revealed that the host stabilized both the reduced forms; particularly the first (cationic) reduction product. Furthermore, the rates of heterogeneous electron transfer for the viologens associated with the OA **2** dimer were significantly attenuated relative to free solution. This was attributed to the association between the anionic poles of the OA **2** capsule and the viologen increasing the average distance of maximum approach between the viologen center and the electrode surface.

Subsequently it was shown that the capsule formed by the dimerization of OA **2** around ferrocene **53** could also (externally) bind ethyl viologen (**54**, R = Et) to form the corresponding quinternary complex.

The Kiafer group subsequently built on this work by demonstrating cationic ferrocene derivative **55** (Figure 16) associates strongly with the outer surface of the OA **2** capsule containing ferrocene **53**, and that this quaternary complex can undergo a homogeneous electron transfer process.[54] PGSE NMR confirmed the quaternary complex, yielding very similar diffusion coefficients from signals corresponding to the capsular complex and **55**. A similar situation was obtained if (*E*)-stilbene (**50**, R = H) replaced the internalized guest **50.**

When the voltammetric behavior of the quaternary assembly was investigated with the encapsulated stilbene, the current levels were depressed relative to **55** alone. However, when stilbene was replaced by guest **53** a number of changes to the cyclic voltammogram were observed. On the forward scan, there was no faradaic response detected where **53** would be directly oxidized, but the oxidation of **55** was observed, albeit at higher current levels than expected. Furthermore, on the reverse scan, two peaks were observed: one corresponding to

the reduction of the ferrocenium form of **55**, and a second corresponding to the reduction of ferrocenium form of **53**. The results demonstrate that once oxidized, the ferrocenium form of **55** accepts an electron from the internalized **53,** to generate the cation (ferrocenium) form **53** inside the capsule. However, this guest is a poor one and it is released to bulk solution. This process was fully reversible and so the OA **2** capsule containing **53** was again formed upon reduction. Control experiments were also carried out with **56**. In this instance, there were no changes in the CV response in the presence of the OA **2** dimer encapsulating either (*E*)-stilbene **50** (R = H) or **53**. Furthermore, the complex of **55** with cucurbit[7]uril was determined to be a poor promoter of the electron transfer process in the system where **55** needs to associate with the outer walls of the OA **2** dimer. Clearly, there must be close association between the internalized and external ferrocene derivatives for electron transfer to occur.

A second example of redox-controlled capsular assembly/disassembly from the Kaifer group focused on tetrathiafulvalene (TTF) **57** (Figure 16) encapsulated inside the OA **2** dimer.[55] As anticipated, ^{1}H and PGSE NMR demonstrated that **57** formed the corresponding 2:1 complex. These studies were performed at 1 mM concentrations, and therefore the complex represents a much higher concentration of **57** 'in water' than is usually possible.

Tetrathiafulvalene **57** and its derivatives undergo two consecutive one-electron oxidations to first generate the corresponding radical cation and eventually the dication form at more positive potentials. However the first oxidation is usually poorly developed in water because of the low solubility of **57**.

The electrochemical behavior of this OA **2** dimer complex containing **57** was analyzed by both CV and SWV. In the absence of OA **2**, two shallow waves at +0.18 V and +0.48 V were observed in the forward scan of the cyclic voltammogram, and no peaks were apparent on the reverse scan. This is consistent with the behavior of **57** in aqueous solution. However, in the presence of two equivalents of OA **2**, the small initial current corresponding to the first oxidation step disappeared entirely and there was a well-developed peak corresponding to the second oxidation process at +0.56 V. In the reverse scan only one small wave was observed corresponding to the second reduction to regenerate neutral **57**. The SWV trace confirmed the hindered voltammetric response associated with encapsulated **57**, which was attributed to the increased distance between it (versus free TTF) and the electrode surface. In contrast, the well-developed second oxidation process was attributed to the release of the cationic form of **57**. The solitary, small peak observed in the reverse process was attributed to the dicationic form of **54** being unstable under basic conditions. Larger tetrathiafulvalene derivatives were also examined in this study, but they were found to not bind to the host.

More recently, electron transfer across the walls of the OA **2** capsule has also been observed by the Ramamurthy group.[56] To demonstrate this, one donor-acceptor pair ideally suited to the capsule formed by OA **2** is 4,4'-dimethylstilbene **50** (R = 4-Me, Figure 15) and *N*-methyl pyridinium **58** or viologen **54** (R = Me, Figure 16). ^{1}H NMR demonstrated that electron donor **50** is strongly encapsulated within the capsule, whilst diffusion NMR revealed that both **54** (R = Me) and **58** associated with the exterior of the capsule via Coulombic forces. Fluorescence spectroscopic analysis of the titration of **54** or **58** into a solution of encapsulated **50** revealed that the pyridinium solutes statically quenched the fluorescence of the encapsulated guest. Laser flash photolysis pin-pointed the cause of this quenching, namely the transient formation of the radical cation of **50**. The presence of two transient absorptions (at 510 and > 700 nm) with identical decay kinetics suggested that the quenching was due to electron transfer from the singlet excited state of **50** to **54** or **58**. In the case of viologen **54** (R = Me) it was also possible to observe the mono-cation radical 'product' resulting from electron transfer. Further supporting electron transfer were similar fluorescence and transient absorption experiments in the presence of cucurbit[7]uril (CB7). CB7 is a strong binder of viologen **54** (R = Me), and consequently its addition restored fluorescence of the internalized **50**, and quenched the observed transient absorption. Laser flash photolysis also revealed that the lifetime of the radical cation of **50** was < 20 ns in the presence of **54** (R = Me) and 4.6 μs in the presence of **58**. This difference was attributed to the fact that the single electron reduction product of the latter is neutral but mono-cationic in the former, and that the mono-cation has a relatively strong affinity with the exterior of the capsule.

Building on this work, photo-induced electron transfer has been recently demonstrated using TiO_2 as an acceptor.[57] In this work, the encapsulated donors were a series of three coumarins including guest **29** (Figure 8) whilst for solution studies viologen **54** (R = Me) was again used as the acceptor that partitioned between bulk solution and the outer wall of the capsule. As anticipated, titration of the acceptor **54** (R = Me) into a solution of the capsular complex resulted in static quenching of the fluorescence of the donor **29**, but that fluorescence could be recovered by the addition of a strong binder of **54** (R = Me) such as CB7. With this knowledge in hand, the emersion of films of TiO_2 (and as a control ZrO_2 films) into solutions of the capsular complex lead to the complex adhering to the surface of the oxides (Fourier Transform, Infra-Red Attenuated Total Reflection spectroscopy, FT-IR-ATR). Furthermore, in the case of the large band-gap ZrO_2 film where electron transfer is not possible, fluorescence spectroscopy indicated that adherence to the surface did not induce capsular breakup and release of the coumarin. In contrast, adherence to the TiO_2 film resulted in full quenching of the

coumarin indicative of electron transfer. Finally, titration of TiO_2 into a solution of the capsular complex of OA **2** and the coumarins was achieved by using colloidal TiO_2. In this experiment the reduction in fluorescence suggested that quenching was again static rather than dynamic.

In a recent collaboration between the Burda and Ramamurthy groups the ultrafast electron transfer dynamics of these processes have been investigated using femtosecond laser spectroscopy.[58] In these studies coumarin-153 (**51**, Figure 15) was used as the encapsulated donor, whilst once more viologen **54** (R = Me) and *N*-methyl pyridinium **58** (Figure 16) served as the solute acceptors. The transient absorption spectra obtained using a 390 nm pump pulse confirmed the existence of the oxidized state of the internal excited guest and the reduced state of viologen **54** (R = Me) associating with the outside of the cavity. A kinetic analysis of the increase of the radical cation of **54** (R = Me) as a function of time, and the corresponding decay of the laser induced fluorescence of the excited donor **51**, gave time constants of $\tau = 20 \pm 1$ and 18 ± 2 ps respectively. Furthermore, the recombination kinetics were measured at $\tau = 724 \pm 38$ ps. These results were in sharp contrast with those obtained in free (30% aqueous acetonitrile) solution, where the electron transfer rate was much lower ($\tau = 631 \pm 50$ ps) and almost identical to the recombination rate.

2.1.2 Applications for Deep-Cavity Cavitands and their Assemblies

a) Novel Separations Strategies

The preferred encapsulation of one guest over another within the capsules – differential compartmentalization – offers many intriguing possibilities vis-à-vis molecular separations. Examples of both physical and chemical-based separations have been documented with the deep-cavity cavitands discussed here. With respect to the former, the Gibb group has reported on the separation of hydrocarbon gases using dimeric capsules formed by OA **2**.[21] This study demonstrated (^{1}H NMR) that when *n*-butane was added to the headspace above a buffered solution of OA **2**, the corresponding 2:2 capsular complex was formed in solution. Furthermore, these experiments revealed that it was possible to store *n*-butane as its 2:2 complex at ca. 200 times its nominal solubility in pure water. The actual physical limit of solubility of this complex may be even higher than this as it was viscosity issues with the chosen sodium tetraborate buffer that restricted NMR analysis. NMR was also used to determine the stability of the 2:2 host-butane complex. As it was not possible to differentiate between the free host and guest and their 1:1 complex, an apparent K value was defined as: $K_{app} = [H_2G_2]/[H_a][G_a]$, with $[H_a] = [H_{free} + HG]$ and $[G_a]\ ) = [G_{free} + HG]$. Values for K_{app} ranged from 1,400 M^{-1} in simple buffer solution to 1×10^6 M^{-1} in 14 mM NaCl. A subsequent competition experiment between propane

and *n*-butane demonstrated that the latter bound an order of magnitude more strongly (K_{rel} = 12), and this led to an investigation to determine whether or not the two gases could be separated. This was indeed the case. Thus, when the head-space above a solution of OA **2** was filled with a 1:1 mixture of propane and *n*-butane, only the latter was complexed leaving a propane-enriched gas-phase in the head space.

The Gibb group has also demonstrated an example of a chemical separation using these types of supramolecular capsules.[59] The focus of this report was on the supramolecular protection of molecules from reactive (hydrolytic) media. More specifically, pairs of difficult to separate, constitutionally isomeric esters were examined in basic media. The idea behind this work was that one guest would be preferentially bound to the capsule formed from OA **2**, leaving the other molecule of the pair to reside in solution and undergo hydrolysis. Hence the supramolecular nanocapsules formed by OA **2** would bias the relative rates of ester hydrolysis and bring about kinetic resolution.[59] Two series of constitutional esters were examined: those composed of thirteen non-hydrogen atoms, and those composed of sixteen non-hydrogen atoms. The former were chosen in part because previously reported data[31] suggested that dodecane and tridecane optimally fill the cavitand by neither being too compressed or by having too much empty space. The latter were a test of what happens to a resolution at the limit of guest encapsulation. The obtained kinetic resolutions were highest with those composed of thirteen non-hydrogen atoms (Figure 17, **59**-**63**) and therefore are the primary focus of our discussion here.

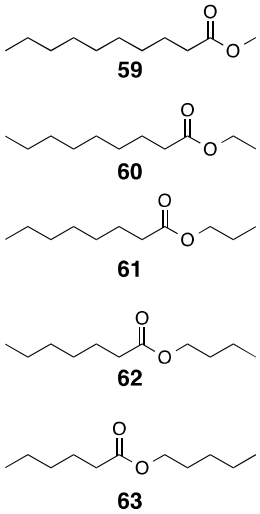

Figure 17: Constitutional isomeric esters for kinetic resolution.

The free esters were hydrolyzed in 3:7 acetone-d_6:D_2O containing 10 mM NaOH to obtain the pseudo first-order hydrolysis rates at room temperature. The methyl ester **59**, and to

a lesser extent the ethyl ester **60**, hydrolyzed slightly faster than the others, but the relative rate (k_{rel}) between the fastest (**59**) and slowest (**62** and **63**) was only three, i.e., insufficient for kinetic resolution in itself. ^{1}H NMR and COSY NMR were conducted to determine the goodness of the fit of the guests in the series, and all were found to form strong 2:1 complexes within the OA **2** dimer. The relative binding constants (K_{rel}) between all the esters were then determined, with the strongest and weakest binding guests found to be **59** and **61** respectively (K_{rel} for esters **59**-**63** were respectively: 165.4 1.8 1.0 10.7 16.4). Two key factors were concluded to influence binding. First, the relative position of the ester group within the cavity presents significant steric clash as it is moved closer to the end of the molecule and hence deeper into the pole-region of the capsule. Second, this steric clash is overcome by compensatory $-CH_3\cdots\pi$ interactions between the methyl of the guest and the walls of the host when the C–H bonds are more polarized by a proximal electronegative atom (the sp^3 O atom). Hence the methyl ester **59** binds strongest, the ethyl- and propyl-esters **60** and **61** the weakest, and the butyl and pentyl-esters **62** and **63** have intermediate affinity. It was noted in the corresponding experiments with the second set of esters that the range of binding affinities was essentially half that found in the first series, presumably because of increased steric strain in the more tightly packed cavity.

Competition experiments between pairs of esters were then carried out in the presence of the capsule formed by OA **2**. As it was noted for a complex of a single ester that even after one month ≤ 5% hydrolysis had occurred at room temperature, all competition experiments were carried out at 100°C. After cooling of each sample the extent of hydrolysis was determined by NMR. When pairs of esters were competed against each other it was determined that for esters with similar K_{rel} kinetic resolution was not possible, but for those with K_{rel} an order of magnitude or more different, fair to good kinetic resolution of isomers was observed. Larger K_{rel} differences still led to very good resolutions. Thus, the best resolution was determined between **59** (the strongest binder) and **61** (the weakest). In this case when all of the latter had reacted, 84% of the former still remained. Subsequent studies in the presence and absence of host indicated that although the rate-determining step in the hydrolysis of free ester is nucleophilic attack by hydroxide, this was not the case for the encapsulated ester where instead the rate-determining step was likely capsule opening. To test this, the authors added a stronger-binding, inert guest (*n*-dodecane, C_{12}) as they monitored the slow hydrolysis of **61**; almost immediately following injection the ester was displaced, and hydrolyzed within 10 minutes. Furthermore, using the projected kinetic data for hydrolysis of free ester at 100 ˚C (via Arrhenius plots), a model based on the notion that capsule opening was the rate-determining step fitted well with the kinetic traces of ester hydrolysis in the presence of a capsule. Overall, these studies demonstrated that

kinetic resolutions can be brought about via selective molecular protection; selective binding one of the reactive molecules biases reactions that, in the absence of the capsule, are otherwise very similar.

b) As Nano-Scale Reactors

As the last example of the previous section demonstrated, encapsulation can protect molecules from reactive external environments. The opposite of this strategy is to use the inner nano-space of capsules as yoctoliter (10^{-24} L) reaction vessels; a popular topic in supramolecular chemistry,[60] and one we discuss in this section.

The vast majority of chemical conversions carried out in the capsules discussed here involve OA **2** and photochemistry. A collaboration between the Gibb and Ramamurthy groups established the foundation for these studies, and from this the Ramamurthy group have built up a flourishing deep-cavity cavitand program within their field of expertise of studying photophysical and photochemical processes within confined media.

Arguably the most studied reaction within the capsule formed by OA has been the photolysis of dibenzyl ketone derivatives; a class of reaction that has shed much light on the ability of capsules formed by OA **2** to bring about unusual photochemical reactions. By way of example,[38] the photolysis of ketone **64** (Scheme 5) in aqueous solution gave, via homolytic cleavage of the C(O)-C bond and decarbonylation, products **65** (AA) **66** (AB) and **67** (BB) in the expected (statistical) 1:2:1 ratio. In contrast, irradiation of **64** encapsulated within the OA **2** dimer led to only type AB products because the radical formed from **64** are – in the timeframe of the photochemical conversion – trapped within the capsule. This exceedingly high (100%) cage effect had only previously been observed in the solid-state. More interestingly, the major products formed from encapsulated **64** were identified as rearrangement product **68** (44%), **66** (41%), and a mixture of various decarbonylated, ortho substituted derivatives such as **69** (15% combined yield). Compound **68** is believed to be formed (Figure 18) via cleavage of the C(O)-C bond, intersystem crossing from the triplet to the singlet radical pair, rapid reorientation of the unsubstituted benzyl radical, recombination and a 1,5 H-shift. Reorientation occurs because whereas the phenylacetyl radical is anchored in place by its *p*-methyl group, the benzyl radical isn't. Consequently, it rotates 180˚ relative to rest of the complex to better pack the cavity and place the benzyl group in the narrow region at the base of the nano-space. A hydrogen shift and recombination of the radicals gives product **68**.

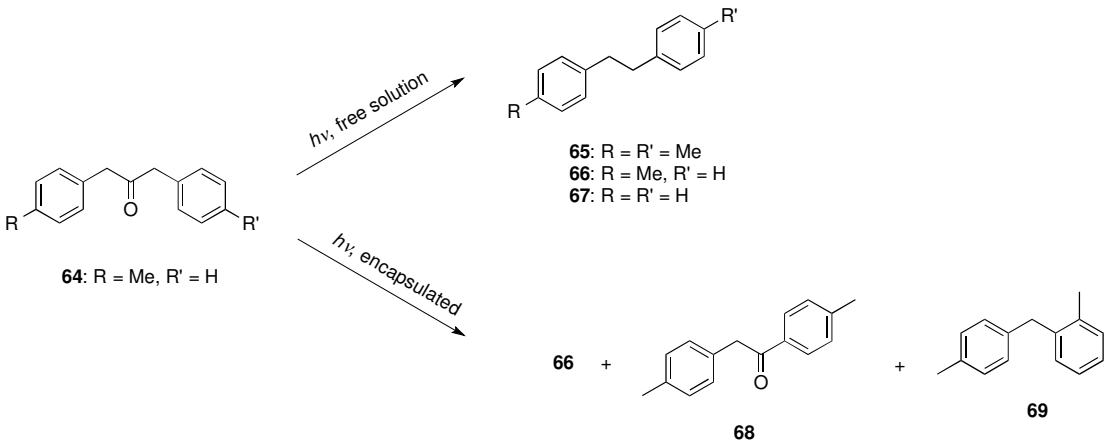

Scheme 5: Major photochemical products from the photolysis of **64** in free solution or encapsulated within the OA **2** dimer.

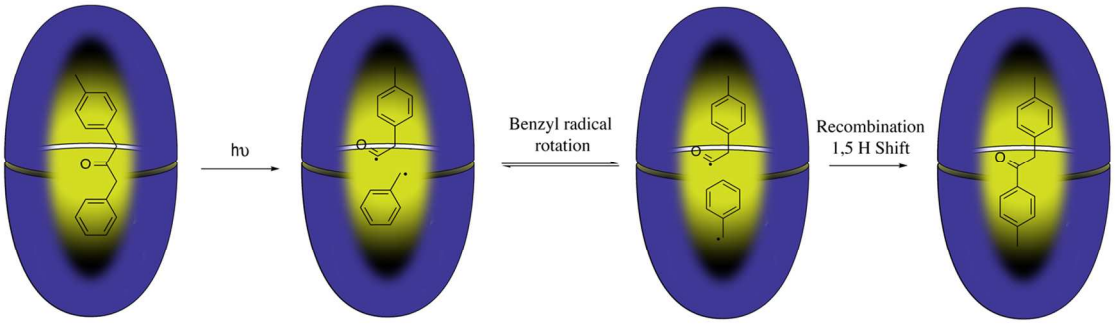

Figure 18: Schematic of the proposed mechanism for the formation of rearranged product **68**.

Extending this work, the Gibb and Ramamurthy groups examined α-(*n*-alkyl) dibenzyl ketones **70** (Scheme 6) where R varied from Me to n-octyl. Extensive NMR analysis including ^{1}H studies, diffusion, and 2D experiments revealed all guests formed 2:1 host-guest complexes with three distinct packing motifs depending on the R group of the guest. For the smaller R groups (R = Me, Et, *n*-Pr) it was found that each phenyl ring occupied the polar regions of the container whilst the R group occupied the equatorial region (Figure 19). In contrast, for mid-sized R groups (R = *n*-Bu *n*-pentyl and *n*-hexyl) it was found that one phenyl ring (distal to the R group) and the R group occupied the polar regions of the container and the proximal phenyl ring occupied the equatorial region. Finally, in the case of the largest R groups examined (R = *n*-heptyl and *n*-octyl) it was found that the guest packed the cavity such that the distal phenyl ring occupies the equatorial region of the capsule.

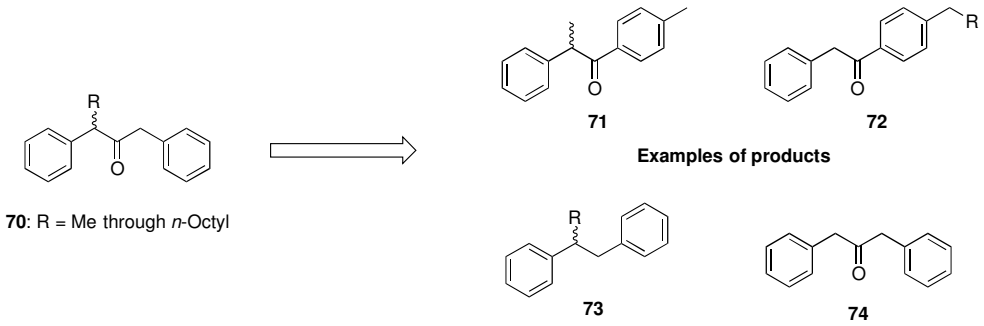

Scheme 6: Examples of photochemical products from the photolysis of **70** (R = various) encapsulated within the OA **2** dimer.

In hexane or buffer solution the majority of products from photolysis of these eight ketones arise via Norrish Type I mechanisms and indicate no cage effect. In contrast, photolysis within the capsule revealed again a 100% cage effect with only AB type products observed. Nevertheless, the relationship between the packing of the capsule and the outcome of photolysis was complex because of the multiple chemical channels in the triplet excited-state surface. Consequently, the guests examined yielded a considerable range of products arising from both Norrish Type I and Norrish Type II (Norrish-Yang) chemistry. Prominent examples include rearranged products **71**, **72** and decarbonylated product **73** via Norrish Type 1 mechanisms, and dealkylated (Norrish-Yang) products such as **74.**

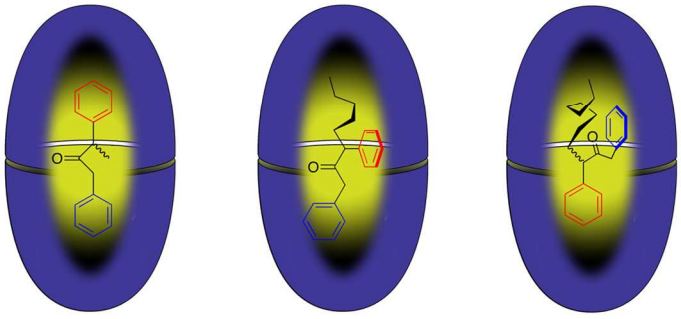

Figure 19: Packing motifs observed for the different guests within the OA **2** capsule.

Although overall many products were formed, the range of products from individual host-guest complexes was much narrower than in free solution and some general conclusions regarding packing and reactivity were possible. First, smaller R groups (R = Me, Et, and *n*-Pr) formed substantial amounts of rearranged product **72** and only trace amounts of the other rearranged product **71**. This was attributed to the faster cleavage of the more substituted C(O)-C bond of **70**, and the fact that the resulting substituted benzyl radicals from the three guests

were able to rotate in the cavity and generate **72**. On the other hand, midsized R groups (*n*-butyl and *n*-pentyl) give roughly equal amounts of both rearranged products **71** and **72**. Although the cleavage of the more substituted C(O)-C bond of **70** would be expected to the faster, apparently the reorientation of the resulting substituted benzyl radical is difficult. Consequently, via recombination of the initially formed phenacetyl and benzyl radicals, the slower cleaving C(O)-C bond that is the first step to product **72** effectively competes. Finally, the largest R groups (*n*-hexyl through *n*-octyl) gave the most Norish-Yang products such as **73**. This was attributed to two phenomena: 1) with little space in the cavity, Type I chemistry and rearrangement processes were disfavored; 2) The conformation preference (Figure 19) for these guests promotes γ-hydrogen abstraction and Type II chemistry.

A different perspective on this encapsulation chemistry was obtained with the series of dibenzyl ketones **75** (R = Et through *n*-hexyl, Scheme 7).[61] With **75**, the outcome of photolysis in hexanes (Scheme 7) is independent of the nature of the R group, with in all cases, a statistical mixture (1:2:1) of the AA, AB, and BB decarbonylated products **76**-**78**. In the case of the encapsulated reactions all the products were again of the AB type (100% cage effect), with the predominant products being **77**, **79**, **80** and **81**. In general, yields of **79** decreased and those of **77** increased as R increased in size, suggesting that with larger and larger R groups rotation of the intermediate benzyl radical became energetically more demanding and the decarbonylation pathway became more competitive. Yields of **80** and **81** were less dependent on the R group size, suggesting that the increase in yield of decarbonylated **77** is at the expense of rearrangement product **79**.

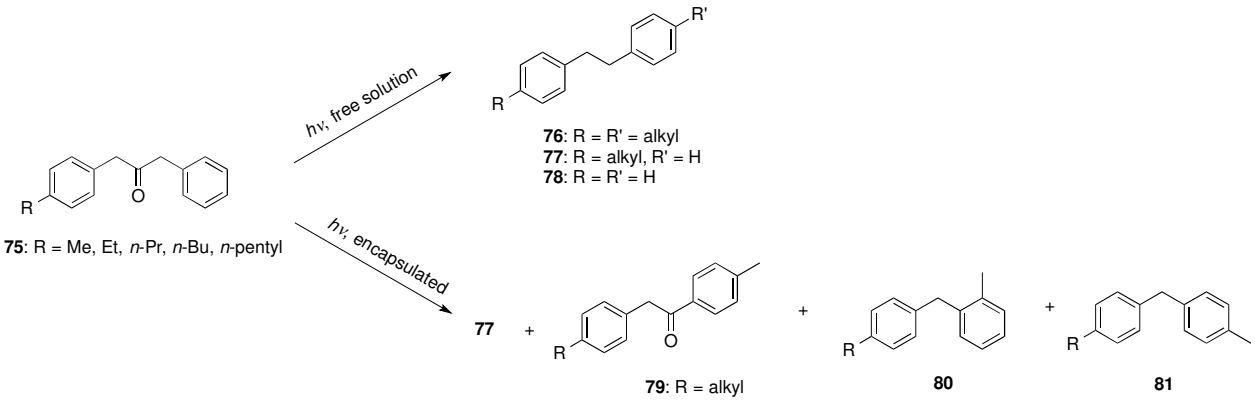

Scheme 7: Major photochemical products from the photolysis of **75** in free solution or encapsulated within the OA **2** dimer.

One question that the photolysis of these different type of dibenzylketones does not reveal is the extent of recombination of the phenylacetyl and benzyl radicals to regenerate the starting ketone (Figure18). To address this question a recent study examined the photolysis of optically pure α-deoxybenzoins (Scheme 8) encapsulated within the dimer capsule formed by OA **2**.[62] These guests can only undergo cleavage on one side of the carbonyl group, and so photolysis of these complexes forms a narrower range of products. With **82** (R = H) only Type I reactions are possible and the rearranged product **83** (R = H) was formed quantitatively. Guest **82** (R = Et) formed mostly **83** (R = Et), but also the Type II products **84** (R^1 = Me) and **85**. In contrast, guests **82** (R = *n*-pentyl and *n*-heptyl) gave no Type I products but only **84** (respectively R_1 = *n*-Bu and *n*-pentyl) and **85**. Equally important, in all cases if photolysis was kept to < 20% the recovered starting material was found to have undergone partial racemization; a phenomenon that necessitates the first step of the Type I mechanism, i.e., formation of the phenylacetyl benzyl radical pair. Two key observations were made from the data: 1) longer chain lengths led to reduced extents of racemization; 2) but even with guests **82** (R = *n*-pentyl and n-heptyl) which gave no Type I products, the first step of the Type I mechanisms is not suppressed. Overall these studies revealed that the reduction of free space in the complex with increasing R group significantly decreases the ability of the guest to undergo Type I chemistry and rearrangement (100% yield of **83** for **82** (R = H), 0% for **82** (R = *n*-pentyl and n-heptyl), but the effect of packing coefficient on the formation of the phenylacetyl/benzyl radical pair and subsequent racemization is much smaller (75:25 er versus 88:12 er for **82** (R = H and *n*-heptyl respectively). In other words, formation of the phenylacetyl benzyl radical pair occurs with all guests, but increasing packing coefficient has more of an effect on the rearrangement reaction to form **83** than on flipping of the benzyl radical necessary for racemization.

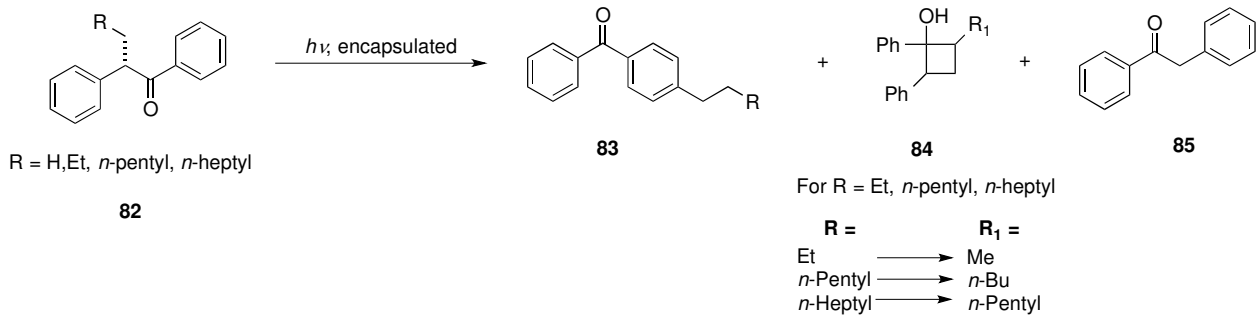

Scheme 8: Major photochemical products from the photolysis of **82** in free solution or encapsulated within the OA **2** dimer.

Studies of the photophysical and photochemical properties of encapsulated stilbenes also reveals that the cavity formed by the dimerization of OA **2** has a profound effect on encapsulated guest molecules.[63] In this work the authors examined a series of *cis*- and *trans*-methyl stilbenes (2-, 3- and 4-substituted) as well as dimethyl stilbenes (2,2'-, 3,3'-, and 4,4'-) **50**. (Figure 15). NMR studies demonstrated that both *cis*- and *trans*-stilbenes readily form 2:1 host-guest complexes, with the latter more efficiently filling the nano-space of the capsule. Furthermore, the NMR shift data between the free and the bound states suggested that it was the 4,4'-disubstituted stilbene that demonstrated the greatest difference between the *cis*- and *trans*-isomers; the more rotund form of the former guest only filled the 'equatorial' region of the capsule, whereas the shape of the latter was sufficient to more efficiently fill the bulk of the interior, and in particular, allow its two methyl groups to bind deeply into the narrow 'polar' regions of the nano-space.

Fluorescence studies revealed that the stilbenes displayed weak aggregate emission in free borate solution, but well-defined monomer emission when encapsulated. Furthermore, the singlet lifetime of all the disubstituted guests was longer than the corresponding values in hexanes solution (the corresponding lifetimes of the mono-substituted stilbenes were too short to measure).

Photochemical studies revealed that the 4,4'-dimethyl stilbene **50** (R = 4–Me) was unique among all the different isomers examined. Free in hexane solution or bound in the capsule, irradiation of the other isomers led to similar *cis*/*trans* ratios in the pseudo-photostationary states (Scheme 9). However, in the case of 4,4'-dimethyl stilbene **50** its pseudo-photostationary state in hexane was 18% *trans* and 76% *cis*, but (a more slowly attained) 85% *trans* and 15% *cis* in the capsule. Furthermore, whereas irradiation in hexane led to high yields of the corresponding phenanthrene **31**, only trace amounts of **31** formed over extended irradiation of the bound 4,4'-dimethyl stilbene **50**. These results demonstrated that the two methyl groups of the guest are uniquely positioned to anchor the two ends of the guest in the nano-space of the capsule, inhibiting the formation of the preferred *cis*-isomer and so preventing the formation of the expected phenanthrene **31**.

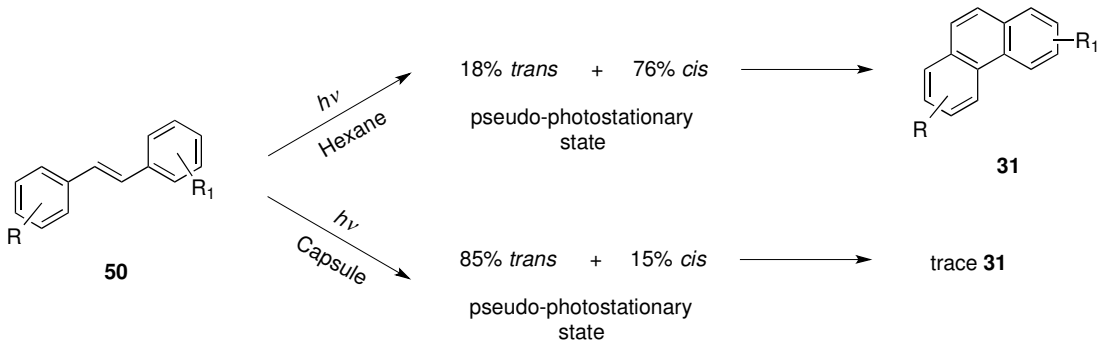

Scheme 9: Major photochemical products from the photolysis of **50** in free solution or encapsulated within the OA **2** dimer.

A recent related paper examined the photophysical and photochemical properties of an expanded array of encapsulated stilbene and stilbene-like guests molecules.[64] In this work, the photostationary states of the different guests were attained via a second OA **2** capsular complex containing a triplet sensitizer. A comparison of qualitative competition studies for the encapsulation of the different *cis*/*trans* isomers, with the photostationary state ratios obtained upon photolysis suggested that the latter is biased in the capsule by the relative binding affinities of the guests. Models explaining the mechanism by which energy is transferred from the encapsulated, excited donor and the encapsulated acceptor were discussed.

A number of other photochemical transformations have been investigated within the confines of the dimeric capsule formed by OA **2**. For example, the dimerization of acenaphthylene **86** in water gives 40% of the *syn*-dimer and 60% of the *anti* stereoisomer (Scheme 10). In the capsule however the *syn*-dimer is formed quantitatively.[65] Interestingly, when the water-soluble triplet sensitizer Eosin-Y is added to the reaction, in the case of free **86** the *syn*:*anti* ratio is 51:49, and in the case of the encapsulated **86** 60:40. The authors tentatively ascribe this increase in the yield of the *anti* isomer in the presence of Eosin-Y to the increase in the triplet lifetime of **86** in the presence of the sensitizer. As a result, the triplet state of **86** may be able to exit the cavity and undergo reaction in free solution. Building on this concept, the general ability of the OA **2** dimer to control photo-dimerization reactions has been illustrated with methyl cinnamates, *p*-methyl styrene, indene, and 4,4-dimethylcyclohex-2-enone.[66]

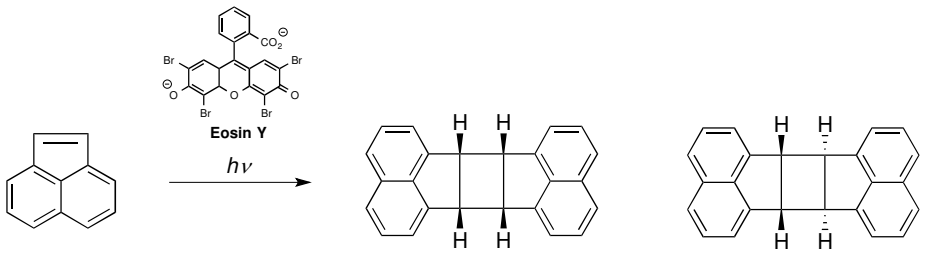

Scheme 10: Major photochemical products formed from **86** in free solution or encapsulated within the OA **2** dimer (see text).

The familiar Photo-Fries reaction has also been studied within the confines of the dimer capsule of OA **2**.[67] In organic solvents the Photo-Fries reaction can produce a bewildering array of products. For example, the naphthyl esters examined by the authors (Scheme 11) gave as many as nine products depending on the nature of the R group. However, in the confines of the capsule formed by OA **2** the three esters examined, **87**-**89** all gave quantitative yields of their respective rearranged products **90**-**92**. As the authors noted, such selectivity in the Photo-Fries reaction had only been observed in zeolites, and suggests little translational and rotational freedom for the excited singlet state and subsequent β-cleavage process.

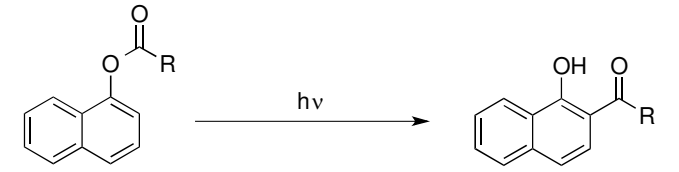

87: R = Ph
88: R = Bn
89: R = $C(CH_3)_2Ph$

90: R = Ph
91: R = Bn
92: R = $C(CH_3)_2Ph$

Scheme 11: Photochemical products from the photolysis of **87-89** encapsulated within the OA **2** dimer.

A fascinating example of the control of a photochemical reaction is the selective oxidation of olefins by singlet oxygen within the OA **2** capsule.[68] Alkenes with multiple allylic positions normally react indiscriminately with singlet oxygen via addition to the double bond and simultaneous abstraction of an allylic hydrogen. However, when alkenes such as 1-methyl cyclohexene were exposed to solutions of OA **2** a 2:2 host-guest complex was spontaneously formed in which each guest adopted a specific orientation with its methyl group filling the narrow polar region of the inner space (Figure 20). As a result, only the C-3 allylic position is accessible via partial opening of the capsule (see Section 2.1.1.d).

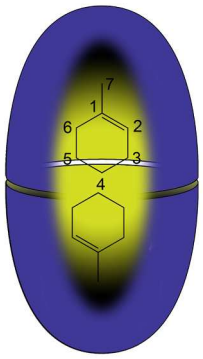

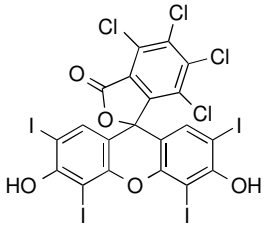

Figure 20: Left: Orientation of 1-methyl cyclohexene with the capsule formed by OA **2**. Right: Structure of Rose Bengal.

In this system singlet oxygen was generated using two sensitizers: water-soluble Rose Bengal (Figure 20), and water insoluble dimethyl benzil (**30**, Figure 9). The latter was itself made water-soluble by encapsulation within an OA **2** capsule. Although mixing of the capsular complexes of substrate and sensitizer **30** did not result in the formation of any hetero-guest complex, irradiation at 500 nm successfully oxidized the encapsulated substrate to give a 95% yield of the product peroxide arising from C-3 abstraction. Elucidation of the mechanism for this conversion began with an examination of the encapsulated dimethyl benzil **30** on its own. Thus, lifetime measurements of singlet oxidation generated by this capsule were 5 and 41 μs in water and D_2O respectively, indicating that singlet oxygen spends most of its time in free solution. Next, the rate constant for oxygen induced quenching of the triplet excited state of encapsulated **30** was determined. Two different approaches gave very similar results; the rate was approximately one order of magnitude slower than diffusion, but faster than through-the-wall energy transfer observed with hemicarcerands.[69] These results suggest that energy transfer from the encapsulated (triplet) guest to oxygen involves partial opening of the container to allow oxygen to enter the capsule, a mechanism facilitated by the relatively long lifetime of the excited sensitizer. Indeed, as was discussed in section 2.1.1.d, sensitizers with much shorter lifetimes were only slightly affected by the presence of oxygen in solution. Based on this information, the overall mechanism proposed involved: 1) generation of triplet encapsulated **30**, 2) capsule breathing to allow contact between oxygen and excited **30** and subsequent energy transfer; 3) exit of singlet oxygen from the capsule into bulk solution; and 4) entry of singlet oxygen into the capsule containing the alkene and regioselective oxidation.

Two papers detailing chiral photochemistry within the capsule formed by OA **2** have also been reported. In the first, the 4e disrotatory cyclization of pyridones was examined (Scheme 12). At its most stereochemically simple level this reaction produces two enantiomers, but the

addition of a chiral R group to the N-atom leads instead to two diastereomeric products. Two related questions raised by such conversions are: 1) even though the chirality of the R group is quite distant from the developing stereocenters, can packing within the capsule formed by OA **2** promote high diastereoselective reaction? 2) How do other groups around the pyridine ring influence reaction outcome?

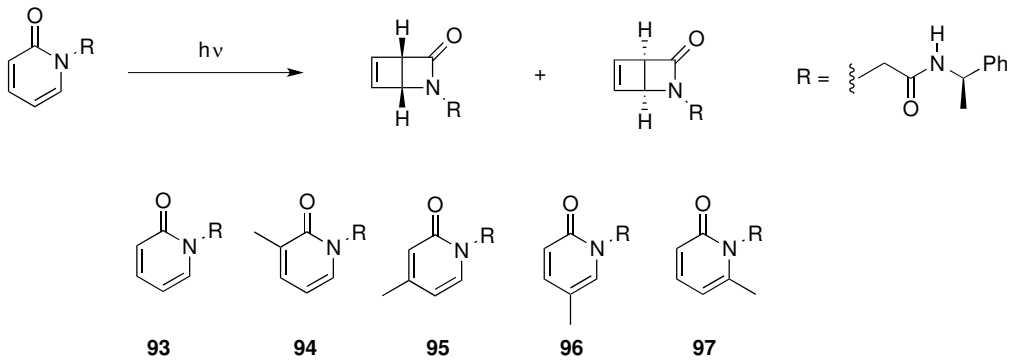

Scheme 12: The 4e disrotatory cyclization of chiral pyridones **93**-**97**.

The described research focused on the five pyridones **93**-**97**. NMR revealed that all formed 2:1 host-guest complexes in the presence of excess OA **2**, with the methyl group of **96** exhibiting the largest shift from the free state indicating that it anchors deeply into the polar region of one of the hemispheres of the capsule. These studies also revealed that the molecules adopt a pole-to-pole orientation with free rotation around the long polar axis, but no flipping of the guest on this axis (Section 2.1.1.e). Presumably, in the dry environment of the capsule a hydrogen bond can exist between the pyridine carbonyl and the N-H of the chiral amide sidechain (Figure 21). Photochemical reaction of these pyridones in free acetonitrile solution resulted in very low diastereoselectivity (diastereoselectivity ratio (dr) < 52:48), presumably because the chiral center in each example cannot transmit its stereochemical information over the relatively long distance between it and the developing stereo-centers. On the other hand, within the capsule good to excellent diastereoselectivity was observed, especially at 278 K. Thus dr values ranged from ~60:40 in the case of **93**, to as high as 96:4 in the case of **94**; contrary to what was observed in solution, the confining effect of the capsule did allow the stereochemical information of the chiral center to be transmitted to the developing centers.

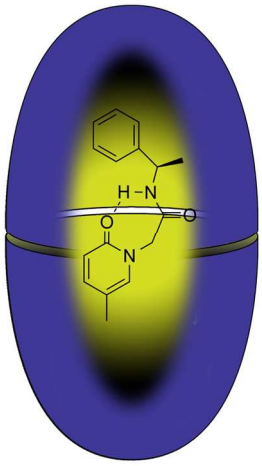

Figure 21: Proposed binding motif of pyridine **96**.

A second paper detailing chiral photochemistry in the capsule formed by OA **2** concerned the encapsulation of tropolone ethers such as **98** and cyclohexadienones such as **99**. The former undergoes a 4e disrotatory cyclization to form [3.2.0]bicycles, whilst the latter undergoes an oxa-di-π-methane rearrangement to form [3.1.0]bicycles (Scheme 13). NMR analysis revealed that both guests form 2:1 host-guest complexes with OA **2** dimer, with their respective 7- and 6-member rings occupying one hemisphere, and their chiral side chains occupying the other. In free solution both molecules gave little or no diastereoselectivity (dr ~ 50:50), but as anticipated, higher diastereoselectivity when encapsulated within the host dimers. Thus tropolone ether **98** and cyclohexadienone **99** gave diastereomeric ratios of their respective compounds of ~68:32 (at 278 K).

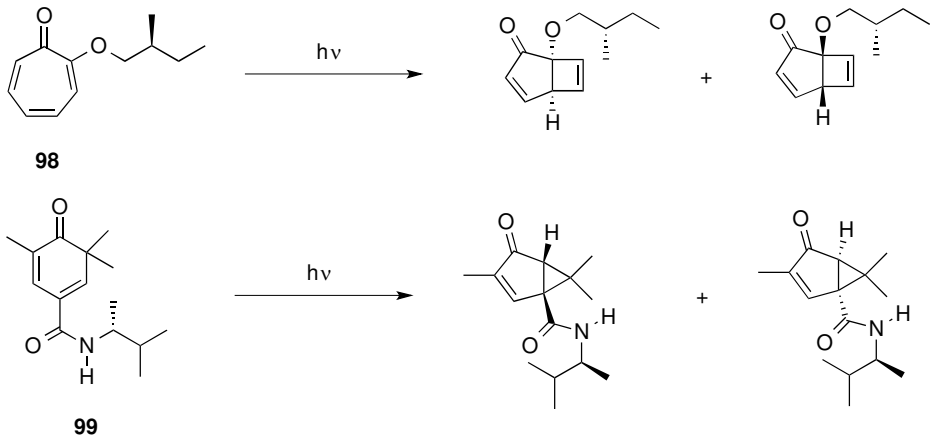

Scheme 13: The photochemistry of tropolone ethers such as **98** and cyclohexadienones such as **99**.

It is not only stereochemical information within a molecule that can be enhanced or biased within the confines of containers, but conformation information too. Cyclohexylphenyl

ketones possess established conformational-dependent photochemistry in solution, and were therefore prime targets to examine within the nano-scape of the OA **2** dimer.[70] Cyclohexylphenyl ketones undergo Type I and Type II Norrish photochemistry (Scheme 14). The Norrish type I reaction is independent of the conformational preference of the cyclohexyl group, whereas the Norrish Type II reaction that occurs in these compounds is dependent on the position of the C-3 hydrogens in relation to the excited phenylacyl carbonyl chromophore. Thus, only when the phenylacyl group is axial are these hydrogens on the same side of the 6-membered ring within reach of the carbonyl group. Two cyclohexylphenyl ketones were examined: **100** (R = H in Scheme 14) and **100** (R = Me), both of which formed the expected 2:1 host-guest complexes with OA **2**. A comparison of the photochemistry of these two ketones in free acetonitrile and encapsulated within the capsule revealed that **100** (R = H) gave mostly the Type II cyclobutanol product in free solution and only the Type I products when encapsulated, whereas **100** (R = Me) gave exclusively the cyclobutanol in free solution and the Type I products when encapsulated. The initial conclusion of these results could be that within the capsule the conformation preference of the 6-membered ring is with an equatorial phenylacyl group whose carbonyl cannot react with the C-3 hydrogens and so Type II chemistry is switched off. However, ^{1}H DQF COSY NMR analysis revealed that in both free solution and within the capsule it is the conformer with the axially positioned phenacyl group that is preferred. Why no Type II chemistry? Molecular dynamics simulations of the complexes formed by **100** (R = H) and **100** (R = Me) reveal that although the phenylacyl group is oriented axially, its carbonyl group is turned away from the 6-membered ring. Thus, assuming a similar packing of the excited state, the carbonyl group is seldom in the position to react with the C-3 hydrogen atoms and form Type II products (Figure 22).

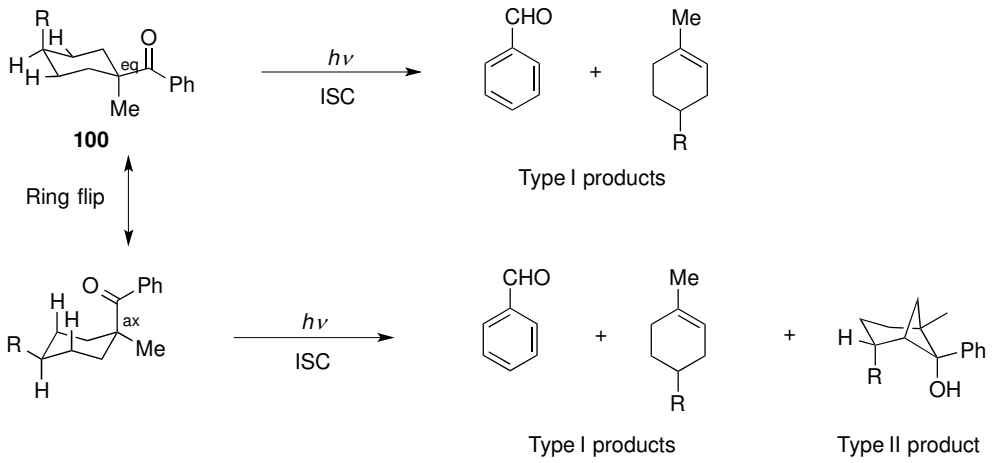

Scheme 14: Type I and Type II Norrish photochemistry of cyclohexylphenyl ketones **100** (R = H) and **100** (R = Me).

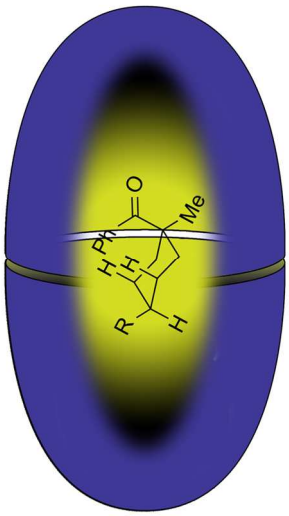

Figure 22: Proposed binding motif of cyclohexylphenyl ketones based on reaction outcome and computer models.

The behavior of carbenes generated within the OA **2** host has recently been investigated.[71] A range of carbenes generated from diazirines **101**-**104** were studied, with initial investigations focused on the types of complex formed between guests **101**-**104** and OA **2**. From a combination of ^{1}H and diffusion NMR studies the authors concluded that **101** formed a 2:2 host-guest complex, but that guests **102**-**104** formed strong (ITC) 1:1 complexes.

In free solution, irradiation of **101**-**104** gave predominantly ketone **106** and alcohol **107** in a combined yield of > 90%. In contrast, irradiation of the corresponding complexes generated different products depending on the guest. In the case of **101**, the 2:2 complex led to an 89% yield of azine **105** (R = H). On the other hand, the 1:1 complex of **102** in OA gave a 92% yield of insertion products **108** and **109** (R = OH) and 8% **106** (R = OH), while the host-guest complexes with **103** and **104** gave 55 and 63% of **106** (R = Cl and Br respectively), and a combined 45% and 37% of the insertion products **108** and **109** (R = Cl and Br respectively). The difference between the 1:1 complex of **102**, and the 1:1 complexes of **103** and **104** was rationalized with the aid of molecular dynamics simulations. Thus, the preferred orientation of **102** in the cavity of OA is with the diazirine group pointing down into the base of the pocket of the host. The corresponding carbene has little reaction options but to therefore undergo insertion reactions. On the other hand, the adamantanes **103** and **104** were predicted to bind with the diazirine group pointing up. Such an orientation allows the resulting carbene to readily react with water and generate a significant amount of the ketone **106**.

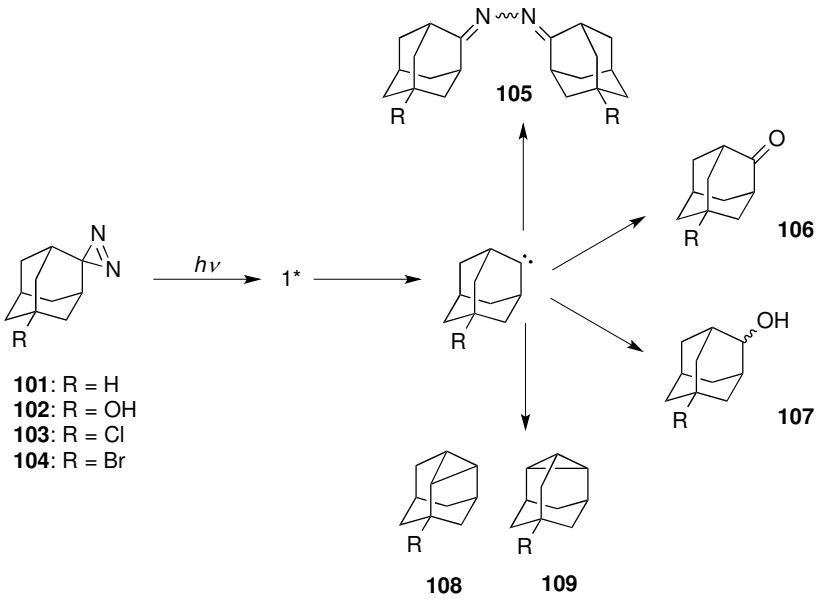

Scheme 15: Diazirines reactivity within OA 2.

Whilst compartmentalization can radically alter photochemistry it can also stop photophysical or photochemical processes normally observed in solution. An excellent example comes in the form of the entrapment of naphthalene **110**, anthracene **111**, and tetracene **112** (Figure 23) within the dimer formed by OA **2**.[38] The smallest of these guests, naphthalene **110**, shows only monomer emission in aqueous solution at 10^{-4} M, but at the same concentration in the presence of the host shows a red-shifted monomer and an excimer emission. NMR spectroscopy reveals why this is so: the guest forms a 2:2 complex with OA **2**, and with two guests inside the capsule they experience an effective concentration of 3 M. Contrastingly, in solution tetracene **112** normally undergoes facile photo-induced dimerization and shows both monomer and excimer emission. The capsular complex of this guest however only demonstrates monomer emission and does not undergo guest dimerization because the size and shape of the guest is such that only one can fit within the capsule formed by OA **2**. Between these two examples is the interesting case of anthracene **111**. Irradiation of solutions of **111** normally leads to rapid and quantitative formation of anthracene dimer, and as a result of the speed and efficiency of this reaction only the weakest of excimer emissions is normally observed along with monomer emission. NMR reveals that this guest forms a 2:2 complex with OA **2**, but rather than promoting dimerization, none is observed. However, there is a strong excimer emission band in the fluorescence spectrum of the complex. Close scrutiny of the ^{1}H NMR spectrum of the complex solved this puzzle. The guests are held out of register with respect to each other (Figure 23), and in this relative position the two pairs of 9,10 atoms cannot

approach each other. As a result, extensive irradiation leads to excimer emission but no dimerization. As might be anticipated, this unusual situation has been shown to be independent of the coating of the cavitand.[22]

Figure 23: Left panel: Structures of naphthalene, anthracene and tetracene (**110**-**112**). Right Panel: Proposed binding motif of anthracene **111** based on NMR evidence and photolysis experiments.

The capsules formed by OA **2** also allow thioketones to phosphoresce at room temperature.[72] Phosphorescence of this class of molecule is normally minimal at best because they demonstrate strong diffusion limited self-quenching as well as diffusion controlled oxygen quenching. Furthermore, singlet oxygen generated by this process reacts with thioketones irreversibly. To examine the effects of encapsulation on thioketones three guests were chosen: camphorthione **113**, fenchthione **114** (Figure 24) and adamantanethione **49** (Figure 15). Guests **113** and **49** are illustrative (Figure 24, right).

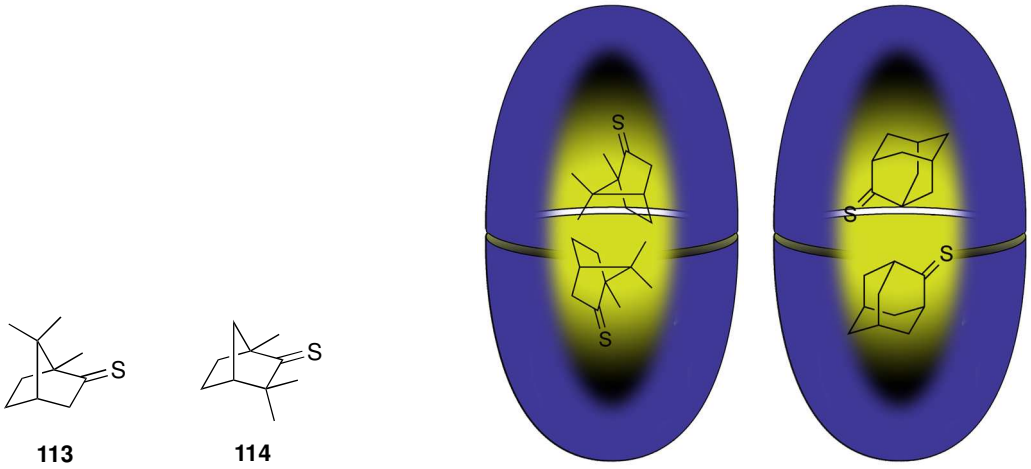

Figure 24: Left panel: Structures of camphorthione **113** and fenchthione **114**. Right Panel: Proposed binding motif of camphorthione **113** and adamantanethione **49** based on NMR evidence and photophysics.

^{1}H, NOESY and diffusion NMR analysis revealed that these two guests have subtly different binding motifs within the capsule. Thus camphorthione **113** binds preferentially with its thioketone groups buried in the deep, 'polar' region of the nano-space, whereas adamantanethione **49** binds in the opposite manner with the two thiol groups of the guests at the equatorial region of the capsule (Figure 24).

Guest **113** demonstrated phosphorescence at a capsule concentration of 10^{-4} M, and possessed a relatively long lifetime in the capsule (conc. 10^{-5} M), exceeding its lifetime at infinite dilution in perfluorodimethylcyclohexane. Its enhanced fluorescence and lifetime suggests that no self-quenching of the guests occurs, even though there are two per capsule with an effective molar concentration in the nano-space. This was attributed to the preferred orientation of the guest within the capsule that inhibits self-quenching and protects the guest from dissolved oxygen. Indeed, when the rate constant for oxygen quenching was measured it was found to be two orders of magnitude lower than in common solvents. Considering the orientation of adamantanethione **49** within the capsule it may be anticipated that the complex demonstrates no phosphorescence. However, this is not the case. Although weaker than the complex with **113**, the adamantanethione **49** possessed phosphorescence much greater than that observed at infinite dilution. Interestingly the lifetime of the phosphorescence from this complex was shorter than that at infinite dilution. Apparently the two guests are oriented relative to one another such that they can partially self-quench and reduce their lifetimes, but cannot adopt the relative orientations attainable in free solution that bring about nearly complete self-quenching. Overall, the ability of the capsule formed by OA **2** to enhance the phosphorescence of these guests (and in capsules formed by related cavitands[22]) was found to be superior to that of comparably sized, but more open, cucurbit[7]uril.

The photophysics and photochemistry discussed thus far has assumed that the capsule formed by OA **2** is an inert container akin to a nano-scale round-bottomed flask. However, very recent results have demonstrated for the first time that this is not actually the case.[73] Thus in their excited state the capsules formed by OA **2** and related cavitand **8** have been shown to be good triplet energy donors to ground state guests, and in their ground state have been shown to be electron donors to excited state species. To investigate the possibility that these hosts can act as triplet sensitizers guests such as **115** – that form distinct products depending on the type of excitation – were included inside the capsule. Guest **115** formed a strong, structurally well-defined 2:2 host-guest complex with OA **2**, and irradiation of this complex led smoothly to a quantitative yield of the triplet product **116**. Guest **115** did likewise with the capsule formed by **8**, but in this instance the transformation to **116** was considerably slower than with OA **2**. With

either host there was no evidence of the singlet product **117**. Benzoate groups are known triplet sensitizers, and so these results strongly support the notion that the benzoate groups of the hosts are excited to the singlet state, undergo intersystem crossing, and transfer their energy to the encapsulated guest; in the case of OA **2**, the more local benzoate groups at the rim of the host are more efficient at transferring their energy than the more distal benzoates in the pendant groups of **8**.

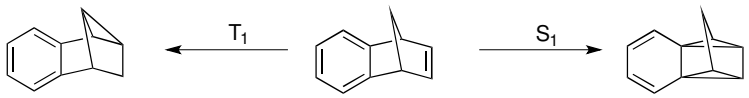

116 **115** **117**

Scheme 16: Singlet and triplet photochemistry of **115**.

The OA **2** capsule is also capable of donating electrons to excited electron acceptors. To take one example, the fluorescence of acridinium **118** was quenched upon the addition of OA **2**, a quenching that was shown to be static rather than dynamic, with a sub-nanosecond rate constant. Since water-soluble cationic guests are known to associate with the outside of the host (Section 2.1.1.f), and considering the higher S_1 energies of OA **2** versus **118**, the observed fluorescence quenching was unlikely to arise from singlet-singlet energy transfer. Considering the likely oxidation potentials of OA **2** and **8**, the authors attributed the loss of fluorescence of excited guests such as **118** to electron transfer.

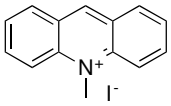

118

There are also rare examples of reactions occurring between the OA **2** capsule and an encapsulated guest. In this regard it is worth highlighting a paper that, although one the edge of the purview of this review, is of significant note[74] Specifically, it has recently been noted that the 1 and 2-azidoadamantanes **119** and **120** (Figure 25) bind to OA **2** to form the corresponding 1:1 complexes. Irradiation of these complexes results in the generation of the corresponding nitrene complexes, and this reactive guest then inserts into one of the four benzal hydrogens of the host to generate 'cavitands' such as **121** (Figure 25).

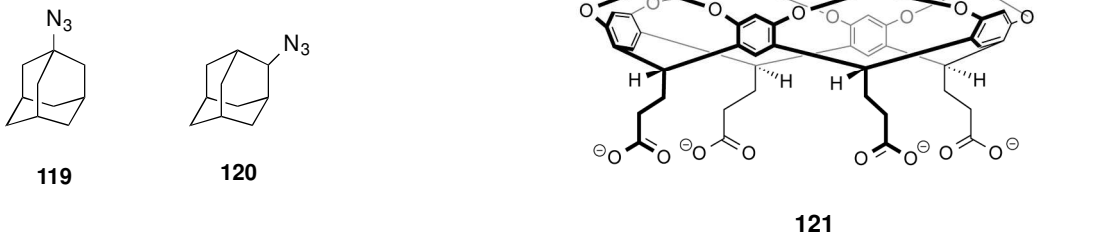

119 120 121

Figure 25: Left panel: Structures of azidoadamantanes **119** and **120**. Right Panel: Structure of insertion product **121** from reaction between OA **2** and a bound nitrene.

And on the topic of photochemical insertion into the capsule formed by OA **2** we turn to the last example on the topic of photoreactions in these cavitand dimers, the release of encapsulated guests via a photo-trigger mechanism.[75] In this work, a series of *p*-methoxyphenacyl esters **122** (R = various) were encapsulated with the OA **2** dimer. In each case the corresponding 2:1 host-guest complex was formed. ^{1}H NMR analysis demonstrated that irradiation of these complexes fragmented the guest which in turn led to the breakdown of the supramolecular capsule. Each guest produced between three and five products, primarily the p-methoxy acetophenone and the corresponding carboxylic acid (Scheme 17), but also in some cases the insertion product where the p-methoxy acetophenone moiety inserted into a benzal C-H bond of the host (c.f. **121**). The wide range of products observed suggested to the authors that more than one mechanism for the decomposition of the guest might be operational. Because the host is a good triplet sensitizer (*vide supra*) it was suggested that the triplet excited state of the bound guest was central to its decomposition. However, further work is required to fully understand this system.

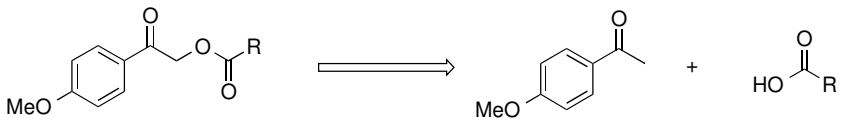

122

Scheme 17: Primary photochemical outcome of **122** encapsulated within the dimer of OA **2**.

c) As Tools for Probing Fluorescent Protein Chromophores

The chromophores of fluorescent proteins exhibit markedly different fluorescence properties when sequestered inside a β-barrel of a protein compared to those observed in free

solution. The effect of sequestration is generally attributed to the control of the overall shape of the 4-(*p*-hydroxybenzylidene)imidazolidin-5-one chromophore. Mimics of this chromophore, e.g. **123** (R_1 and R_2 = various) have been investigated to examine how changes to the dihedral angle of the benzylidene single and double bond influence their fluorescence properties. To gain further insight, a group of researchers led by Tolbert examined the encapsulation of **123** (R_1 and R_2 = various) by the OA **2** dimer capsule.[76] As anticipated, the *para*-alkyl derivatives exhibited strong shielding of both the *para*-alkyl and N-alkyl group signals, suggesting that groups in this position are anchored at the polar region of the capsule. However, neither *para*- nor *meta*-substituents were efficient at ameliorating internal conversion of the guest. In contrast, *ortho*-substituents led to a one order of magnitude increase in the fluorescence quantum yield relative to benzene solution.

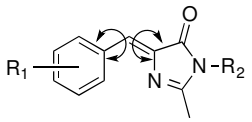

123

All of the 2:1 complexes of the guests examined were biased towards their *trans*-isomer, with photo-stationary states as high as 94:6 for the *trans* to *cis* ratio. As has been discussed above, this bias for alkene geometry reflects a more efficient filling of the cavity of the *trans* isomer. Interestingly, contrary to what has been observed with stilbenes, the propensity for *cis* to *trans* isomerization did not correlate with the internal conversion efficiency. Thus, the presence of an *ortho*-substituent in **123** attenuated internal conversion without inhibiting isomerization. The conclusion of the authors was therefore that within the capsule formed by OA **2** the *ortho*-substituent prevents rotation around the benzylidene single bond, decreasing internal conversion, and allowing either fluorescence or double bond isomerization. In contrast, in solution the combination of a double bond isomerization with efficient single bond rotation allows both efficient isomerization and efficient internal conversion.

More recently, the range of chromophores encapsulated within the confines of the OA **2** dimer was expanded considerably.[77] Specifically, the choice of R_1 groups was expanded to include a range of *ortho*-, *meta*-, and *para*- substituents covering the gamut of common electron withdrawing and donating groups. With the exception of cases where the guest had an *ortho* ethyl group, all the chromophores formed the expected 2:1 host-guest complexes. In each case fluorescence quantum yields were measured and fitted (linear regression analysis) to an equation based on a linear free energy relationship involving a Hammett substituent constant and a density functional theory derived volume change from replacing an H-atom in the parent with the substituent. An analysis of the resulting correlation factors from the data obtained with

the chromophores in free solution revealed that electronic effects dominated the fluorescence of the different molecules in the case of *meta*- or *para*-substituents, but that steric factors as large as 12% were apparent with *ortho*-substituents. On the other hand, the effect of R_2 was negligible. In addition, this analysis also revealed that there is substantial negative charge transfer to the aryl ring in the transition state for decay.

In contrast, a similar analysis for the data obtained from the chromophores encapsulated within the OA **2** dimer revealed that the remote R_2 group did have a significant effect, approaching that of *ortho*-substituents, but that the effect of R_2 decreased in the order: *ortho* > *meta* > *para* for the position of the R_1 group. Unusually, this analysis also revealed that as R_1 was kept constant and R_2 increased in size there was a non-monotonic relationship with quantum yield; the quantum yield increased for methyl through propyl, and then decreased with larger R_2 groups. This was attributed to conformational locking of the guest with increasing size, and then an over-crowding of the capsule. Comparing the steric effects of the *ortho*-, *meta*-, and *para*- substituents, guest conformational locking was more apparent with the *ortho*- and *meta*-substituents; the *para*-substituents could not prevent aryl group rotation. Finally, a comparison of the data from benzene with that of the encapsulated guest demonstrated that internal conversion within the capsule must require more charge transfer back to the ground state; an observation that may reflect a larger amount of twist in the guest when bound within the capsule.

d) Cavitands and Capsules on Surfaces

A range of cavitands has been investigated on solid surfaces. For example, with a long-term goal of examining photochemistry on inert solid supports, the photophysical properties of complexes formed by OA **2**, and cavitands **7** and **8** have been studied on silica surfaces.[22] Whereas the fluorescence of **30** (Figure 9) and phosphorescence of **113** (Figure 24) are weak at best when adhered to silica, the corresponding adhered cavitand complexes both showed strong phosphorescence, suggesting that they remained intact upon binding to the silica. Similarly, when adsorbed onto silica the capsular complex of anthracene **111** (Figure 23) showed strong excimer emission consistent with the stable 2:2 capsular complex observed in solution.[78] Perhaps the strongest evidence for successful capsule formation on silica came from guest **64** (Scheme 5). As has been discussed, in solution irradiation of the OA **2** complex with **64** produces a high yield of rearranged product **68**, and likewise complexes of this guest with OA **2**, **7** and **8** absorbed onto silica gave comparable yields of this benzyl phenyl ketone.

The unusual optical and electronic properties of gold nano-particles have led to much interest in their potential biomedical and opto-electronic applications. With this in mind, the

Ramamurthy group has synthesized a number of amine-coated and thiol-footed cavitands for functionalizing gold nano-particles.[79] Nano-particles coated with the former did not behave well and will therefore not be discussed here, but within this thiol-group several cavitands were studied in aqueous solution. Hosts **124** and **125** are representative examples.

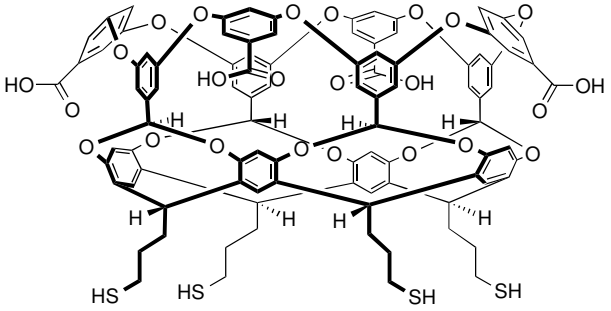

124

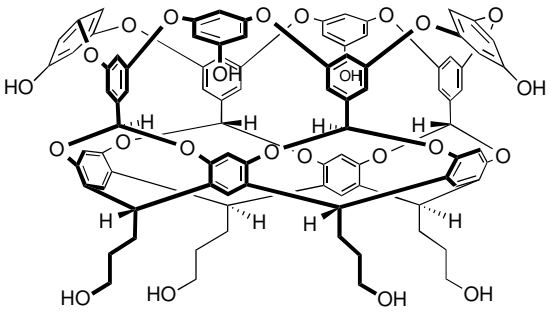

125

Gold particles were synthesized with **124** on their surface and characterized with a combination of Transmission Electron Microscopy (TEM), UV-vis absorption, IR, ^{1}H NMR, Dynamic Light Scattering (DLS), and Thermogravimetric Analysis (TGA). All of these techniques indicated successful inclusion of the cavitands onto the gold surface. Regarding host-guest complexation, although hampered by the expected signal broadening NMR studies confirmed that guests could form 1:1 host-guest complexes with the bound cavitands. Furthermore, with guests such as **30** (Figure 9) NMR suggested that capsular complexes were formed on the surface of the gold. Taking this one step further, a mixture of gold nano-particles coated with **124**, guest **30**, and excess cavitand **125** in free solution, suggested a degree of hetero-capsule formation on the surface of the nano-particle. Apparently, the hydrophobic effect is in operation at the surface of these gold nano-particles and that capsular complexes similar to the ones constituting the bulk of this review can be formed.

2.2 Velcrands

Velcrands are resorcinarene-based cavitands that, because of the two-atom bridging between pairs of opposing resorcinarene oxygen atoms, can exist as either in a 'flat' (C_{2v}) kite form, or a deeper concave (C_{4v}) vase form (Scheme 18). The rather flat nature of the kite form means that it readily undergoes self-assembly to form the corresponding dimer devoid of binding properties. On the other hand, the vase form has a rich record of host-guest chemistry that goes back some three decades.[80] One prominent thrust of the Rebek group has been the development of novel water-soluble velcrands. The majority of this work has focused on solution

studies, but as we discuss below some amphiphilic velcrands have also been studied having been imbedded into micelles or membranes. We highlight these studies where they are carried out in conjunction with solution work. Readers should note in passing though that papers describing micelles composed of amphiphilic velcrands,[81] and papers centered solely on micelle bound velcrands[82] have also appeared in the literature.

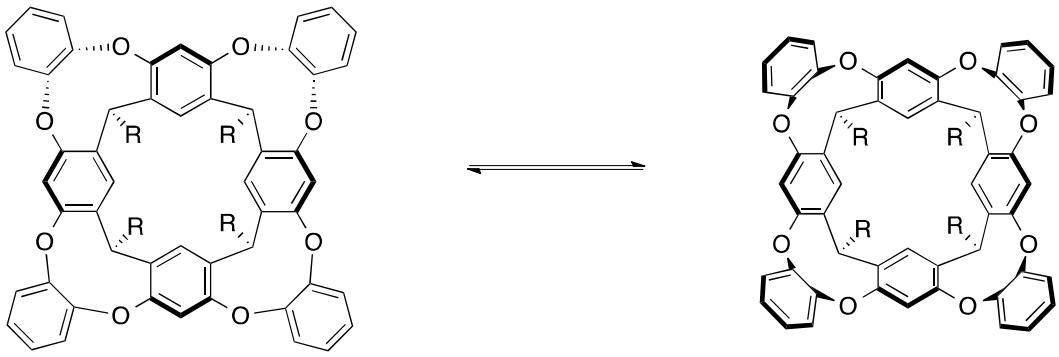

Scheme 18: C_{2v} Kite (left) and C_{4v} vase (right) forms of velcrands.

An early example of a water-soluble velcrand **126** (Scheme 19) was synthesized in three steps from the octa-nitro derivative **127**; itself available from bridging the corresponding resorcinarene **128** with 1,2-difluoro-4,5-dinitrobenzene.[83]

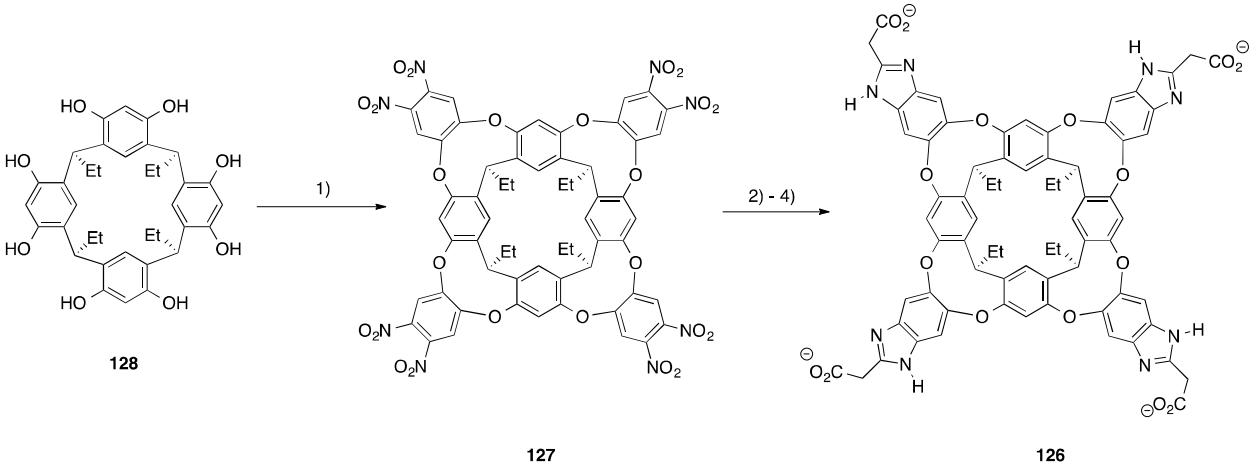

Scheme 19: Synthesis of tetra-acid velcrand **126**. Reagents are: 1) 1,2-difluoro-4,5-dinitrobenzene Et_3N, DMF; 2) $SnCl_2$, HCl; 3) Ethyl 3-ethoxy-3-iminopropanoate; 4) NaOH, THF/H_2O.

The carboxylate appended host **126** was shown to exist only in the vase form under aqueous conditions, in large part because water molecules can bridge the benzimadazole groups and help seam the host together. In addition though, the 'free' host was found to contain

a single adventitious molecule of THF bound to the cavity that resisted removal even by heating to 100 ˚C under high vacuum. This uninvited guest was however displaced in the presence of suitable alternative guests.

In passing it is worth noting that in further work,[84] it was shown that when the solvent in the final step for the preparation of **126** (Scheme 19) was switched from THF/H_2O to EtOH/H_2O, the THF-free host could be isolated. However, ^{1}H and DOSY NMR, as well as electrospray MS demonstrated that this 'free' host existed in the aqueous and gas phase as the kite-form dimer. The dimer was however quite weak; one equivalent of THF was sufficient to form the monomeric vase form. Consequently, all studies on **126** focused on the THF-containing monomeric host.

Tetraalkylammonium ions as large as tetraethylammonium were found to bind to host **126**, but larger guests such as tetrapropylammonium did not. To take one successful example, tetramethylammonium bound with an association constant of K_a = 3800 M^{-1}. Binding of these guests was slow on the ^{1}H NMR timescale, and 2D NOESY experiments revealed that the egression rate of bound tetramethylammonium was 8.2 s^{-1}. This corresponds to a relatively high energy-barrier of 16 kcal mol^{-1}. Binding was not just a question of size, shape and charge complementarity. For example, primary and secondary ammoniums of similar size to the aforementioned tetraalkylammoniums were rejected by the host, presumably because they have much stronger hydration shells. However, larger ammoniums that could simultaneously present a relatively hydrophobic moiety for binding to the pocket and an ammonium group for the rim carboxylates, were found to bind strongly. Examples include *S*-nicotinium **129** and rimantadium **130** (Figure 26). Acetylcholine **131** and choline **132** were also found to bind strongly to the host (K_a = 14,600 and 25,900 M^{-1} respectively), but the related L-carnitine **133** was found to only weakly bind (K_a = 150 M^{-1}). This was attributed to the fact that the carboxylate of the guest is in close proximity to the negatively charged upper rim of the host. Although ITC data suggested that Coulombic forces were important in these complexations, the Hydrophobic Effect also plays a role. Thus, host **126** could readily extract adamantane **134** from the solid state into a D_2O solution.

Preliminary investigations of the effects of buffer and salts (the Hofmeister Effect) on the solubility of host **126** revealed complex and poorly understood physicochemical properties.

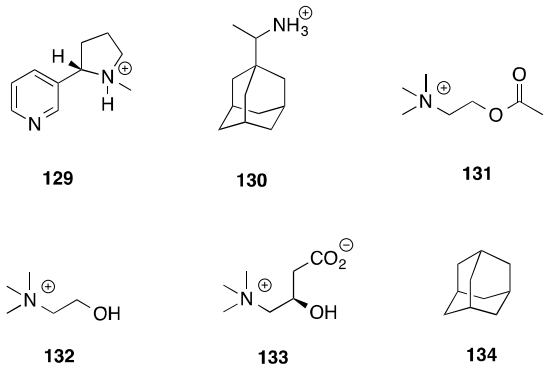

Figure 26: Guests for host **126**.

Trembleau and Rebek also used host **126** to demonstrate the first helical motif of an encapsulated guest.[43a] A 2 mM solution of **126** and dodecyl phosphocholine (DPC, **135**) resulted in an ^{1}H NMR spectra showing individual signals for each methylene unit of the hydrocarbon chain and the terminal methyl, with upfield shifts for the proton signals of eight carbons as high as $\Delta\delta$ = 5 ppm. However, the internal environment of **126** can only accommodate at most six carbons in an extended motif. As the 2 mM concentration of DPC is above its critical micelle concentration (CMC) of 1 mM, analogous experiments were conducted with sodium dodecyl sulfate (SDS, **136**) below its ~8 mM CMC. These produced similar results, with far upfield shifted signals for the methylene units and terminal methyl group. A comparison of the NMR of free and bound **135** and **136** revealed little difference between the guests indicating they bind in a similar fashion.

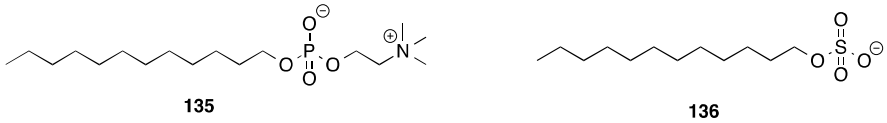

Figure 27: Helix-adopting guests for host **126**.

This data can only be readily explained by assuming the alkyl chain coils up inside the pocket of the host. This preference for the coiled motif was attributed by the authors to the release of "ordered" water molecules from the surface of the hydrocarbon chain and from the interior of the cavity. Additionally, in the coiled form more C-H bonds of the guest can form attractive interactions with the aromatic π-surfaces of the benzene moieties that line the cavity. Finally, the authors noted size complementarity exists between the dodecyl chain (126 Å^3) and the inside of the cavity (225 Å^3), a close to ideal packing coefficient of 0.56. These factors

combine to overcome the roughly 2.5 – 3.0 kcal mol^{-1} of straining *gauche* interactions that this conformation imposes on the coiled chain.

Further examination of the NMR spectra of these complexes reveals slightly broadened bound guest peaks in the upfield region. Since the exchange process must overcome a 15-20 kcal mol^{-1} barrier afforded by the breaking and refolding of the seam of hydrogen (deuterium) bonds that enforces the vase form of the receptor, and as the helical guest motif within the cavity should produce diastereomeric complexes, the broadening of the proton signals was attributed to time-averaging of the signals from multiple conformations.

In related work the same group looked at the interaction between SDS **136** and water soluble cavitand **126** as a function of increasing amounts of surfactant.[85] As just discussed, with one equivalent of **136** the guest forms a kinetically stable complex with host **126**. However, in the presence of a slight excess of guest (*ca.* 1.3 equiv.) the exchange rate becomes rapid relative to the NMR timescale and the upfield resonances diminish as the chemical shifts relating to the free and bound species average. With a concentration of 10 mM **136**, i.e., above the CMC, the host NMR signals broaden somewhat, whilst at very high concentrations of **136** (20 – 40 mM) a new set of broad signals appeared. Considering the amphiphilic nature of the host, the authors hypothesized that the host was being included into micelles, and to test this diffusion (DOSY) NMR measurements were performed. The first of these indicated that host **126** was monomeric between 0.2 mM – 4 mM, and in the presence of one equivalent of **136** a similarly sized 1:1 complex was observed. Further DOSY measurements on **136** alone indicated a decreasing diffusion coefficient with increasing concentration; below 3.7 mM ($D = 4.2 \times 10^{-6}$ cm^2 s^{-1}) the surfactant was essentially monomeric, whilst above the CMC there existed an equilibrium between micelle and monomer. Finally, at 40 mM SDS ($D = 1.3 \times 10^{-6}$ cm^2 s^{-1}) the apparent hydrodynamic radius of the micelle was calculated to be 15.4 Å. For the mixture of 40 mM surfactant and 1 mM **126** the diffusion coefficient of the latter was noted to have decreased to just 0.8×10^{-6} cm^2 s^{-1}; a corresponding hydrodynamic radius of approximately 25 Å. These data indicate each cavitand is associated within a micelle composed of approximately 60 amphiphiles. Incorporated into the surfactant micelle, there was no evidence of lipid tail binding into the pocket of the host. Furthermore, the host retained the ability to bind guests from the exterior aqueous solution. For example, acetylcholine bound with an affinity of $K_a \approx 1.7 \times 10^4$.

The Rebek group have also reported on a comprehensive analysis of the binding of acyclic and cyclic hydrocarbons to host **126**.[84, 86] As just discussed, in the case of DPC **135** and SDS **136** the guest adopts a helical packing motif to maximize the number of methylene groups shielded from the outer aqueous environment. For small *n*-alkanes, NMR illustrated well that

they do not bind in quite the same way. For the smallest guests (C_3 – C_5) peaks are broad, presumably because of relatively fast exchange. However, even the larger guests (C_6 – C_{12}) gave broad and/or clustered peaks on the NMR spectra indicative of coiled motifs that were rapidly tumbling within the cavity. In addition, with guest lengths too long to be accommodated within the cavity (C_9 or larger) binding was quite weak and competing THF binding prevented full complexation. Branched alkanes also bound, but with slower tumbling and broad ill-defined NMR signals.

Entropic costs with confinement were smaller for cyclic guests, and these proved to be generally stronger than the acyclic counterparts. Overall competitive binding studies revealed that cyclohexane was the best guest.

Small aromatic guests on the other hand are rigid and therefore cannot adopt differing conformations to optimally fill the cavity space. Consequently, these showed only weak affinity to the cavity. Larger aromatic guests did however bind. 4,4'-Dimethylbiphenyl **137** (Figure 28) was the longest guest bound, and anthracene (**111**), stilbene (**50** (R = H), and 1,4-di-*tert*-butylbenzene **138** also bound efficiently.

137 **138**

Figure 28: Examples of aromatic guests for host **126**.

The insolubility of these aliphatic and aromatic alkanes in water precluded quantification of the thermodynamics for binding. Consequently, a series of neutral, amphiphilic guests were also chosen as guests to study by ITC. Guests included a number of cyclic and adamantyl alcohols and ketones which all bound with the neutral hydrophobic moiety inside the cavity and the polar head group at the cavity rim. Binding constants were typically $>10^5$ M^{-1}. Complexation of these guests was noted to be strongly entropically driven with only a small contribution made by enthalpy. This latter point was attributed to the absence of cation–π interactions. As expected for complexations driven by the Hydrophobic Effect, complexation was associated with a negative heat capacity change (ΔC°_p).

Two dimensional EXSY NMR experiments were used to determine the exchange rates of the various guests. For the different guests examined egression rates varied from 1.7 to 14.6 s^{-1}, which correspond to free energies of activation $\Delta G^\ddagger$ from 17.2 to 16.0 kcal mol^{-1}. The similarity of these values, coupled with the concentration independence of the guest exchange rates, suggests that host **126** must fully unfold for a guest to vacate the cavity.

Velcrand **126** has been shown to act as a phase-transfer catalysts for transporting hydrophobic species into aqueous solution to bring about their reaction.[87] The reaction in question was between organic-phase maleimides (**139**) and a water-soluble thiol (Scheme 20).

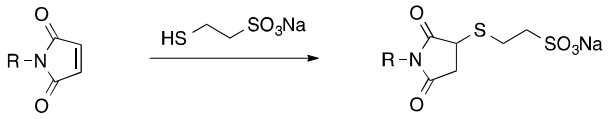

139: R = various

Scheme 20: Reaction between a water-soluble thiol to a maleimide **139**.

Host **126** readily transferred a number of *N*-substituted maleimides by complexation to the R group of the substrate, whereupon the resulting complex rapidly reacted with the thiol. Owing to the charge on each product, the resulting products were poorer guests than their corresponding starting materials. Hence product inhibition was avoided and efficient catalysis seen at levels as low as 0.5 mol%. Variations on the nature of the R group in **139** highlighted several important factors necessary for efficient and rapid transfer and reaction. First, if the starting material was a poor guest and poorly soluble in water then it would undergo only very slow reaction. Second, if **139** was partially soluble in water then although the presence of **126** accelerated the reaction, the fast background rate meant low relative rate acceleration. Third, the rate of the overall process was determined by the transfer rates of the maleimide into the aqueous layer, and this in turn was linked to the binding affinity of the R group. Good complementarity led to high relative rates (assuming **139** was insoluble in water). Finally, with selected pairs of maleimides significant reaction selectivities could be achieved.

Kaifer and Rebek have studied the electrochemistry of ferrocene derivatives bound to the hydrophobic pocket of cavitand **126**.[88] This work showed that a 1.0 mM solution of **126** increased the solubility of ferrocene **53** (Figure 16) from 50 μM in 0.1 M NaCl to fully soluble at like salt concentrations. As expected, NMR analysis of the mixture indicated guest inclusion within the hydrophobic pocket; an association constant of ~9 × 10^4 M^{-1} was estimated based on the fact that with a 1:1 stoichiometry of host and guest there was no free guest observed by NMR, and the very reasonable assumption this corresponded to at least 90% guest complexation. Similar studies with partially water-soluble guests **55** (Figure 16) and ferrocenemethanol **140** allowed association constants to be accurately determined. Thus, **55** bound with an affinity of K_a = 1300 M^{-1}, whilst **140** had an association constant of K_a = 4800 M^{-}. In all cases NMR demonstrated slow exchanging systems with the expected insertion of the

ferrocene moiety into the hydrophobic cavity, and where present, the polar group exposed to the exterior environment.

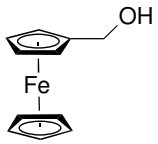

140

The included guests were also investigated using cyclic voltammetry (CV). Of particular note is that in the presence of equimolar amounts of host **126**, the voltammogram was essentially flat with no observed faradaic response. In the case of excess guest **55** and **140** (**53** did not possess sufficient solubility) a cyclic voltammetric response was observed. Complete encapsulation of these guests within the dimer formed by OA **2** (Section 2.1.1 f) was previously noted to completely switch off their electrochemistry,[53] but this was not anticipated in the open 1:1 complex with **126**. Precisely why **126** has such an effect on these guests is yet to be determined.

Host **141** is an interesting variation on **126**. The aryl groups of tetra-acid **141** effectively act as revolving doors to the cavity and modulate both the thermodynamics and kinetics of guest binding.[89] For example, the presence of the doors means that **141** has a preference for cyclopentane over cyclohexane. For **126** the reverse was true. Correspondingly, in a competition study between these two hosts, **141** preferentially bound cyclopentane (7.5:1), but in a similar study with cyclohexane **126** outcompeted **141** by two to one. Additionally, the residency time of guests within host **141** are much longer than for host **126**. Thus, EXSY NMR revealed that for cyclohexane as guest entry and egression rates are approximately two orders of magnitude slower in the case of **141**.

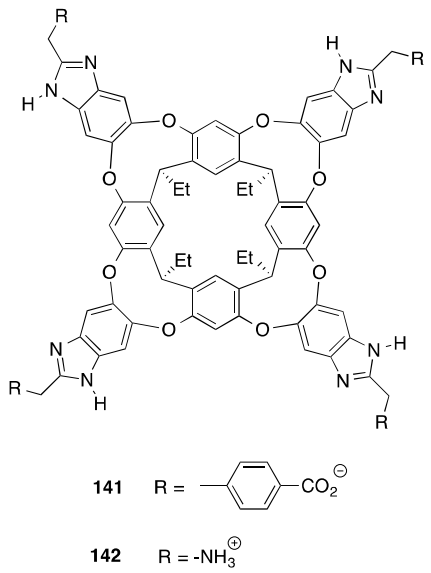

Figure 28: A gated cavitand **141** and tetra-ammonium cavitand **142**.

We close on the topic of ethyl-footed velcrands with a passing note concerning tetra-ammonium cavitand **142**.[90] The bromide salt of this cavitand had good solubility in water, and existed solely in the kite form in aqueous solution. In contrast to **126** however, the addition of THF did not trigger the formation of the vase form. In fact, formation of the vase form required substantial amounts of a water-miscible co-solvent. Consequently, its hosting properties could not be investigated in water but in 3:1 D_2O:DMSO solutions instead.

An alternative family of water-soluble velcrands is shown in Scheme 21. The formation of carbohydrate-conjugated cavitand **143** utilized tetrahydroxy resorcinarene **3**,[91] and was based on earlier related examples of water-soluble velcrands.[92] The tetrakis(β-D-glucosyl) moieties of **143** was added by a late-stage azide–alkyne “click” reaction between a lower-rim functionalized tetrazido cavitand and a propargyl glycoside. As with other hosts of this type, the eight amide groups at the rim help to stabilize the vase conformation. NMR evidence suggested that host **143** exists in a kite-conformation in order to minimize solvent-exposed hydrophobic surfaces. However, addition of guests induced vase conformation with concomitant complexation.

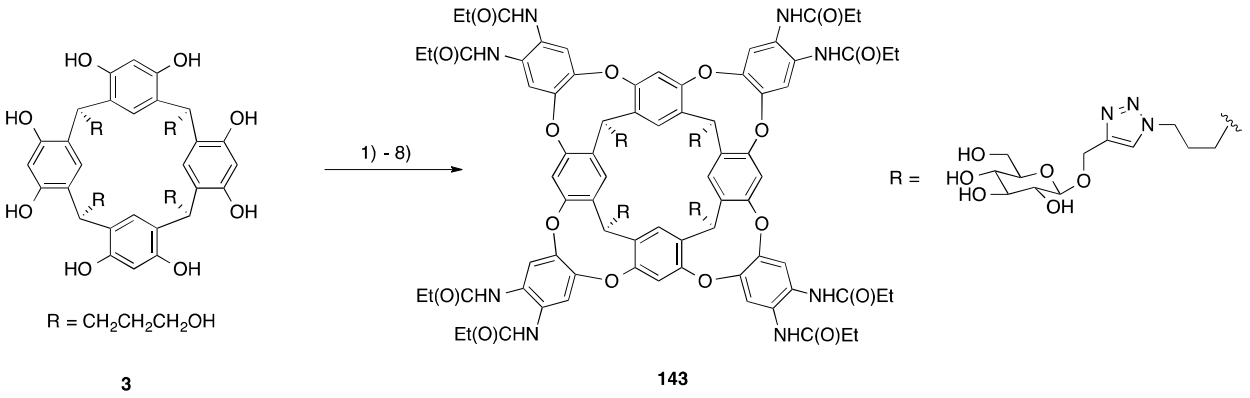

3 **143**

Scheme 21: Synthesis of tetrakis(β-D)glucosyl velcrand **143**. Reagents are: 1) 1,2-difluoro-4,5-dinitrobenzene Et_3N, DMF; 2) Propionyl chloride, Et_3N, THF; 3) Ra-Ni, H_2, THF. 4) Propionyl chloride, Et_3N, THF, -45˚C. 5) K_2CO_3, MeOH. 6) MsCl, Et_3N, THF, 0 ˚C. 7) NaN_3, DMF, 70 ˚C. 8) propargyl glycoside, Cu(I)I, TBTA, THF, 40 ˚C. 9) K_2CO_3, MeOH.

NMR studies revealed that this cavitand bound a range of water-soluble guests containing hydrophobic alkane surfaces including: cylcohexanesulfonate **144**, (1R)-(—)-10-camphorsulfonic acid **145**, quinuclidine hydrochloride **146**, and adamantylamine hydrochloride **147** (Figure 29). EXSY NMR experiments revealed for **146** a guest dissociation barrier of 13.6 kcal mol^{-1} at 37 ˚C. However, under strongly basic conditions the neutral form of this guest did not bind. Similar studies have also been performed for a velcrand with tetraethylene glycol pendant groups possessing pH-independent water solubility.[93]

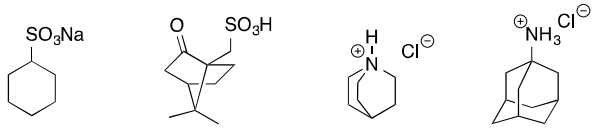

144 **145** **146** **147**

Figure 29: Examples of aromatic guests for host **143**.

When exposed to SDS micelles host **143** was successfully incorporated (DOSY NMR). Within the micelle the host adopted the vase form and could bind small molecules such as **146**. Other molecules that did not bind to the host in free solution were also bound by **143** when it itself was within the micelle, the interpretation being that the absence of any dimeric kite form in the micelle enhanced the binding properties of the host. Guest **146** also dissociated more slowly from the micelle-associated caviplex, with a barrier of 14.4 kcal mol^{-1} at 37 ˚C.

Interestingly, the binding properties of **143** remained even after dissolution in human serum. Furthermore, in a subsequent report it was noted that this host could bind and detect guests **146** and **147** (a FDA approved drug for influenza and Parkinson's disease) in spiked

samples of human urine.[94]. In lyophilized human urine reconstituted with deuterium oxide, **143** existed as a soluble dimer velcrand, i.e., no constituents of human urine can occupy the binding site of the host and enforce the vase form. Unfortunately, the detection limit for this technique was in the millimolar range and therefore of limited application.

The Rebek group also showed the ability of a guanidinium-footed cavitand **148** to incorporate in a dodecylphosphocholine (DPC, **135**) micelles.[95] The host was prepared in one step from tetra-amine **149** (Scheme 22), itself available in ten steps from commercially available materials.[92b] Cavitand **148** was soluble up to 2.0 mM in D_2O and adopted the characteristic non-binding kite form. In contrast, the vase form was only observed in solutions of acetone.

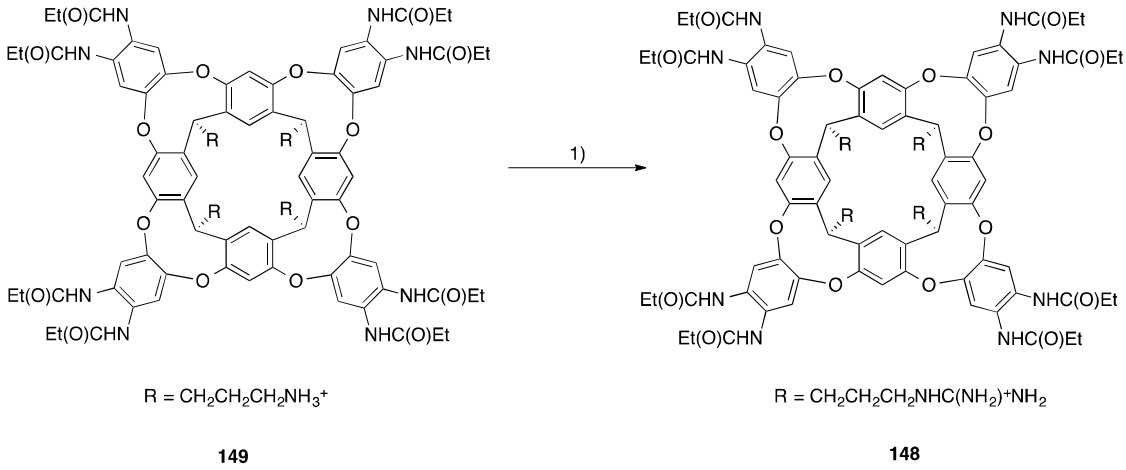

149 **148**

Scheme 22: Synthesis of the octa-amide, guanidinium footed velcrand **148**. Reagents are: 1) 1-H-pyrazole-1-carboxamidine hydrochloride, *i*-Pr_2NEt, $CHCl_3$.

In aqueous solution, **148** modestly bound a variety of cationic and neutral guests, in each case with any nonpolar group of the guest buried deep within the pocket. One possibility for the relatively weak binding was the lack of any unoccupied vase form of **148**. Thus, for a guest to bind to the host it must first overcome the dimerization of the kite form of the host. Although functioning as a cation and neutral guest binder, the addition of anionic species induced precipitation of the host.

When **148** was included in a solution containing dodecylphosphocholine (DPC, **135**) micelles (20 mM), the NMR spectrum showed signals characteristic of the vase form and an additional upfield signal at -0.4 ppm. ROESY NMR studies showed resonance between this peak and the trimethylammonium group of **135** and not the nonpolar tail group, suggesting that the host was located near the surface of the micelle. Approximately 25% of the host was occupied by lipid. Experiments below the critical micelle concentration of **135** showed no

appreciable binding between **148** and either terminal of the phospholipid, suggesting that preorganization of the vase form by the micelle enhances the binding ability of **148**. As such, **148** serves as both a guest to the micelle and host to the lipid head-group.

Molecular dynamics simulations on the incorporation of **148** into a 65-molecule DPC micelle were then carried out. The simulation began with **148** at the interface, but over time it submerged itself into the micelle to the point that its hydrophobic portions were surrounded by alkyl chains of **135** whilst its open-end remained accessible to bulk solvent. Subsequent to this, as observed by NMR, an ammonium group from the phospholipid bound into the pocket of the cavitand.

Binding studies using the micelle-incorporated host demonstrated that all of the guests tested in aqueous solution still bound to **148**. In addition, guest binding was much stronger, with as much as a 230-fold increase in K_a. Van't Hoff plots for the case of **146** binding to the cavitand, in both free solution and within the micelle, revealed a favorable enthalpy of binding in both cases (ΔH = –3.0 and –8.1 kcal mol^{-1} respectively). The difference between the ΔH for complexation in water versus the micelle was tentatively attributed to the greater preorganization of the host in the latter. These studies also revealed a small entropic penalty of ΔS = -8.4 and -9.7 cal K^{-1} mol^{-1} in water and DPC micelles respectively. Interestingly, other related cavitands usually give strongly positive ΔS values in water. Because the NMR spectra of **148** showed very well resolved signals, this difference was tentatively attributed to a lack of aggregation of host **143**. The more negative entropy of formation in the presence of the micelle is, as the authors noted, consistent with the reduction of the degrees of freedom of the micelle-bound complex.

A variation on velcrand **149** is the chiral derivative **150**.[96] This host possesses a unique benzimidazole bridge with an appended carboxylic acid group that dangles into its binding pocket. Consequently it can form a hydrogen bond/salt bridge with amine guests that bind to the pocket. In the absence of a suitable guest **150** adopts a kite form, but the addition of a suitable binder such as quinuclidine hydrochloride **146** results in the vase form. The association constant of this guest is over two orders of magnitude larger than that between **146** and **149**. This corresponds to an enhancement of -2.7 kcal mol^{-1}, a stabilization attributed in large part to the buried hydrogen bond between host and guest. A more rigorous determination using a free-energy cycle gave a value of this hydrogen bond of -3.0 kcal mol^{-1}. EXSY NMR studies suggested that the introverted carboxylic acid also affected the rate of guest exchange. An energy barrier for guest egression from **150** was measure at 19 kcal mol^{-1} in the case of guest **146**, a full 2 kcal mol^{-1} more than for host **149**. Regardless, this relatively high barrier strongly supports the common guest exchange mechanism seen with these type of velcrands: such a

mechanism requires a change from the vase to kite form costs (ca. 10-12 kcal mol^{-1}), plus the rupture of the seam of hydrogen bonds (5-7 kcal mol^{-1}).

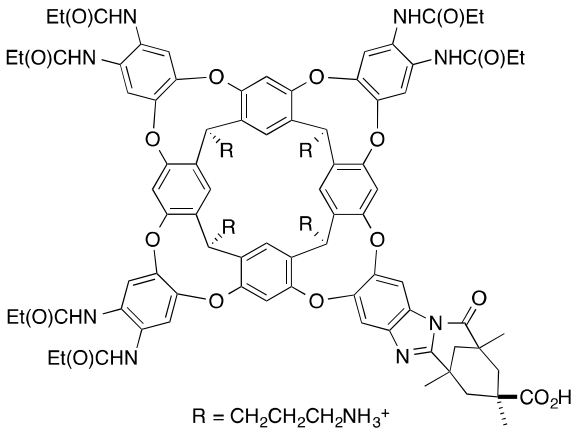

150

The Hooley, Cheng, and Rebek groups have examined the immobilization of cavitands on gold substrates for protein recognition.[97] This study centered round cavitand **151**, which by virtue of its thioether-functionalized feet could be readily appended onto gold surfaces. A combination of Surface Plasmon Resonance (SPR) and Surface Plasmon Resonance Imaging (SPRi) was used to study the binding properties of this host.

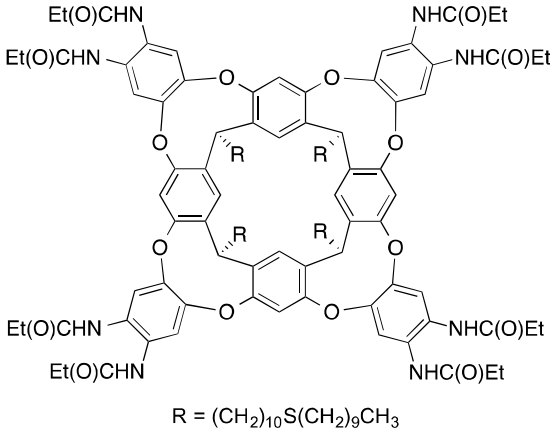

151

The host was first deposited as a self-assembled monolayer (SAM) onto a cleaned gold electrode by immersing the electrode in a 0.5 mM solution of **151** in *n*-butanol containing a 10:1 ratio of **151** and either *N*-octadecanethiol (ODT) or 11-mercaptoundecanoic acid (MUA). The

ODT or MUA were needed as fillers to enhance the predominance of the vase form of **151** and completely inhibit CV current; the SAM of **151** alone incompletely filled the gold chip and resulted in limited insulation of the electrode surface.

Focusing first on the NMe_3^+-tagged fluorescein **152** (Figure 30), it was noted that the strongest SPR response was for the SAM composed of **151** alone, but that sufficient although more modest signal could be obtained with the mixed SAM composed of **151** and ODT. Unfortunately, tests revealed that the SAM composed of just ODT also had a strong response to **152**. Consequently, attention turned to the MUA filler, and as expected, monolayers of MUA alone showed no affinity for **152** whereas the mixed monolayer with **151** and MAU did.

A number of additional ammonium guests were bound to the immobilized **151**, and although changes in resonance angle upon binding were modest, they were significant. To take this one step further, the authors then turned to guest binding detection using SPRi, which, because it is a micro-array compatibility makes the approach amenable to large-scale screening of targets in the fields of drug discovery. Briefly, a similar sample preparation led to successful surface deposition in defined arrays, and these could be used in label-free guest binding determinations.

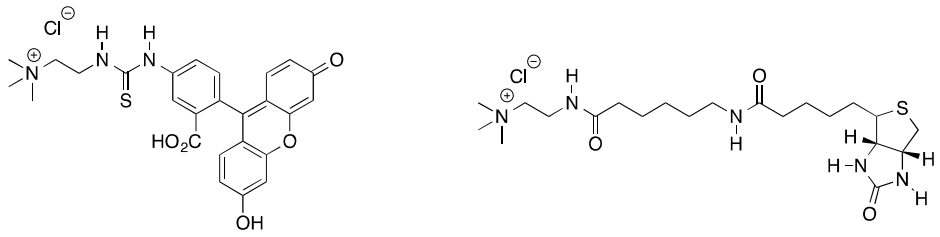

152 **153**

Figure 30: Examples of aromatic guests for host **151**.

Finally, the group turned to protein recognition by SPR. For this they first demonstrated that the mixed monolayer with **151** and MAU successfully bound biotin derivative **153**. Subsequent addition of a solution of streptavidin induced an increase in resonance angle indicative of immobilization of the streptavidin at the surface. Cross-checks demonstrate that **153** was essential for streptavidin recognition, and that no signal was observed in the absence of the cavitand. In combination these experiments proved that neither the guest nor the protein can be immobilized by MUA alone, and biosensing required the complete set of specific non-covalent interactions involving the cavitand, the biotin guest **153**, and streptavidin.

Most recently the Rebek group have utilized velcrands to form capsules that form in water. As we will see, whilst hydrogen bonding is important in their formation, the Hydrophobic Effect also plays a key role in their formation. This program is based on velcrand **154**, a host that is based on an early example of a velcrand capsule devised by De Mendoza.[98] The dimeric capsule of **154** is held together by sixteen hydrogen bonds between the hydrogen bond acceptors and donor groups of the benzimidazolone rim, whilst its water-solubility arises from the eight pyridinium pendant groups.

Host **154** is synthesized in eight steps and exists in both the kite and vase forms at low concentrations. The first guests reported that confirmed capsule formation were *n*-undecane through *n*-tetradecane (C_{11}-C_{14}). NMR demonstrated that the guest *n*-undecane fits comfortably in an extended conformation, while the longer alkanes adopt *gauche* conformations within the capsule. Absolute binding affinities could not be determined because of the very low water solubility of these guests, but competitive studies revealed a relative order for binding affinity to be: $C_{11} > C_{12} > C_{13} > C_{14}$.

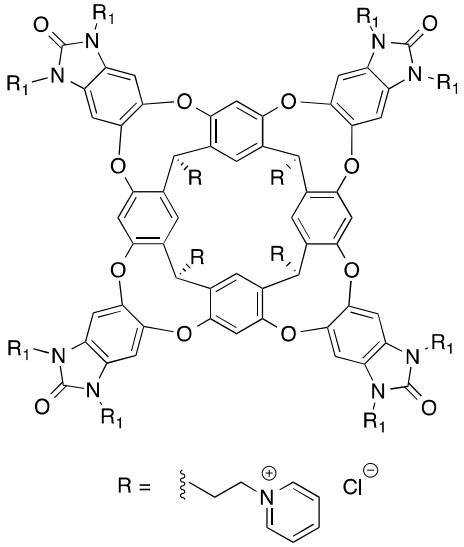

154: R_1 = H
155: R_1 = Me

A series of rigid molecules with subtly differing lengths, including stilbene **50** (Figure 15) and viologen **54** (R = Me, Figure 16), were used to probe both the length of the inner-space and the guest preferences of the **154** dimer. The initially report data suggested that uncharged guests bound more strongly that isosteric pyridinium salts.

The photophysical behavior of encapsulated stilbene derivative **50** also provided indirect evidence of the robustness of the seam of hydrogen bonds at the capsule equator. The fluorescence of **50** was strong in mesitylene but completely quenched upon encapsulation within the dimer formed by **154**. This supports the idea that the capsule must be quite robust in shape, for if it were dynamic or ill-defined the host could adapt to accommodate a planar stilbene guest and allow fluorescence. In reality, the seam of hydrogen bonds stoutly defines the shape of the inner-space such that the rings of a stilbene guest cannot be coplanar while inside and its fluorescence is quenched.

In a follow-up communication, the short *n*-alkanes (C_7 through C_{11}), and the appetite stimulant peptide grehlin were respectively encapsulated and complexed by **154**.[99] The smallest guest *n*-alkanes heptane, octane, and nonane all formed the corresponding 1:1 complex with the host. These rotated rapidly in the internal hydrophobic environment created by the monomeric host and their corresponding ^{1}H NMR signals were broad and the spectra highly symmetrized. Interestingly, *n*-decane formed both a 1:1 and a 2:1 complex with the host. Tell-tail characteristics of the two complexes were: in the 1:1 complex the guest exhibited ^{1}H NMR signals over a narrow range indicative of *gauche* interactions and an overall compressed guest motif; in the 2:1 complex the same signals for the bound guest were spread out over a wide ppm range indicating an extended motif in a symmetrical environment. It was noted that the ratio of the two complexes was temperature dependent, with the capsular assembly predominating at elevated temperatures and exclusively so above 340 K.

Exposure to amphiphiles such as octanoic acid also resulted in a 1:1 complex, with as anticipated, the alkane chain imbedded in the host cavity. Similarly the peptide ghrelin – a 28 amino-acid peptide that contains an octanoyl ester moiety at the third (serine) residue – was also bound in a 1:1 manner. Similar results were obtained for rat ghrelin, a truncated 10 amino acid peptide. The binding constant of both ghrelin and rat-ghrelin were too large to determine by NMR, but ITC titrations with rat-ghrelin showed $K_a = 2.5 \times 10^5$ M^{-1}, and both favorable enthalpy and entropy of binding.

Per-methylation of the benzamidazolones groups of host **154** leads to **155**, a velcrand which exhibited water solubility up to 10 mM in the kite form. Host **155** was expected to have more flexible walls because whereas the vase form of **154** is stitched together by hydrogen bonds to “bridging” water molecules, this is not possible with **155**. Correspondingly, the vase form of **155** could potentially hold wide guests (or wider guest motifs). It transpires that this is indeed the case.

Brief sonication and/or heating with a series of *n*-alkanes (C_6 to C_{14}) gave characteristic spectra associated with the vase form, but with noticeably compressed signal ranges for the bound-guest. Hence for the smallest guests this range spanned only about 0.6 ppm, whilst for C_{13} and C_{14} this range was still a relatively modest 2 ppm. As expected, for the short *n*-alkanes (C_6 to C_{10}) the furthest upfield shifted signals were those of the terminal methyl protons; time-averaged as they tumbled quickly on the NMR time-scale with the one end pointed to the solvent exterior and the other nestled deep within the pocket.

In contrast, were the longer alkanes (C_{12} to C_{14}) whose terminal methyls were unexpectedly, furthest *downfield* on the ^{1}H NMR. Typically terminal methyl groups reside the deepest within the cavitand pocket and as such are shielded the most by the aromatic walls of the host. Hence they have the largest $\Delta\delta$ values with upfield shifts of 4.0 ppm or more. However, in the case of these guests within **155** it was the central methylene protons that possessed the largest upfield shift, demonstrating that the mid-section of these guests is closest to the base of the pocket. Correspondingly, the terminal methyl group signals were the furthest downfield shifted of the bound guest region in the NMR. In combination, this data indicates that the *n*-alkanes C_{12}-C_{14} adopt U-shaped motifs within the binding pocket of **155**. Because of the small range of signals in the NMR spectra, these guests likely “writhe” in the defined space and adopt many low energy variations on the idealized U-shaped motif.

To probe this type of binding further the authors turned to a series of *n*-alcohols. NMR investigations confirmed that the terminal methyls reside deep within the cavity for *n*-octanol and *n*-nonanol (-3.4 ppm, $\Delta\delta$ = -4.2 ppm), but as the carbon chain length increases the terminal methyl becomes less and less shielded. With *n*-decyl (C_{10}) and *n*-undecyl alcohols (C_{11}) the methyl signals are still the furthest upfield but have shifted significantly downfield to -3.1 ppm and -2.6 ppm, respectively, indicating the methyl is in the wider more capacious interior of the cavity. The guest adopts a J-shaped motif. For the longest homologue, tetradecanol (C_{14}), the bound methyl signal appeared at only -0.3ppm, suggesting that this longer guest adopts a U-shaped motif. Supporting this ^{1}H NMR information, COSY NMR indicated the carbon chains adopt helical and/or folded conformations within the cavity as the terminal methyl is pushed further and further out of the base of the pocket. Among other groups tested, α,ω diols also exhibited similar folding patterns.

2.3 Amphiphilic Cogs

The Shionoya group has developed two water-soluble self-assemblies driven by the Hydrophobic Effect. The requisite amphiphiles were based on pyridine containing tris-monodentate ligands **156** (Figure 31), which had previously been shown to self-assemble in organic media to form either cages and capsules depending on the stoichiometry of Hg^{2+} and whether or not a cryptand was also present.[100] The cages (Hg_6**156**$_4$) required no templating guest, whilst the fluorescently active capsules (Hg_6**156**$_8$) were templated by an encapsulated cryptand guest.

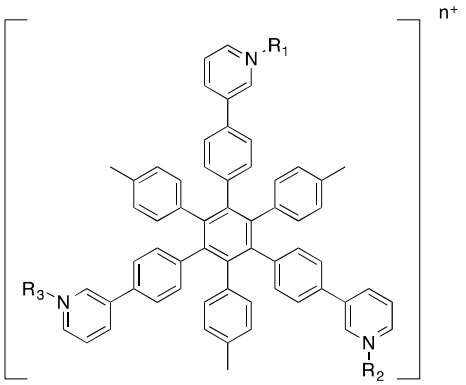

156: $R_1 = R_2 = R_3$ = lone pair
157: $R_1 = R_2$ = lone pair, R_3 = Me
158: R_1 = lone pair, $R_2 = R_3$ = Me
159: $R_1 = R_2 = R_3$ = Me

Figure 31: Amphiphilic cogs **156**-**159**.

As a stepping-stone to working in pure water, the amphiphile **156** was shown to self-assemble in aqueous methanol to form box-shaped hexamers (**156**$_6$).[101] Suggestive of the importance of the hydrophobic effect in this assembly, water was required to form the hexamer; the subunit was monomeric in pure methanol. Optimal assembly required the encapsulation of two templating molecules. Thus, with tribromomesitylene **160** (Figure 32) as guest a crystal structure of the assembly was obtained. As is so often the case with templated assemblies, the nature of the template had a large influence on the success of assembly. Thus, hexamethylbenzene **161** and mesitylene **162** were shown by NMR to be good templates for this process, whereas 1,3-5-trichlorobenzene **163** proved too small and hexabromobenzene **164** too big to template assembly.

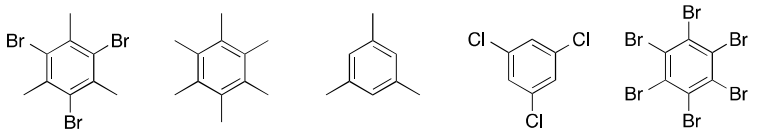

160 **161** **162** **163** **164**

Figure 32: Guests and templates for the assembly of amphiphilic cogs **160**-**164**.

Furthermore, in a subsequent publication it was revealed that when adamantane **134** was used as a template, the product formed was a tetrameric assembly $\mathbf{156}_4$ with the template encapsulated within.[102] X-ray crystallography, NMR and MS were all used to characterize the assemby. Similar self-assembled inclusion complexes were also formed upon addition of pseudo-spherical species such as Me_4Si or CBr_4, to a solution of **156**.

Methylation of **156** gave the *N*-methylpyridinium amphiphiles **157**-**159**,[103] of which **157** was insoluble in pure water whereas **158** and **159** were fully water-soluble. NMR and X-ray crystallography demonstrated that cog **158** had the predisposition to self-assembled into box-shaped hexamer $\mathbf{158}_6$, and when a suitable guest molecule such as **160** was present the assembly encapsulated the guest to form the corresponding complex.

The ^{1}H NMR spectrum of **158** in deuterated methanol was remarkably simple showing monomeric **158** with C_{2v} symmetry, whereas the spectrum in D_2O indicated several upfield shifted proton signals indicating an aggregate. Examination of the non-equivalent *N*-methyl and *p*-tolyl signals indicated a highly symmetric box-shaped container was exclusively formed. The formation of the hexameric aggregate was confirmed by PGSE NMR measurement (*log D* = -9.9; $D = 1.26 \times 10^{-10}$ m^2 s^{-1}) consistent with a 2 nm box. X-ray crystallography revealed that the stability of the assembly was in part due to interactions between electron-rich pyridyl groups sandwiched between pairs of electron-deficient pyridiniums.

The box-shaped aggregate of $\mathbf{158}_6$ was shown to be remarkably stable; heating to 353 K produced noticeably sharp NMR spectra with no signs of dissociated monomer in solution. By contrast, heating aggregate $\mathbf{156}_6$ in CD_3OD:D_2O (3:1) afforded primarily the monomeric species at only 333 K. Additionally, the critical concentration required for capsular assembly was shown to be significantly lower than 1 μM: a 1 mM solution of **158** in MeOH showed characteristic UV absorption at 265 and 287 nm corresponding to the monomeric species, while an increasing fraction of H_2O caused a significant lessening of the absorption bands; examination of the concentration effect on absorbance in pure H_2O showed no hypochromism at all in the concentration range from 1 μM to 100 μM.

The inner space formed by $\mathbf{158}_6$ is 0.8 nm × 0.8 nm and as such can comfortably house two copies of the guest **160** in its internal cavity; addition of water insoluble **160** to a D_2O

solution containing **158**$_6$ resulted in rapid internalization of the guests and downfield shifts of the ^{1}H NMR signals of the methyl groups from δ = 2.64 ppm (in CD_3OD) to δ = 3.49 ppm in D_2O.

In contrast to the properties of C_{2v} symmetric **158**, C_{3h} subunit **159** with three pyridinium groups formed a tetrameric assembly around a templating adamantane **134** molecule. In the absence of the template **159** actually forms a 1:9 ratio of the tetramer and hexamer, but the addition of template **134** leads to the quantitative formation of the tetramer.

3.0 Conclusions and Outlook

This review has discussed three classes of molecules that have been used by researchers to investigate self-assembly in aqueous solution. The use of resorcinarene-based hosts dominates the area, but all approaches demonstrate the importance of preorganization of arrays of rigid (aromatic) moieties to define a specific form predisposed to bind, fold, or assemble. Studying these molecules and their properties is: 1) teaching us how to control supramolecular chemistry in water; 2) shedding light on some dark corners of aqueous solutions chemistry, and; 3) illustrating novel applications that necessitate water being the solvent.

Regarding the first of these, supramolecular chemists are familiar with the concept of a functional group driving and/or directing binding or assembly. Thus the directionality of a hydrogen bond – a notion derived from the variance on ΔH° on the angle between donor and acceptor – may help drive a molecule to form an assembly of specific form (constitution, and relative position and orientation of subunits). The molecules discussed in this review suggest modifications to this concept, namely that: directionality can be free energy based rather than enthalpically based, and that the definition of a “functional group” can be expanded from a list useful to synthetic chemists, to include moieties useful to supramolecular chemists. In all the examples highlighted here, careful crafting of structure resulted in functional groups (to use the just expanded definition) that bind, fold, or assemble… in water.

The second and third points listed above are for the future; but we are confident much can be learned from aqueous supramolecular chemistry. Continued investigations involving the aforementioned families of molecules, and potentially new classes of molecules that are yet to be developed, will shed more light on the mysteries of water and undoubtedly engender new and useful applications. The details are certainly murky, but the bigger picture seems quite clear.

Acknowledgements

BCG acknowledges the financial support from the National Science Foundation (CHE 1244024).

References

1. Reichardt, C.; Welton, T., *Solvents and Solvent Effects in Organic Chemistry*. 4 ed.; VCH: New York, 2011.
2. Oshovsky, G. V.; Reinhoudt, D. N.; Verboom, W., *Angewandte Chemie* **2007,** *46* (14), 2366-93.
3. Lynden-Bell, R. M.; Morris, S. C.; Barrow, J. D.; Finney, J. L.; Harper, R. L. J., *Water and Life*. CRC Press: Boca Raton, 2010.
4. (a) Michal, G.; Schomburg, D., *Biochemical Pathways: An Atlas of Biochemistry and Molecular Biology*. 2 ed.; John Wiley and Sons: New York, 2012; (b) Ball, P., *Chem. Rev.* **2008,** *108*, 74-108.
5. (a) Maddox, J.; Randi, J.; Stewart, W. W., *Nature* **1988,** *334*, 287-290; (b) Davenas, E.; Beauvais, F.; Amara, J.; Oberbaum, M.; Robinzon, B.; Miadonna, A.; Tedeschi, A.; Pomeranz, B.; Fortner, P.; Belon, P.; Sainte-Laudy, J.; Poitevin, B.; Benveniste, J., *Nature* **1988,** *333*, 816-818; (c) Rousseau, D. L., *Am. Sci.* **1992,** *80*, 54-63; (d) Lippincott, E. R.; Stromberg, R. R.; Grant, W. H.; Cessac, G. L., *Science* **1969,** *164* (3887), 1482-7.
6. (a) Ovchinnikova, K.; Pollack, G. H., *Langmuir* **2009,** *25*, 542-547; (b) Corti, H. R.; Colussi, A. J., *Langmuir* **2009,** *25* (11), 6587-6589.
7. Clark, G. N.; Hura, G. L.; Teixeira, J.; Soper, A. K.; Head-Gordon, T., *Proc Natl Acad Sci U S A* **2010,** *107* (32), 14003-7.
8. Petersen, P. B.; Johnson, J. C.; Knutsen, K. P.; Saykally, R. J., *Chemical Physics Letters* **2004,** *397* (1-3), 46-50.
9. Petersen, P. B.; Saykally, R. J., *Annu. Rev. Phys. Chem.* **2006,** *57*, 333-64.
10. (a) Lum, K.; Chandler, D.; Weeks, J. D., *J. Phys. Chem. B.* **1999,** *103* (22), 4570-4577; (b) Chandler, D., *Nat. Biotechnol.* **2007,** *445*, 831-832.
11. (a) Israelachvili, J. N., *Intermolecular & Surface Forces*. Academic Press: San Diego, 2011; (b) Wang, L.; Friesner, R. A.; Berne, B. J., *Journal of Physical Chemistry B* **2010,** *114*, 7294–7301.
12. (a) Baron, R.; Setny, P.; McCammon, J. A., *J. Am. Chem. Soc.* **2010,** *132* (34), 12091-7; (b) Setny, P.; Baron, R.; McCammon, J. A., *Journal of Chemical Theory and Computation* **2010,** *6*, 2866-2871; (c) Ewell, J.; Gibb, B. C.; Rick, S. W., *J. Phys. Chem. B* **2008,** *112*, 10272-10279.
13. (a) Rowan, S. J.; Cantrill, S. J.; Cousins, G. R. L.; Sanders, J. K. M.; Stoddart, J. F., *Angew. Chem. Int. Ed.* **2002,** *41*, 898-952; (b) Belowich, M. E.; Stoddart, J. F., *Chem. Soc. Rev.* **2012,** *41*, 2003-2014; (c) Sun, J.; Bennett, J. L.; Emge, T. J.; Warmuth, R., *J. Am. Chem. Soc.* **2011,** *133* (10), 3268-3271; (d) Xu, D.; Warmuth, R., *J. Am. Chem. Soc.* **2008,** *130* (24), 7520-7521; (e) Liu, X.; Warmuth, R., *J. Am. Chem. Soc.* **2006,** *128* (43), 14120-14127.
14. (a) Warmuth, R. In *Carcerands and hemicarcerands*, John Wiley & Sons Ltd.: 2012; pp 917-954; (b) Jasat, A.; Sherman, J. C., *Chem. Rev.* **1999,** *99*, 932-967.
15. (a) Fujita, M.; Tominaga, M.; Hori, A.; Therrien, B., *Acc Chem Res* **2005,** *38* (4), 369-78; (b) Klosterman, J. K.; Yamauchi, Y.; Fujita, M., *Chem Soc Rev* **2009,** *38* (6), 1714-25; (c) Yoshizawa, M.; Klosterman, J. K.; Fujita, M., *Angew. Chemie* **2009,** *48*, 3418-3438; (d) Pluth, M. D.; Raymond, K. N., *Chem. Soc. Rev.* **2007,** *36*, 161-171; (e) Nitschke, J. R., *Acc Chem Res* **2007,** *40* (2), 103-12.
16. (a) Gibb, C. L. D.; Stevens, E. D.; Gibb, B. C., *Journal of the American Chemical Society* **2001,** *123* (24), 5849-5850; (b) Gibb, C. L. D.; Li, X.; Gibb, B. C., *Proc. Nat. Acad. Sci. U.S.A.* **2002,** *99*, 4857-4862; (c) Laughrey, Z. R.; Gibb, C. L. D.; Senechal, T.; Gibb, B. C., *Chem. - Eur. J.* **2003,** *9* (1), 130-139; (d) Xi, H.; Gibb, C. L. D.; Gibb, B. C., *J. Org. Chem.* **1999,** *64*, 9286-9288; (e) Xi, H.; Gibb, C. L. D.; Stevens, E. D.; Gibb, B. C., *Chem. Commun.* **1998**, 1743-1744.
17. Gibb, C. L. D.; Gibb, B. C., *J. Am. Chem. Soc.* **2004,** *126* (37), 11408-11409.

18. Liu, S.; Whisenhunt-Ioup, S. E.; Gibb, C. L. D.; Gibb, B. C., *Supramol. Chem.* **2011,** *23* (6), 480-485.
19. Green, J. O.; Baird, J. H.; Gibb, B. C., *Org Lett* **2000,** *2* (24), 3845-8.
20. Rowan, S. J.; Hamilton, D. G.; Brady, P. A.; Sanders, J. K. M., *J. Am. Chem. Soc.* **1997,** *119*, 2578-2579.
21. Gibb, C. L. D.; Gibb, B. C., *J. Am. Chem. Soc.* **2006,** *128* (51), 16498-16499.
22. Ramasamy, E.; Jayaraj, N.; Porel, M.; Ramamurthy, V., *Langmuir* **2012,** *28* (1), 10-16.
23. (a) Giles, M. D.; Liu, S.; Emanuel, R. L.; Gibb, B. C.; Grayson, S. M., *J. Am. Chem. Soc.* **2008,** *130* (44), 14430-14431; (b) Giles, M. D.; Liu, S.; Emanuel, R. L.; Gibb, B. C.; Grayson, S. M., *Isr. J. Chem.* **2009,** (49), 31-40; (c) Grayson, S. M.; Gibb, B. C., *Soft Matter* **2010,** *6*, 1377-1382.
24. (a) Kulasekharan, R.; Ramamurthy, V., *Org. Lett.* **2011,** *13* (19), 5092-5095; (b) Ishida, Y.; Kulasekharan, R.; Shimada, T.; Takagi, S.; Ramamurthy, V., *Langmuir* **2013,** *29* (6), 1748-53; (c) Ishida, Y.; Kulasekharan, R.; Shimada, T.; Ramamurthy, V.; Takagi, S., *The Journal of Physical Chemistry C* **2014,** *118* (19), 10198-10203.
25. Da Silva, J. P.; Kulasekharan, R.; Cordeiro, C.; Jockusch, S.; Turro, N. J.; Ramamurthy, V., *Org. Lett.* **2012,** *14* (2), 560-563.
26. Sun, H.; Gibb, C. L. D.; Gibb, B. C., *Supramol. Chem.* **2008,** *20* (1&2), 141-147.
27. Jayaraj, N.; Zhao, Y.; Parthasarathy, A.; Porel, M.; Liu, R. S. H.; Ramamurthy, V., *Langmuir* **2009,** *25* (18), 10575-10586.
28. Gibb, C. L. D.; Gibb, B. C., *J Comput Aided Mol Des* **2013**, Ahead of Print.
29. Gibb, C. L. D.; Gibb, B. C., *J. Am. Chem. Soc.* **2011,** *133* (19), 7344-7347.
30. Liu, S.; Gibb, B. C., *Chem. Commun. (Cambridge, U. K.)* **2011,** *47* (12), 3574-3576.
31. Gibb, C. L. D.; Gibb, B. C., *Chem. Commun.* **2007,** (16), 1635-1637.
32. Gibb, C. L. D.; Gibb, B. C., *Tetrahedron* **2009,** *65* (35), 7240-7248.
33. Gan, H.; Benjamin, C. J.; Gibb, B. C., *J. Am. Chem. Soc.* **2011,** *133* (13), 4770-4773.
34. Gan, H.; Gibb, B. C., *Chem. Commun. (Cambridge, U. K.)* **2012,** *48* (11), 1656-1658.
35. Gan, H.; Gibb, B. C., *Chem. Commun. (Cambridge, U. K.)* **2013,** *49* (14), 1395-1397.
36. (a) MacGillivray, L. R.; Atwood, J. L., *Nature* **1997,** *389*, 469-472; (b) Rissanen, K., *Angew. Chemie Int. Ed.* **2005,** *44*, 3652-3654.
37. Ewell, J.; Gibb, B. C.; Rick, S. W., *J. Phys. Chem. B* **2008,** *112* (33), 10272-10279.
38. Kaanumalle, L. S.; Gibb, C. L. D.; Gibb, B. C.; Ramamurthy, V., *J. Am. Chem. Soc.* **2004,** *126* (44), 14366-14367.
39. Porel, M.; Jayaraj, N.; Kaanumalle, L. S.; Maddipatla, M. V. S. N.; Parthasarathy, A.; Ramamurthy, V., *Langmuir* **2009,** *25* (6), 3473-3481.
40. Jayaraj, N.; Jockusch, S.; Kaanumalle, L. S.; Turro, N. J.; Ramamurthy, V., *Can. J. Chem.* **2011,** *89* (2), 203-213.
41. Tang, H.; de Oliveira, C. S.; Sonntag, G.; Gibb, C. L. D.; Gibb, B. C.; Bohne, C., *J. Am. Chem. Soc.* **2012,** *134* (12), 5544-5547.
42. Kulasekharan, R.; Jayaraj, N.; Porel, M.; Choudhury, R.; Sundaresan, A. K.; Parthasarathy, A.; Ottaviani, M. F.; Jockusch, S.; Turro, N. J.; Ramamurthy, V., *Langmuir* **2010,** *26* (10), 6943-6953.
43. (a) Trembleau, L.; Rebek, J., Jr., *Science* **2003,** *301* (5637), 1219-20; (b) Scarso, A.; Trembleau, L.; Rebek, J., Jr., *J. Am. Chem. Soc.* **2004,** *126*, 13512-13518; (c) Ajami, D.; Rebek, J., Jr., *J Am Chem Soc* **2006,** *128* (47), 15038-9.
44. Choudhury, R.; Barman, A.; Prabhakar, R.; Ramamurthy, V., *J Phys Chem B* **2013,** *117* (1), 398-407.
45. Furuhashi, M.; Hotamisligil, G. S., *Nature reviews* **2008,** *7*, 489-503.
46. Ko, Y. H.; Kim, H.; Kim, Y.; Kim, K., *Angew. Chem. Int. Ed.* **2008,** *47*, 4106-4109.
47. Liu, S.; Russell, D. H.; Zinnel, N. F.; Gibb, B. C., *J. Am. Chem. Soc.* **2013,** *135* (11), 4314-4324.

48. Porel, M.; Jayaraj, N.; Raghothama, S.; Ramamurthy, V., *Org. Lett.* **2010,** *12* (20), 4544-4547.
49. Chen, J. Y.-C.; Jayaraj, N.; Jockusch, S.; Ottaviani, M. F.; Ramamurthy, V.; Turro, N. J., *J. Am. Chem. Soc.* **2008,** *130*, 7206-7207.
50. Jockusch, S.; Zeika, O.; Jayaraj, N.; Ramamurthy, V.; Turro, N. J., *J. Phys. Chem. Lett.* **2010,** *1* (18), 2628-2632.
51. Jockusch, S.; Porel, M.; Ramamurthy, V.; Turro, N. J., *J. Phys. Chem. Lett.* **2011,** *2* (22), 2877-2880.
52. Gupta, S.; Adhikari, A.; Mandal, A. K.; Bhattacharyya, K.; Ramamurthy, V., *J. Phys. Chem. C* **2011,** *115* (19), 9593-9600.
53. Podkoscielny, D.; Philip, I.; Gibb, C. L. D.; Gibb, B. C.; Kaifer, A. E., *Chem. - Eur. J.* **2008,** *14* (15), 4704-4710.
54. Podkoscielny, D.; Gadde, S.; Kaifer, A. E., *J. Am. Chem. Soc.* **2009,** *131* (36), 12876-12877.
55. Qiu, Y.; Yi, S.; Kaifer, A. E., *Org. Lett.* **2011,** *13* (7), 1770-1773.
56. Porel, M.; Jockusch, S.; Parthasarathy, A.; Rao, V. J.; Turro, N. J.; Ramamurthy, V., *Chem. Commun. (Cambridge, U. K.)* **2012,** *48* (21), 2710-2712.
57. Porel, M.; Klimczak, A.; Freitag, M.; Galoppini, E.; Ramamurthy, V., *Langmuir* **2012,** *28* (7), 3355-3359.
58. Porel, M.; Chuang, C.-H.; Burda, C.; Ramamurthy, V., *J. Am. Chem. Soc.* **2012,** *134* (36), 14718-14721.
59. Liu, S.; Gan, H.; Hermann, A. T.; Rick, S. W.; Gibb, B. C., *Nat. Chem.* **2010,** *2* (10), 847-852.
60. Vriezema, D. M.; Comellas Aragones, M.; Elemans, J. A.; Cornelissen, J. J.; Rowan, A. E.; Nolte, R. J., *Chem Rev* **2005,** *105* (4), 1445-89.
61. (a) Sundaresan, A. K.; Ramamurthy, V., *Org. Lett.* **2007,** *9* (18), 3575-3578; (b) Sundaresan, A. K.; Ramamurthy, V., *Photochem. Photobiol. Sci.* **2008,** *7* (12), 1555-1564.
62. Kulasekharan, R.; Maddipatla, M. V. S. N.; Parthasarathy, A.; Ramamurthy, V., *J. Org. Chem.* **2013,** *78* (3), 942-949.
63. (a) Parthasarathy, A.; Kaanumalle, L. S.; Ramamurthy, V., *Org. Lett.* **2007,** *9* (24), 5059-5062; (b) Parthasarathy, A.; Ramamurthy, V., *Photochem. Photobiol. Sci.* **2011,** *10* (9), 1455-1462.
64. Samanta, S. R.; Parthasarathy, A.; Ramamurthy, V., *Photochem. Photobiol. Sci.* **2012,** *11* (11), 1652-1660.
65. Kaanumalle, L. S.; Ramamurthy, V., *Chem. Commun. (Cambridge, U. K.)* **2007,** (10), 1062-1064.
66. Parthasarathy, A.; Samanta, S. R.; Ramamurthy, V., *Res. Chem. Intermed.* **2013,** *39* (1), 73-87.
67. Kaanumalle, L. S.; Gibb, C. L. D.; Gibb, B. C.; Ramamurthy, V., *Org. Biomol. Chem.* **2007,** *5* (2), 236-238.
68. Natarajan, A.; Kaanumalle, L. S.; Jockusch, S.; Gibb, C. L. D.; Gibb, B. C.; Turro, N. J.; Ramamurthy, V., *J. Am. Chem. Soc.* **2007,** *129*, 4132-4133.
69. (a) Pina, F.; Parola, A. J.; Ferreira, E.; Maestri, M.; N., A.; Ballardini, R.; Balzani, V., *J. Phys. Chem.* **1995,** *99*, 12701-12703; (b) Place, I.; Farran, A.; Deshayes, K.; Piotrowiak, P., *J. Am. Chem. Soc.* **1998,** *120*, 12626-12633.
70. Kulasekharan, R.; Choudhury, R.; Prabhakar, R.; Ramamurthy, V., *Chem. Commun. (Cambridge, U. K.)* **2011,** *47* (10), 2841-2843.
71. Gupta, S.; Choudhury, R.; Krois, D.; Wagner, G.; Brinker, U. H.; Ramamurthy, V., *Org. Lett.* **2011,** *13* (22), 6074-6077.
72. Jayaraj, N.; Maddipatla, M. V. S. N.; Prabhakar, R.; Jockusch, S.; Turro, N. J.; Ramamurthy, V., *J. Phys. Chem. B* **2010,** *114* (45), 14320-14328.
73. Jagadesan, P.; Mondal, B.; Parthasarathy, A.; Rao, V. J.; Ramamurthy, V., *Org. Lett.* **2013,** *15* (6), 1326-1329.

74. Choudhury, R.; Gupta, S.; Da Silva, J. P.; Ramamurthy, V., *J. Org. Chem.* **2013,** *78* (5), 1824-1832.
75. Jayaraj, N.; Jagadesan, P.; Samanta, S. R.; Da Silva, J. P.; Ramamurthy, V., *Org. Lett.* **2013,** *15* (17), 4374-4377.
76. Baldridge, A.; Samanta, S. R.; Jayaraj, N.; Ramamurthy, V.; Tolbert, L. M., *J. Am. Chem. Soc.* **2010,** *132* (5), 1498-1499.
77. Baldridge, A.; Samanta, S. R.; Jayaraj, N.; Ramamurthy, V.; Tolbert, L. M., *J. Am. Chem. Soc.* **2011,** *133* (4), 712-715.
78. Kaanumalle, L. S.; Gibb, C. L. D.; Gibb, B. C.; Ramamurthy, V., *J. Am. Chem. Soc.* **2005,** *127* (11), 3674-3675.
79. (a) Samanta, S. R.; Kulasekharan, R.; Choudhury, R.; Jagadesan, P.; Jayaraj, N.; Ramamurthy, V., *Langmuir* **2012,** *28* (32), 11920-11928; (b) Mondal, B.; Kamatham, N.; Samanta, S. R.; Jagadesan, P.; He, J.; Ramamurthy, V., *Langmuir* **2013,** *29* (41), 12703-12709.
80. (a) Moran, J. R.; Karbach, S.; Cram, D. J., *Journal of the American Chemical Society* **1982,** *104* (21), 5826-5828; (b) Moran, J. R.; Ericson, J. L.; Dalcanale, E.; Bryant, J. A.; Knobler, C. B.; Cram, D. J., *J. Am. Chem. Soc.* **1991,** *113*, 5707-5714.
81. Kubitschke, J.; Javor, S.; Rebek, J., Jr., *Chem Commun (Camb)* **2012,** *48* (74), 9251-3.
82. Schramm, M. P.; Hooley, R. J.; Rebek, J., Jr., *J Am Chem Soc* **2007,** *129* (31), 9773-9.
83. (a) Hof, F.; Trembleau, L.; Ullrich, E. C.; Rebek, J., Jr.,, *Angew. Chem. Int. Ed.* **2003,** *42*, 3150-3153; (b) Biros, S. M.; Ullrich, E. C.; Hof, F.; Trembleau, L.; Rebek, J., Jr., *J Am Chem Soc* **2004,** *126* (9), 2870-6.
84. Hooley, R. J.; Anda, H. J. V.; Rebek, J., Jr.,, *J. Am. Chem. Soc.* **2007,** *129*, 13464-13473.
85. Trembleau, L.; Rebek, J., Jr., *Chem. Commun.* **2004**, 58-59.
86. Hooley, R. J.; Biros, S. M.; Rebek, J., Jr., *Chem Commun (Camb)* **2006,** (5), 509-10.
87. Hooley, R. J.; Biros, S. M.; Rebek, J., Jr., *Angewandte Chemie* **2006,** *45* (21), 3517-9.
88. Podkoscielny, D.; Hooley, R. J.; Rebek, J., Jr.,; Kaifer, A. E., *Organic Letters* **2008,** *10* (13), 2865-2868.
89. Hooley, R. J.; Van Anda, H. J.; Rebek, J., Jr., *J Am Chem Soc* **2006,** *128* (12), 3894-5.
90. Haas, C. H.; Biros, S. M.; Rebek, J., Jr., *Chem Commun (Camb)* **2005,** (48), 6044-5.
91. Ryan, D. A.; Rebek, J., *J. Am. Chem. Soc.* **2011,** *133* (49), 19653-19655.
92. (a) Haino, T.; Rudkevich, D. M.; Rebek, J., Jr., *J. Am. Chem. Soc.* **1999,** *121*, 11253-11254; (b) Haino, T.; Rudkevich, D. M.; Shivanyuk, A.; Rissanen, K.; Rebek, J., Jr., *Chemistry* **2000,** *6* (20), 3797-805.
93. Lledo, A.; Rebek, J., Jr., *Chem Commun (Camb)* **2010,** *46* (45), 8630-2.
94. Ryan, D. A.; Rebek, J., *Analyst (Cambridge, U. K.)* **2013,** *138* (4), 1008-1010.
95. Javor, S.; Rebek, J., Jr., *J Am Chem Soc* **2011,** *133* (43), 17473-8.
96. Butterfield, S. M.; Rebek, J., Jr., *J Am Chem Soc* **2006,** *128* (48), 15366-7.
97. Liu, Y.; Taira, T.; Young, M. C.; Ajami, D.; Rebek, J.; Cheng, Q.; Hooley, R. J., *Langmuir* **2012,** *28* (2), 1391-1398.
98. Ebbing, M. H.; Villa, M. J.; Valpuesta, J. M.; Prados, P.; de Mendoza, J., *Proc Natl Acad Sci U S A* **2002,** *99* (8), 4962-6.
99. Zhang, K. D.; Ajami, D.; Gavette, J. V.; Rebek, J., Jr., *Chem Commun (Camb)* **2014,** *50* (38), 4895-7.
100. Harano, K.; Hiraoka, S.; Shionoya, M., *J. Am. Chem. Soc.* **2007,** *129* (17), 5300-5301.
101. Hiraoka, S.; Harano, K.; Shiro, M.; Shionoya, M., *J Am Chem Soc* **2008,** *130* (44), 14368-9.
102. Hiraoka, S.; Harano, K.; Nakamura, T.; Shiro, M.; Shionoya, M., *Angewandte Chemie* **2009,** *48* (38), 7006-9.
103. Hiraoka, S.; Nakamura, T.; Shiro, M.; Shionoya, M., *J. Am. Chem. Soc.* **2010,** *132* (38), 13223-13225.